SAHC

Flexural out-of-plane retrofitting of masonry walls in historical constructions

Barna Csikai

Portugal | 2013

ADVANCED MASTERS IN STRUCTURAL ANALYSIS
OF MONUMENTS AND HISTORICAL CONSTRUCTIONS

Master's Thesis

Barna Csikai

Flexural out-of-plane retrofitting of masonry walls in historical constructions

University of Minho

UNIVERSITAT POLITÈCNICA DE CATALUNYA

Education and Culture

Erasmus Mundus

ADVANCED MASTERS IN STRUCTURAL ANALYSIS
OF MONUMENTS AND HISTORICAL CONSTRUCTIONS

Master's Thesis

Barna Csikai

Flexural out-of-plane retrofitting of masonry walls in historical constructions

This Masters Course has been funded with support from the European Commission. This publication reflects the views only of the author, and the Commission cannot be held responsible for any use which may be made of the information contained therein.

Portugal | 2013

DECLARATION

Name: Barna Csikai

Email: csikai.barna@gmail.com

Title of the Msc Dissertation: Flexural out-of-plane retrofitting of masonry walls in historical constructions

Supervisor: Professor Luís F. Ramos

Year: 2013

I hereby declare that all information in this document has been obtained and presented in accordance with academic rules and ethical conduct. I also declare that, as required by these rules and conduct, I have fully cited and referenced all material and results that are not original to this work.

I hereby declare that the MSc Consortium responsible for the Advanced Masters in Structural Analysis of Monuments and Historical Constructions is allowed to store and make available electronically the present MSc Dissertation.

University: Universidade do Minho

Date: 08.07.2013

Signature: _____

I am dedicating this work to my family.

ACKNOWLEDGEMENTS

I would like to express my sincere gratitude to Professor Luís F. Ramos, my supervisor, for his continuous support, motivation, guidance, enthusiasm and most of all for his kind personality and expertise.

I also wish to thank to Susana Moreira, Phd. student at University of Minho, for her persistent help in preparation of the experiments, for introducing the laboratory, and being a reliable friend during my short stay.

My sincere thanks the Polytechnic University of Catalonia (UPC) for hosting me in the semester of coursework. Especially to Pere Roca Fabregat and Lúca Pelá professors, for believing in me, and for highly contributing to my development with their expertise and kindness.

Thank you for the Consortium for granting me with a scholarship.

I would never forget the great support of Professor István Sajtos, who kept being enthusiastic about my attendance in the SAHC program, giving me great motivation.

Many thanks to all of my classmates, for the quality teamwork and for all the fun that we had together in such short time.

I cannot find words to express my gratitude to my loving family for supporting me in every possible way. Thank you very much for everything.

ABSTRACT

Historic ruins are often peculiar types of masonry structures. These constructions are extremely vulnerable to out-of-plane actions – such as seismic movements and wind effects - often being left without any transversal bracing. Their historical, social and economical values however, make it very important to save them for the future. A comprehensive literature review revealed several techniques for the internal and external strengthening of walls, but applying these techniques to un-rendered heritage constructions often cause visual damage, which cannot be tolerated.

This work aims to develop a reinforcing technique for the flexural strengthening of heritage masonry walls. Extending the idea of an existent technique, adding an enhanced constituent for anchoring, the method comprises an irregular grid that follows the joint texture of the wall. The insertion procedure is much alike a shallow repointing. As a result the technique upgrades the mechanical performance against out-of-plane actions (flexural) and increases the integrity of a structure, without causing visual impact.

Applicability and workability issues remained key aspects of the investigation, which involved experimental and analytical studies. The constituents of the technique were tested individually. Based on the gathered information and on the analytical investigation, monotonic bending tests were prepared finally. The results proved the adequacy of the new technique and allowed decisions on future development. Improvement of anchors and pre-stressing the grid is necessary. For future numerical modeling, the bond behavior of the improved anchors needs to be tested in both axial and transversal direction.

Finally a case study was presented with the discussion of the theoretical application of the new technique on the Alcáçova wall in Guimarães Castle, Portugal. The study showed the practical limits of the technique given by the geometrical constraints of the joint texture of the wall. It also demonstrated that the design abacus – proposed in the analytical investigation – is a powerful tool to define the failure modes and resistance of a strengthened construction.

Conclusions were made on the future development of the technique, giving ideas about the protection of the reinforcement, the improvement of the anchors, alternative materials for the reinforcing grid, and necessary experiments to gather information for numerical modeling.

RESUMO

As ruínas de construções históricas em alvenaria constituem, geralmente, estruturas muito peculiares do ponto de vista estrutural. As ruínas são extremamente vulneráveis a ações para fora do plano - como a ação sísmica ou do vento – sendo muitas vezes deixadas sem a presença de travamento horizontal. Dado o valor patrimonial intangível e a sua importância económica na generalidade dos sítios históricos, torna-se muito importante a sua salvaguarda.

A literatura científica mostra que existem várias técnicas de reforço para paredes de alvenaria, aplicáveis quer no interior, quer no exterior das paredes. Contudo, a sua aplicação a paredes de alvenaria sem revestimento – o caso da generalidade das ruínas – é muito limitada, dado que a maioria das técnicas introduz impactos visuais incompatíveis com este tipo de construções históricas.

Esta tese visa o desenvolvimento de uma técnica de reforço à flexão para paredes de construções com valor patrimonial elevado tendo em conta a mínima intrusividade na construção. Trata-se de um melhoramento de uma técnica existente através da introdução de elementos que melhoram a ancoragem do reforço nas paredes de alvenaria. Concretamente, o método de reforço consiste na introdução de uma armadura flexível e irregular que consegue acompanhar a geometria das juntas das paredes de alvenaria, podendo ser posteriormente escondida nas juntas de argamassa. Como resultado, a técnica aumenta a capacidade de carga a esforços de flexão para fora do plano das paredes e aumenta a integridade estrutural sem causar impacto visual.

Os pontos fortes desta investigação foram a análise da aplicabilidade e trabalhabilidade desta técnica a construções históricas, em comparação com o melhoramento do seu desempenho estrutural. Após uma análise analítica da aplicabilidade da técnica, foram escolhidos e testados todos os componentes do sistema, culminando numa campanha experimental que incluiu ensaios à flexão em paredes reforçadas à escala reduzida. Os resultados obtidos comprovam a adequabilidade da técnica e apontam alguns melhoramentos necessários para o sistema de reforço ser mais eficiente.

É também apresentado um caso de estudo sobre a aplicabilidade do sistema de reforço na parede da Alcáçova (em ruina) no Castelo de Guimarães. O caso de estudo demonstrou os limites da aplicabilidade da técnica e permitiu aferir aspetos práticos e de dimensionamento, através da análise da geometria da parede e do recurso a um ábaco de dimensionamento desenvolvido para o efeito, prospectivamente.

Finalmente foram apontadas algumas recomendações para futuros desenvolvimentos da técnica, nomeadamente relacionados com a proteção das armaduras, o melhoramento do sistema de ancoragem, materiais alternativos para o reforço e ensaios necessários para realizar análises numéricas do sistema.

ABSZTRAKT

A dolgozat magyar címe: Történeti falazatok síkra merőleges hajlításokra történő megerősítése

A történeti romok gyakran bármilyen merőleges megtámasztás nélküli, falazott szerkezetekből állnak. Ezek a szerkezetek különösen érzékenyek az őket érő transzverzális hatásokra (szeizmikus hatások, szélterhek). Megmentésük a jövő számára különösen fontos, hiszen történelmi, gazdasági és társadalmi értékük felbecsülhetetlen.
Az irodalmi áttekintés kitért a fellelhető megerősítési technikákra. A kutatás azt a következtetést engedte levonni, hogy a technikák többsége nehezen, vagy egyáltalán nem alkalmazható vakolatlan történeti szerkezetek megerősítésére, az okozott vizuális elváltozások miatt.

A dolgozat célja egy új, hajlításra történő erősítési technológia kifejlesztése volt történeti falazatok számára. Egy meglévő módszer elméletének kiterjesztésével, valamint egy egyedi fejlesztésű lehorgonyzó elem alkalmazásával, az új rendszer egy a falazat hézagstruktúráját követő, szabálytalan hálóból áll. E háló elhelyezéséhez szükséges a habarcshézagok külső 2-3 cm-ének eltávolítása, majd pótlása a műveletek végeztével. Eredményképpen, a rendszer fejleszti a szerkezet hajlításokra történő működését, valamint fokozza a falazat integritását anélkül, hogy közben károsan érintené annak vizuális megjelenését.

Az alkalmazhatóság és az egyszerű megmunkálhatóság kérdései kulcsszerepet játszottak a kutatás során, mely különböző kísérleteket, és analitikai tanulmányozást is magába foglalt. Végül lehetőség volt hajlítási tesztek elvégzésére is, 1:2 arányú falazott kőfalak alkalmazásával, valamint az új rendszer kipróbálásával. Az eredmények amellett, hogy igazolták a technológia alkalmazhatóságát, segítettek új fejlesztési irányok kijelölésében is a kutatás további folytatásához: Az egyedi lehorgonyzó elemek továbbfejlesztése, valamint előfeszítési eljárás kifejlesztése szükséges. Továbbá szükséges az egyedi kapcsolóelemek lehorgonyzási viselkedésének kiterjedt kísérleti és elméleti jellemzése – tengely, valamint tengelyre merőleges irányban –, esetlegesen numerikus modellezéshez is.

Végül egy esettanulmány keretein beül került sor az új rendszer alkalmazhatósági kérdéseinek elméleti tárgyalására. A megerősítendő szerkezet a Guimaraes-i Kastély északi fala, az Alcáçova fal volt, Portugáliában. A tanulmány bemutatja az alkalmazhatósági korlátokat, valamint demonstrálja a tervezési segédlet használhatóságát a különböző tönkremeneteli módok, valamint a teljes ellenállási görbe meghatározásában (a tervezési segédlet létrehozása az analitikai tanulmány részét képezte).

A végértékelés magába foglalta a további fejlesztési irányok következő kérdéseit: Erősítő kábelek fokozott védelme; lehorgonyzó elemek fejlesztése; előfeszítés; alternatív háló anyag; valamint további kísérletek elvégzése információgyűjtéshez, numerikus modellezéshez.

TABLE OF CONTENTS

LIST OF FIGURES:

LIST OF TABLES:

1

INTRODUCTION

1.1 Motivation

Historic ruins - vacant buildings without floors and roofs; parts of ancient walls; partially destroyed castle walls or archaeological sites - representing high heritage value are unlike the current masonry buildings. These buildings are often only supported in their foundations, cantilevering with no connection to any other construction element that would function as bracing. Other types are left without horizontal support between the roof structures and their foundations, acting as thin supported wall beams. These structures are extremely vulnerable to seismic and wind effects, as they can have very low resistance against out-of-plane actions. It is difficult to find a technique, which is especially developed for the structural consolidation of these types of constructions and at the same time does not adversely affect their authenticity (see on Figure 1).

Figure 1: Additional bracing structures visibly damaging the authenticity of ruins in seismic area

Figure 2 shows the ruins of the Castle of Regéc in Hungary.

Figure 2: The ruins of the Castle of Regéc in Hungary

Such ruins are common in Hungary memorising the defensive castle building period from the Ottoman invasions till the Habsburg regime. Despite the common belief about the tactical demolition of the forts by the Habsburg kings, in most of the cases the castles were destructed in other circumstances (rebel movements, material reuse by local people). One way or another, these existing remains are dangerously vulnerable. Seismic risk in Hungary is not significant but present. However, the seismic performance of the built heritage is not yet evaluated. Hence an earthquake affecting specific locations is extremely dangerous to these important structures, both to their visitors. For these reasons, developing new strengthening techniques that do not damage the authenticity of these special constructions is a noble challenge.

1.2 Objectives

The cultural, social, historical and economical importance of heritage structures gives support to present thesis work. Its objective is to carry out an investigation to develop a new alternative way of strengthening historic walls against out-of plane actions.

After studying the existing techniques it becomes clear that most of the strengthening methods are not applicable to un-rendered ancient walls, because of their visual impact. Further disadvantages may appear in workability. Present thesis aims to run a series of experimental investigations to mechanically and physically define a new alternative strengthening technique. Workability issues are taken into account, and reduced visual impact is kept as one of the most important factors. Supplementary to the proposal, analytical investigation is prepared to provide design instructions for the application. Finally, theoretical application of the technique is to be discussed on one of the existing important structures.

1.3 Thesis outline

The present thesis is divided in eight chapters with the following structure:

Chapter 1 gives the introduction to the thesis motivation, describes the objectives and presents the document structure.

Chapter 2 consists of a literature review involving the existing techniques of strengthening, code recommendations, and test procedures with a concentration on the out-of-plane capacity of masonry walls. Based on the gathered information and conclusions made by the author, the aim of the chapter is to define the appropriate way of strengthening, taking into account different aspects, such as mechanical improvement, compatibility, aesthetical damage, workability and sustainability.

In Chapter 3 a reinforcing system is proposed with the aim of increasing the out-of-plane bending resistance of a stone masonry walls and reducing visual impact on structure. First

the general aspects of the system are discussed. Than a detailed description of the comprised elements are given.

In Chapter 4, experimental investigation on individual constituents can be found. The results were used to conclude on the further development of the proposed strengthening technique, and to make the preliminary calculations for the scaled wall tests. The experimental research comprised tensile tests of stainless steel cables, tensile tests of synthetic ropes, and pull-out tests of helibars from mortar cylinders.

Chapter 5 consists of an analytical study, which was prepared to investigate cost efficiency issues, to define reinforcement on wall specimens for bending tests, and to provide an analytical guide for designing the proposed technique for future practice.

Chapter 6 consists of the discussion of scaled stone masonry wall bending tests, with and without the application of the proposed strengthening technique. The tests were undertaken after a reduced curing time of 21 days, and conclusions were based on the relation between mechanical performance, applicability and workability issues.

In Chapter 7 a case study of the Alcáçova wall is presented. Practical and analytical investigation on the application of the new technique is presented, together with a literature review about the historical construction.

Chapter 8 involves the conclusions for the evaluation of the research. Ideas for future development are also presented.

2

STRENGTHENING OF HISTORIC MASONRY WALLS

Introduction:

The following chapter consists of a literature review involving the existing techniques of strengthening, code recommendations, and test procedures with a concentration on the out-of-plane capacity of masonry walls. Based on the gathered information and conclusions made by the author, the aim of the chapter is to define the appropriate way of strengthening, taking into account different aspects, such as mechanical improvement, compatibility, aesthetical damage, workability and sustainability.

2.1 Structural safety of historical stone masonry walls

Assessment of the structural safety of historical stone masonry walls is hard, and needs to be done case by case (Binda, et al., 1997; Gelmi, et al., 1993). This problem lies in the peculiar construction type of the walls that is characterized by the: lack of uniformity in geometry; lack of uniformity in material properties; lack of uniformity in cross section (multiple leaf configuration); horizontal and vertical joint texture; shape of units; bond efficiency between units and matrix (see it on Figure 3).

Figure 3: Different shapes of units and different cross-section configuration in stone masonry walls (Binda, et al., 1997).

The most important feature of a stone wall is the bonding of units as it is responsible for the structural integrity of a wall. It is possible to restore and upgrade the integrity of walls with the injection of proper materials into the structure, creating effective bond between units (Binda, et al., 1997; Binda, et al., 1993).

In areas with high seismic risk further strengthening of these structures might be necessary in order to increase the safety level. The global structural role of a wall becomes important. In-plane behaviour of shear walls was discussed in several publications and recommendations for strengthening techniques can be found also in codes (CNR-DT, 200/2004).

Out of-plane deformational capacity of a wall depends on: the boundary conditions and structural integrity of a building; the equilibrium of a rigid body subjected to transversal overturning forces; and transversal flexural capacity of “wall beams” (see representation on Figure 4).

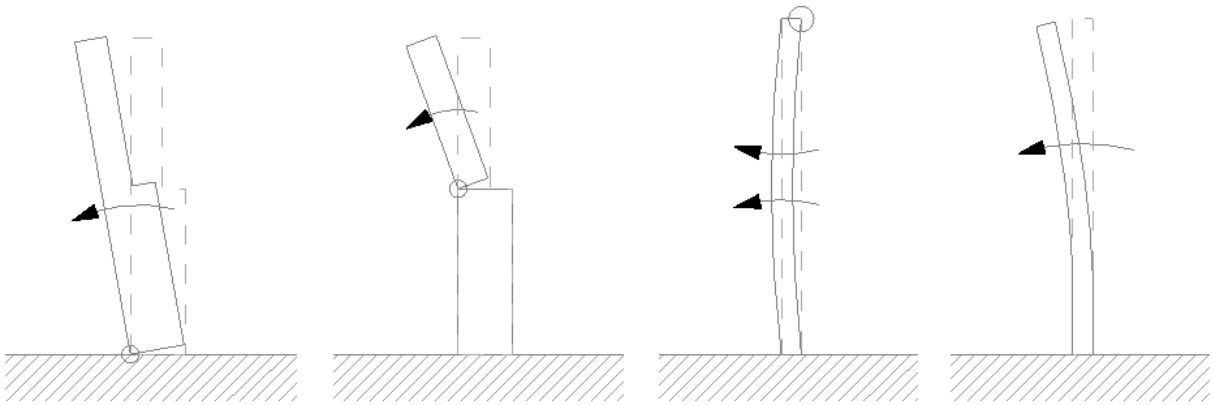

Figure 4: Overturning mechanisms of rigid bodies (a,b) and elastic flexural behaviour of wall beams (c,d)

The bearing capacity of masonry walls against out-of-plane actions is very weak compared to their efficiency against in-plane forces. Therefore it is desirable to avoid transversal actions by improving the connections between horizontal and vertical structural elements (floors and walls) and improving the stiffness of floors. By enhancing the global structural (box-) behaviour horizontal forces can be transported to the shear walls and out-of-plane actions can be released. However, in several cases box behaviour is hard or not possible to be activated (Milani, 2013). If more structural integrity cannot be provided, the historical walls need to be strengthened against out-of-plane actions. In this case, increasing flexural capacity and stabilization becomes important.

2.2 Existing techniques for the improvement of flexural capacity

The literature review involved several techniques for the improvement of flexural capacity not only for masonry structures but with the extension to reinforced concrete structures. Advantages-disadvantages, difficulties in application are discussed briefly in the following sections.

2.2.1 Internal anchoring with post-tensioning tendons

Internal anchoring is done by coring through the wall to be strengthened, and applying noncorrosive tendons inside the vertical drill-holes, creating anchorage in the substructure, foundation or soil. A sketch of a strengthened wall can be seen on Figure 5.

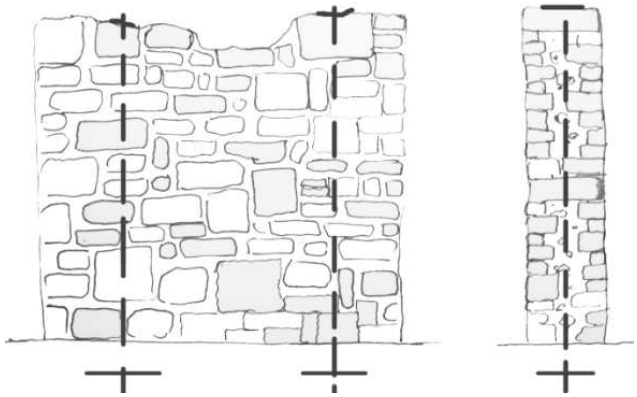

Figure 5: Internal anchoring applied on irregular stone masonry wall

Prestressed tendons with bearing plates are adequate to produce stresses in hinge zones by distributing axial stresses at an angle of 45^{o} in the wall. The flexural capacity of strengthened wall can be estimated with the following formulas (Ismail, et al., 2009).

$$M_c = \frac{I_n}{c}\left[f_r + \left(\frac{P_v + P_{sw} + A_{ps} f_{se}}{A_n}\right)\right] \quad (1)$$

$$M_n = \left(P_v + P_{sw} + A_{ps} f_{se}\right)\left[d_{eff} - \frac{(P_v + P_{sw} + A_{ps} f_{ps})}{2(\lambda_n f_m^b)}\right] \quad (2)$$

where:

M_c is the applied moment at crack penetration
M_n is the moment capacity at nominal strength
I_n is the net moment of inertia of the masonry
c is the distance of extreme compression fibre to neutral axis
f_r is the modulus of rupture
P_v is the overburden vertical load producing axial compression on the masonry
P_{sw} is the axial load due to self-weight
A_{ps} is the area of pre-stressing steel
f_{ps} is the tensile stress in pre-stressing tendons at nominal strength
f_{se} is the effective stress in pre-stressing tendons after all losses
A_n is the net cross sectional area of the masonry,
d_{eff} is the distance of extreme compression fibre to the center of tension reinforcement,
λ_n is a parameter representing the fraction of maximum compressive stress at nominal strength.
f_m is the specified compressive strength of masonry
b is the width of cross section

The technique is not damaging visibly the historical wall, respecting its heritage value, and effectively improves the resistance against out-of-plane actions, such as seismic movement of ground or wind load. Supplementary to the vertical ties, horizontal tie beam can be applied to provide extra integrity by extending the effect of prestressed tendons (see Figure 6).

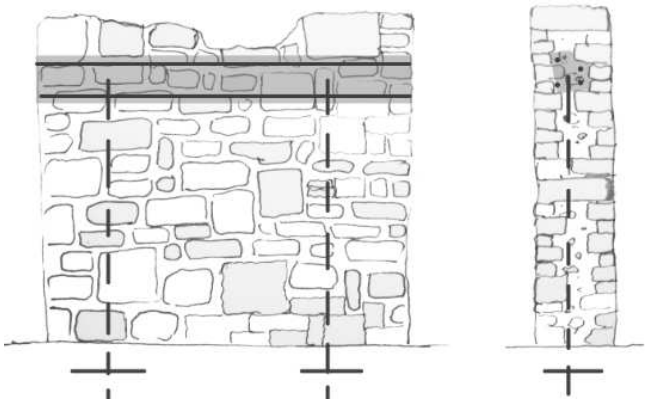

Figure 6: Internal anchors applied to irregular stone masonry wall supplemented by a load distributing tie beam

2.2.2 Near surface mounted reinforcement

In the developing field of the application of fibre reinforced polymers, the near surface mounted technique is relatively recent, and under testing. It was applied successfully to increase the flexural capacity of concrete and masonry structures (Griffith, et al., 2012; Ismail & Ingham, 2012; Barros, et al., 2008). The reinforcing material is inserted into a small groove on surface, allowing better bond between structure and strengthening. As a consequence the inserted material's capacity can be utilized more than in case of external bond.

For irregular ancient stone masonry walls the applicability of the technique depends on the type of stone, as grooves need to be cut on surface. The irregular geometry makes it hard to predict the maximum depth of the groove, and although, the technique seems less "invasive" than the external bonded materials - from an aesthetic point of view – the vertical lines of the cuts remain visibly deteriorating, as can be seen on Figure 7.

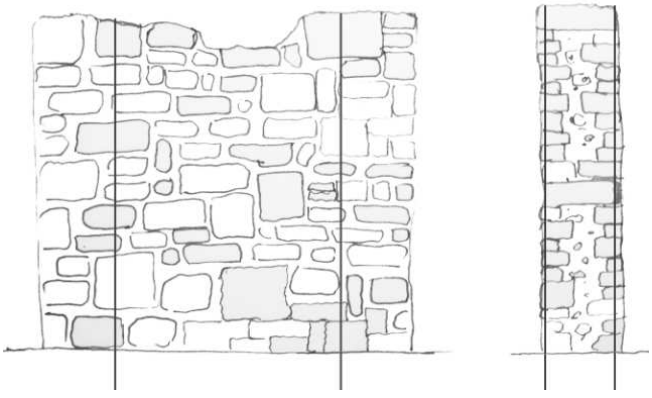

Figure 7: Sketch of NSM technique applied to irregular stone masonry wall

2.2.3 Jacketing and strengthening covers

Jacketing is a well-known technique for increasing in-plane capacity of shear walls, and drastically improving the overall performance of walls with low integrity (Churilov & Dumova-Jovanoska, 2013; Papanicolaou, et al., 2011). The technique consists on the application of strengthening layers on both sides of the wall, using reinforcing grids (steel or polymer) and covering mortar (lime, cement, earthen etc.). The layers are also connected through the wall with connector elements, to improve the efficiency. A sketch of the technique can be seen on Figure 8.

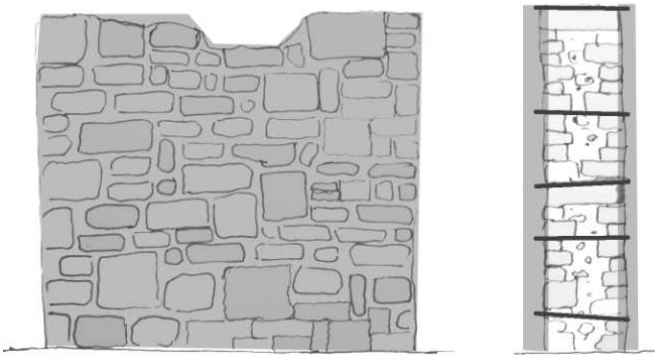

Figure 8: Jacketing technique applied on irregular stone wall

Durability problems of embedded steel seem to be overcome by the usage of fibre reinforced polymeric grids and textile meshes, e.g. textile reinforced mortar (Bernat, et al., 2013). New covering systems take advantage of short fibres mixed with a cementitious matrix, such as Strain Hardening Cementitious Composites (SHCC); and Steel Fibre Reinforced Self-Compacting Concrete (SFRSCC). In a recent work (Esmaeeli, et al., 2013) SHCC was successfully applied to masonry beams as flexural strengthening.

Related to the present thesis work, the key character of any covering technique is that they cannot be applied to walls that sustain heritage value, because of the invasiveness and visibly damage they cause.

2.2.4 External bonded / mechanically fixed materials

Mechanically fixed steel plates and external bonded FRP materials can be applied as tension members. The strengthening materials are forming vertical or horizontal stripes respecting the purpose of strengthening. In case of irregular, historic stone masonry the technique is questionable; the aesthetic features are not pleasing, material bond is hard issue due to irregularity of geometry (see the representing sketch on Figure 9).

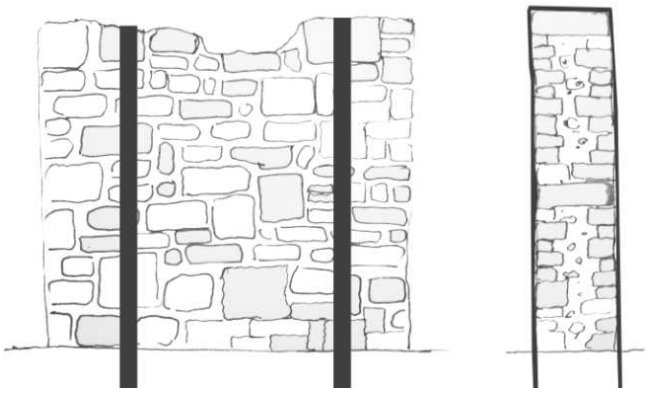

Figure 9: External bond materials applied on irregular stone wall increasing flexural capacity

2.2.5 Reticulatus

An innovative technique was developed by Borri in Italy (Borri, et al., 2011).

The technique consists of a continuous mesh of steel (or polyethylene) cords, embedded in the repointed mortar joints, the nodes of which are anchored to the wall by means of transversal metal bars, as can be seen on Figure 10 and Figure 11. Alternatively Polyethylene cords were used in the experiment to increase resistibility of mesh.

Strengthened historic wall prisms were subjected to shear tests. Increase of capacity in compression and flexure was also expected, however yet not proved by experimental tests.

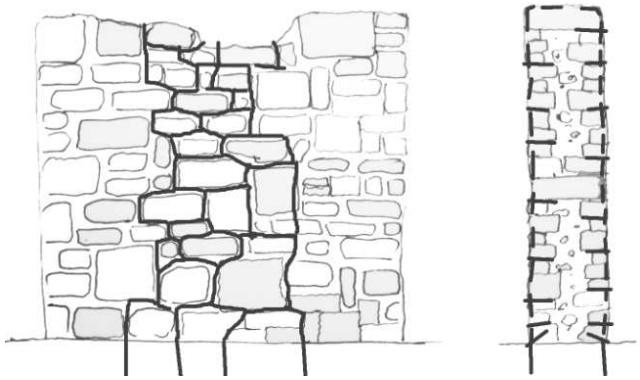

Figure 10: "Reticulatus" technique applied for flexural strengthening: frontage and cross-section

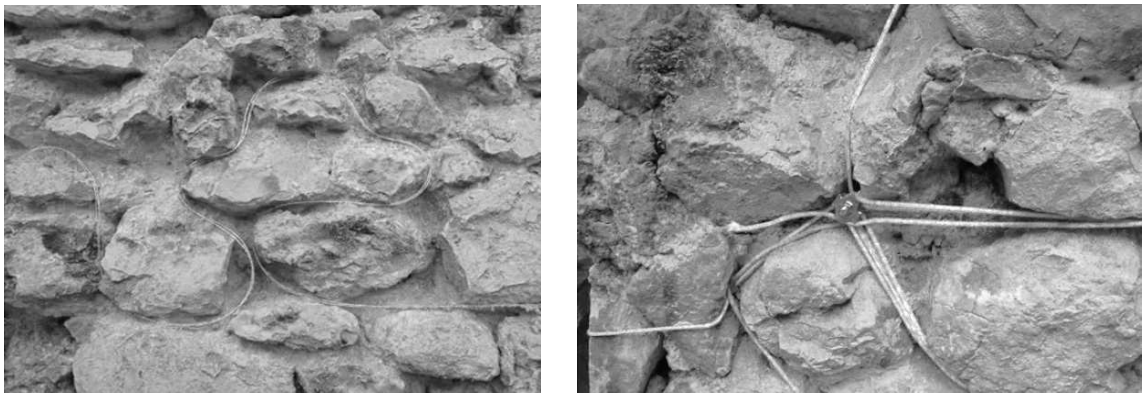

a) **b)**

Figure 11: Reticulatus: (a) Ultra High Tensile Strength Steel (UHTTS) cords; (b) Ultra High Molecular Weight Polyethylene (UHMWPE) cords (Borri, et al., 2011).

First experimental results showed the new technique's efficiency, providing better results compared to jacketing with GFRP mesh.

The special external strengthening technique can be applied to irregular stone walls in an aesthetically pleasant way. However, only few experiments were done till now, and the increased labour time appears to be a disadvantage. Further investigation is needed.

2.3 Eurocode recommendations

In the following sections recommendations for basic design concepts of unreinforced and reinforced masonry are collected, concerning flexural capacity and reinforcing details.

2.3.1 Characteristic Flexural Strength

In Eurocode 6 general recommendations can be found for the evaluation of flexural capacity of un-strengthened masonry walls (Eurocode-6, 2005). Two types of failure planes are mentioned with respect to their position related to the bed joints (see on Figure 12).

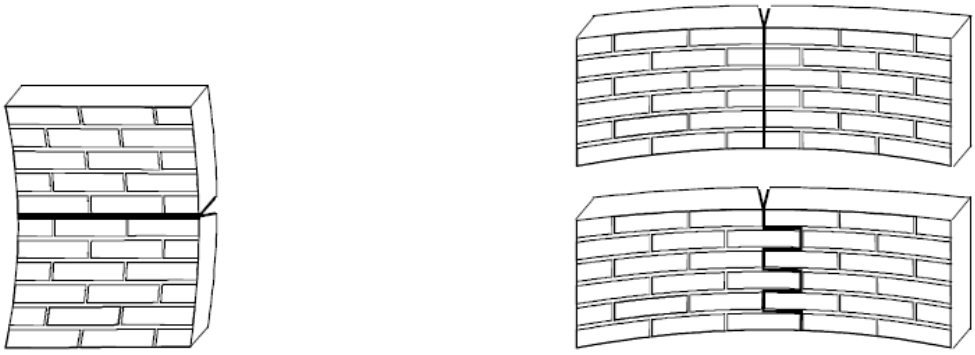

a) **b)**

Figure 12: a) plane of failure parallel to bed joints; f_{xk1} b) plane of failure perpendicular to bed joints; f_{xk2} (Eurocode-6, 2005)

The characteristic flexural strength of the wall depends on the direction of the flexural plane, f_{xk1} *and* f_{xk2}, (Figure 12). For the evaluation of characteristic flexural strength Eurocode 6 recommends values for the mortar strength and the flexural strength of individual units (see Table 1). However, in the case of historical, irregular stone masonry walls it is advisable to obtain the values by experimental tests, as it is cited from Eurocode 6.

Table 1: Values of f_{xk1}, for plane of failure parallel to bed joints (Eurocode-6, 2005)

Masonry Unit	f_{xk1} (N/mm^2)			
	General purpose mortar		Thin layer mortar	Lightweight mortar
	f_m< 5 N/mm^2	f_m > 5 N/mm^2		
Clay	0,10	0,10	0,15	0,10
Calcium silicate	0,05	0,10	0,20	not used
Aggregate concrete	0,05	0,10	0,20	not used
Autoclaved concrete	0,05	0,10	0,15	0,10
Manufactured stone	0,05	0,10	not used	not used
Dimensioned natural stone	0,05	0,10	0,15	not used

2.3.2 Unreinforced masonry walls subjected to lateral loading

At the ultimate limit state, the design value of the moment applied to the masonry wall, M_{Ed} (see EC6 Section 5.5.5), shall be less than or equal to the design value of the moment of resistance of the wall, M_{Rd}, such that:

$$M_{Ed} \leq M_{Rd} \tag{3}$$

The design value of the lateral moment of resistance of a masonry wall, M_{Rd}, per unit height or length, is given by:

$$M_{Rd} = f_{xd} \times Z \quad (4)$$

where:

f_{xd} is the design flexural strength appropriate to the plane of bending,
Z is the elastic section modulus of unit height or length of the wall.

2.3.3 Characteristic anchorage strength of reinforcement:

The characteristic anchorage strength of reinforcement bedded in mortar or concrete shall be obtained from the results of tests. Recommendations can be found for the evaluation of regular reinforcing steel bars bedded in concrete or mortar.

Table 2 can be used for comparison between test results using special anchorage elements (addressed by present work) and code recommendations for using regular steel bars.

Table 2: Characteristic anchorage strength of reinforcement in mortar or concrete not confined within masonry units (Eurocode-6, 2005)

Strength class of	**Mortar**	**M2-5**	**M5-9**	**M10-14**	**M15-19**	**M20**
	Concrete	**not used**	**C12/15**	**C16/20**	**C20/25**	**C25/30 <**
f_{bok} for plain carbon steel bars (N/mm^2)		0,5	0,7	1,2	1,4	1,4
f_{bok} for high-bond carbon steel and stainless steel bars (N/mm^2)		0,5	1,0	1,5	2,0	3,4

2.3.4 Verification of reinforced masonry members subjected to bending and / or axial loading

Externally reinforced masonry subjected to bending can be calculated using the same theory as for the calculation of reinforced concrete bended elements (EC6- Section 6.6.2), as can be seen in Figure 13.

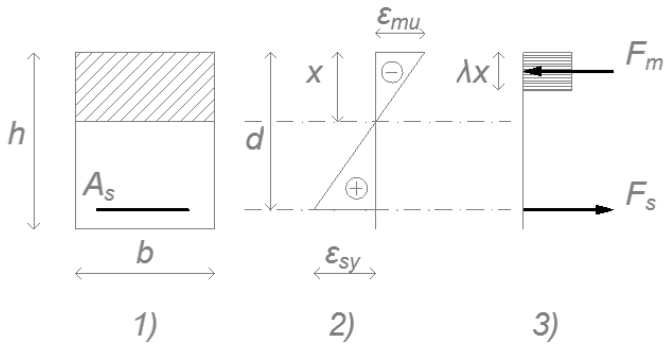

Figure 13: Stress and strain distribution. Cross section (1) strains (2) internal forces (3)

For the case of a singly reinforced rectangular cross-section, subjected to bending only, the design value of the moment of resistance, M_{Rd}, may be taken as:

$$M_{Rd} = A_s \times f_{yd} \times z \quad (5)$$

where, based on the simplification illustrated in Figure 13, the lever arm, *z*, may be taken, for a section when the maximum compression and tension are reached together, as:

$$z = d \times (1 - 0.5 \frac{A_s \times f_{yd}}{b \times d f_d}) \leq 0.95 \times d \quad (6)$$

where:

b is the width of the section;
d is the effective depth of the section;
As is the cross-sectional area of the reinforcement in tension;

fd is the design compressive strength of masonry in the direction of loading
fyd is the design strength of reinforcing steel.

Additional information can be found for the special case of reinforced masonry cantilever walls subjected to bending.

To calculate the moment of resistance, M_{Rd}, , the design compressive strength, f_d, in Figure 13, may be taken over the depth from the compressed edge of the cross-section, λx, when the design value of the moment of resistance, M_{Rd}, in compression, should not be taken to be greater than:

$$M_{Rd} = 0.4 \times f_d \times b \times d$$ for Group 1 units other than lightweight aggregate units (EC6- equation 6.24a) (7)

and

$$M_{Rd} = 0.3 \times f_d \times b \times d$$ for Group 2, 3 and 4 and Group 1 lightweight aggregate units. (EC6- equation 6.24b) (8)

where:

b is the width of the section;
d is the effective depth of the section;
fd is the design compressive strength of masonry;
x is the depth to the neutral axis.

The basic design concepts for evaluation of strengthened masonry walls have been discussed here. More specifications and notes can be found in EC6 (Eurocode-6, 2005).

2.4 Further recommendations

Italian and other recommendations were reviewed for the better understanding of the mechanical behaviour of historical masonry.

2.4.1 Mechanical parameters of masonry types

Magenes and Penna proposed a table (herein Table 3) for the evaluation of mechanical parameters of different masonry types (Magenes & Penna, 2009). After the in-situ recognition of typology and quality of materials, the table can be used to associate the results with other mechanical properties. The table is compiled on the basis of the experimental data obtained and collected by the authors. However, no information was found about the leaf configuration of reference structures.

Table 3: Reference values of the mechanical parameters and average specific weights for selected types of masonry (extracted from Table C8A.2.2. of Circ. NTC08, 2009). Note: f_m=compression strength; τ_o=shear strength; E=Young modulus; G=Shear modulus; W=average specific weight

Masonry typology	f_m (N/mm^2)	τ_o (N/mm^2)	E (N/mm^2)	G (N/mm^2)	W (kN/m^3)
	min-max	**min-max**	**min-max**	**min-max**	
Irregular stone masonry (pebbles, erratic, irregular stone)	1,0 1,8	0,020 0,032	690 1050	230 350	19
Uncut stone masonry with facing walls of limited thickness and infill core	2,0 3,0	0,035 0,051	1020 1440	340 480	20
Cut stone with good bonding	2,6 3,8	0,056 0,074	1500 1980	500 660	21
Soft stone masonry (tuff, limestone, etc.)	1,4 2,4	0,028 0,042	900 1260	300 420	16
Dressed rectangular (ashlar) stone masonry	6,0 8,0	0,090 0,120	2400 3200	780 940	22
Soli brick masonry with lime mortar	2,4 4,0	0,060 0,090	1200 1800	400 600	18

The parameters are varying and rather low compared to other experimental investigations.

An overview of experimental results is given by different authors with mechanical parameters of one masonry type. The difficulty in determining general parameters for different masonry types becomes understandable after checking the comparison in Table 4.

Table 4: Mechanical characteristics of stone masonry determined by various authors; Note: E= Elastic modulus; G= Shear modulus; f_m= compression strength; f_t= tensile strength; τ_u= shear strength; ν= Poisson's ration; ε_u= ultimate strain

Material Properties	Chiostrini et a.l (2000)	Rao et al. (1997)	Henriques et al. (2005)	Sorour et al. (2009)	Tomaževič (2010)	Lutman (2010)	Binda & Modena (1998)	Vintzileou et al. (2006)
E [GPa]	–	–	1770 - 2720	1900	321 - 390	–	470 - 1380	1000 - 1500
G [GPa]	140 - 360	–	–	–	65 - 170	–	–	–
f_m [MPa]	–	0.71 - 0.98	**5.80 - 15.1**	1.500	0.33 - 0.98	0.90 - 3.00	1.87-2.26	1.74-2.26
f_t [MPa]	–	0.60 -1.40	0.09 - 0.14	–	0.02 - 0.32	0.04 - 0.18	–	~0.10
τ_u [MPa]	0.07 - 0.23	–	0.08-0.09	–	–	–	–	–
ν	–	–	0.10 - 0.15	0.250	–	–	0.07 - 0.20	–
ε_u	–	–	-	<0.003	–	–	–	<0.0016 - 0.0026
Type of results	In-situ	Lab.	Lab.	Lab.	In-situ	Ref. of Buildings	Double flat-jack	Lab.

2.4.2 Non-linear kinematic approach

The method stands for the special cases, when the above mentioned box behaviour cannot be activated. In this case the structural performance of a building is defined by the behaviour of local mechanisms (see Figure 14). Based on the equilibrium equation of rigid blocks, the kinematic approach allows the determination of the horizontal action that activates the mechanism (Circolare-C8A). The structure is progressively able to stand with the evolution of the mechanism, until the annulment of the affecting horizontal force, as illustrated in Figure 15.

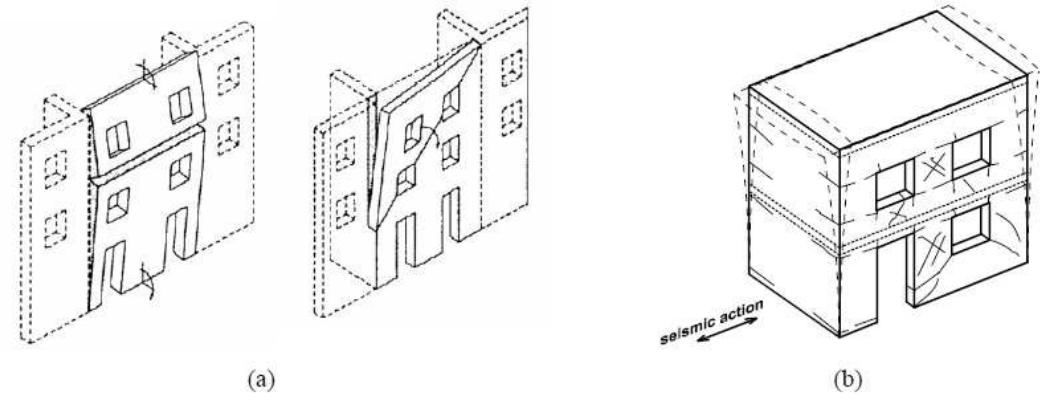

Figure 14: Examples of first-mode "local" damage mechanisms (a, from D'Ayala & Speranza, 2003) and global response mechanism (b).

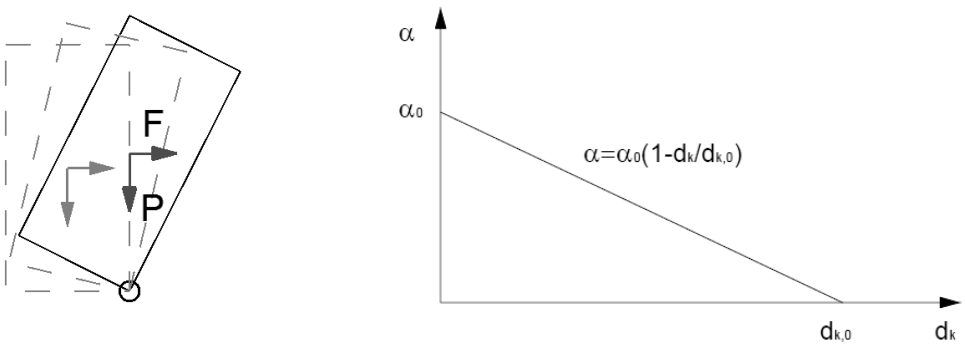

$$F_i = \propto P_i$$

α_0 is the multiplier that activates the mechanism (damage limitation state)

d_k displacement of a suitable control point k of the system (for example the center of the mass)

$d_{k,0}$ displacement of a suitable control point k of the system, for which the multiplier of the horizontal loads is void (α=0)

Figure 15: Application of the kinematic method, and the linear capacity curve

Formulas are available for the safety verification in

- Damage Limit State (DLS): Structural components remain in the elastic range
- Ultimate Limit State (ULS): Structural components suffer repairable damage

Damage Limit State:

The safety verification with reference to the DLS is satisfied when the spectral acceleration for the activation of the mechanism a^*_0 is greater than the acceleration of the elastic spectrum, defined in the point 3.2.6 of the ordinance

$$a_0^* \geq \frac{a_g S}{2{,}5}\left(1 + 1{,}5\frac{Z}{H}\right) \quad (9)$$

where:

Z is the height of the centre of the masses that generate horizontal forces on the elements of the kinematic chain, because they are not effectively transmitted to other parts of the buildings,

H is the height of the whole structure

In case of local mechanisms, the damage limitation state corresponds to the arising of cracking that interests not the whole but only a part of the structure.

Ultimate Limit State:

The ultimate limit state verification of the local mechanism is mandatory, in order to assure the safety with respect of the collapse. This verification can be developed through the following criteria:

a) Simplified verification with structure factor q (linear kinematic analysis):

$$a_0^* \geq \frac{a_g S}{\mathrm{q}} \left(1 + 1{,}5 \frac{Z}{H}\right) \tag{10}$$

where:

Z is the height of the centre of the masses that generate horizontal forces on the elements of the kinematic chain, because they are not effectively transmitted to other parts of the buildings,
H is the height of the whole structure,
q is the structure factor assumed equivalent to 2.

b) Verification through capacity spectrum (non-linear kinematic analysis):

The corresponding formulas can be found in the ordinance chapter C8A 4.2

2.5 Experimental testing of masonry

Recommendations for four-point-bending test of masonry were found in Eurocode (EN-1052-2, 1999). The tests are recommended to be performed vertically. The configuration can be seen in Figure 16 and dimensional details of the specimens can be read in Table 5.

Explanations of signs are listed here:

f_{xd} is the flexural strength of an individual masonry specimen, (N/mm^2)
f_{mean} is the mean flexural strength of the masonry specimens, (N/mm^2)
f_{xk} is the characteristic flexural strength of masonry, (N/mm^2)
h_u is the height of masonry unit, (mm)
k is the numerical factor
l_s is the length of a masonry specimen in the direction of span, (mm)
l_u is the length of masonry unit, (mm)
l_1 is the spacing of the outer bearings, (mm)
l_2 is the spacing of the inner bearings, (mm)
n is the number of specimens
s is the standard deviation of the log values
t_u is width of masonry unit (mm)

Configuration of test and dimensions of specimens:

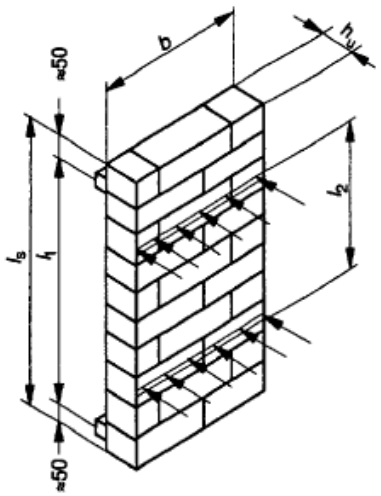

a) Flexural strength for a plane of failure parallel to the bed joints

$b \approx 2l_u$ and $b \geq 400$ mm and $h_u \leq 250$ mm and more than two bed joints in l_2

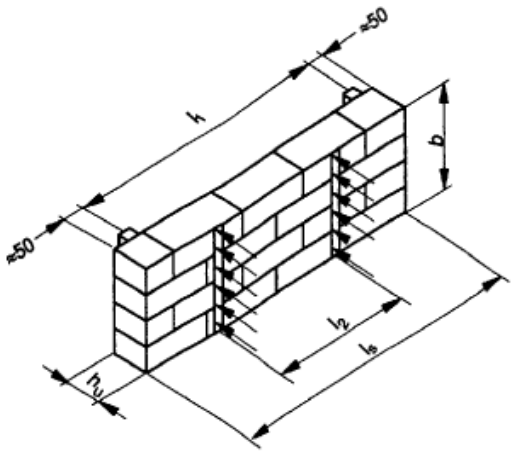

b) Flexural strength for a plane of failure perpendicular to the bed joints

$b \approx 4h_u$ and $b \geq 240$ mm and $h_u \leq 250$ mm and a minimum of one head joint in l_2

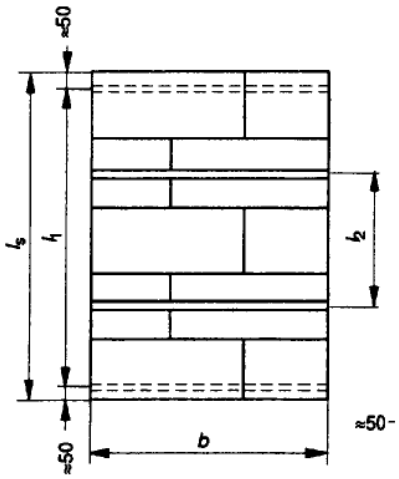

a) Flexural strength for a plane of failure parallel to the bed joints

$b \approx 2l_u$ and $b \geq 400$ mm and $h_u \leq 250$ mm and more than two bed joints in l_2

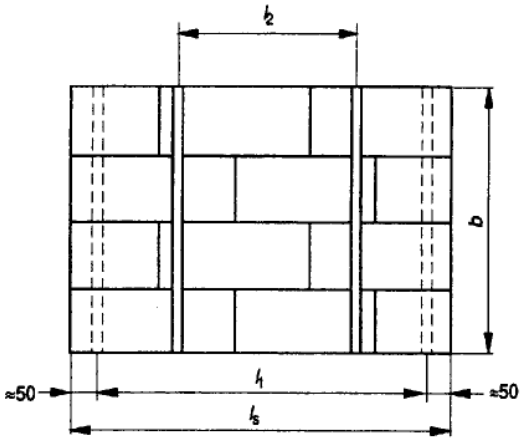

b) Flexural strength for a plane of failure perpendicular to the bed joints

$b \approx 4h_u$ and $b \geq 240$ mm and $h_u \leq 250$ mm and a minimum of one head joint in l_2

Figure 16: Typical examples of masonry test specimens meeting the requirements of Table 5

Table 5: Specimen sizes for testing the flexural strength of masonry (EN-1052-2, 1999)

Direction	h_u (mm)	b (mm)	Additional conditions
Flexural strength for a plane of failure parallel to the bed joints	any	≥ 400 and $\geq 1{,}5\ l_u$	minimum 2 bed joints within l_2
Flexural strength for a plane of failure perpendicular to the bed joints	≤ 250	≥ 240 and $\geq 3\ h_u$	minimum 1 head joint every course within l_2
	> 250	≥ 1000	minimum 1 bed joint and minimum 1 head joint every course within l_2

Loading:

Increasing the flexural stress at a rate between 0,03 N/mm^2/min and 0,30 N/mm^2/min is advisable.

Construction and the curing of the specimens:

Construction of a specimen should not be later than 30 minutes after the conditioning of units. Curing of specimens should be 28 ± 1 day before testing. For lime-based mortars an alternative curing regime and period may be necessary, and this should be specified. Tests shall take place at same age.

Calculation:

The formula for the calculation of flexural strength of each un-strengthened specimen:

$$f_{xi} = \frac{3F_i \max(l_1 - l_2)}{2bt_u^2}\ N/mm^2 \qquad (11)$$

where:

f_{xi} is the flexural strength of the unstrengthened specimen
F_i is the load
l_1 is the spacing of the outer bearings, (mm)
l_2 is the spacing of the inner bearings, (mm)
b is width of masonry wall specimen
t_u is width of masonry unit (mm)

Mean value can be evaluated from the different results.

2.6 Conclusions:

Starting from a general point of view, the state of art review discussed the problems of irregular stone masonry, with special attention to the out-of-plane behaviour and the improvement of flexural capacity. Existing strengthening techniques were listed in relation to the main topic, with an extension to other materials, such as reinforced concrete. The question of applicability was discussed in terms of aesthetics and safeguarding heritage value. As a conclusion, most of the existing methods are not applicable to un-rendered stone masonry walls, as visibly deteriorating techniques cannot be used (e.g.: jacketing, covering, external bonded materials). The insertion of internal tendons was proved to be adequate, but alternative solutions could be necessary. The "reticulatus" technique advocated by A. Borri can solve the aesthetic problems of external strengthening, by the insertion of an irregular grid into the joints of masonry. However, there is a need for experimental investigation of the application as flexural strengthening. Based on the main advantages of "reticulatus" technique, a new flexural strengthening technique is going to be outlined in present thesis work, applicable to irregular and regular masonry walls bearing heritage value.

3

PROPOSAL FOR STRENGTHENING TECHNOLOGY

Introduction:

In the following chapter a reinforcing system is proposed with the aim of increasing the out-of-plane bending resistance of stone masonry walls and reducing visual impact on structure. First the general aspects of the system are discussed. Than a detailed description of the comprised elements are given.

3.1 General description of system

Considering the key aspects of the “reticulatus” (Borri, et al., 2011), an external strengthening technique is proposed for the flexural strengthening of historic masonry. The reinforcement is chosen in a way to be able to follow the joint texture in shallow depth, and to adapt even 90° in intersections of joints (see the sketch of the technique in Figure 17). With appropriate refilling of joints, the reinforcement is hidden, and no visual damage is done on the structure.

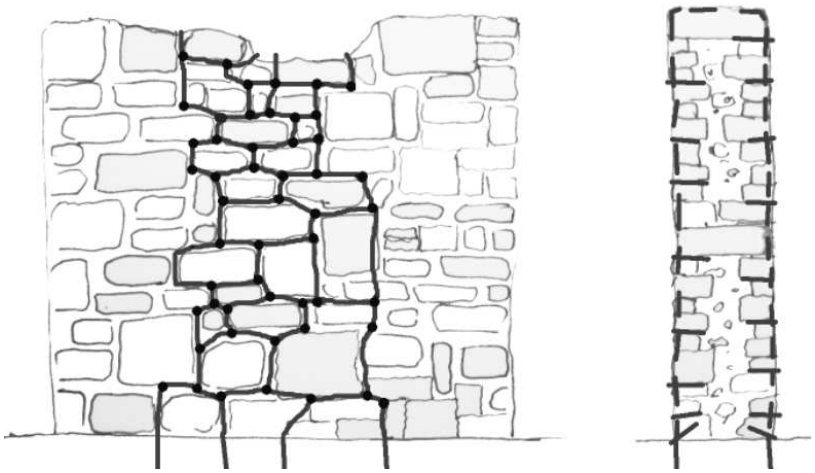

Figure 17: Implementation of “reticulatus” as flexural strengthening technique

The system includes the following steps in application

- Removal of the mortar from the joints in a depth of 2 to 3 cm, to be able to embed the reinforcing grid (see it on Figure 18);

Figure 18: cleaning of joints with hammer driller

- Introduction of helical stainless steel needles in masonry cross joints (where horizontal and vertical joints meet). Before the application of needles a pre-drill is made with a diameter smaller than the diameter of the heli-needles, in order to make the insertion easier. Subsequently the connectors are inserted by hammering with a device designed for this purpose;

- The end of the needles close to the wall surface, is equipped with a head which allows the passage of cables or ropes (see Figure 19);

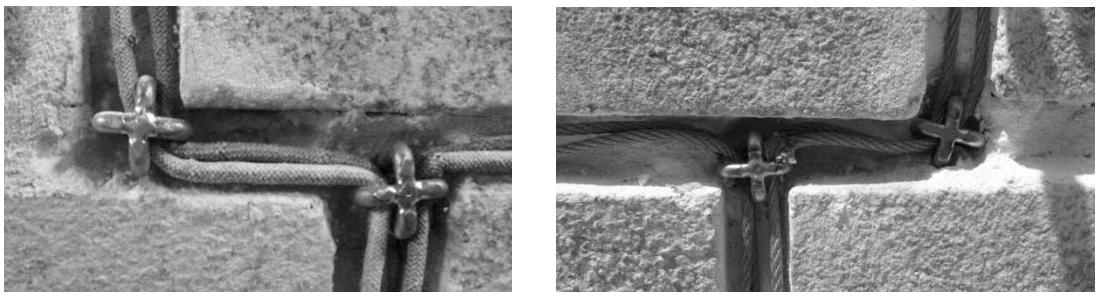

Figure 19: Synthetic and wire ropes passing in the joints

- The cables / ropes together with the special connectors are creating irregular, distributed armour in the joints. The cables have 2 or 4 mm in diameter, in order to be flexible enough to follow the mortar joints and adapt angles of 90°. The cables should be placed to provide the desired orientation for a better resistance against bending stresses;

- After the application of cables, all joints are repointed with the appropriate mortar, so that the reinforcement system would not be visible.

When the walls - reinforced with this system - are subjected to out-of-plane bending forces, the cables / ropes will work in tension. The adaption of helical rods for anchoring the cables is expected to improve the efficiency.

The main characteristics of this system are:

- cables can be applied on both sides of the wall, so the strengthened structure can resist positive as well as negative bending moments;

- As the reinforcement is placed near surface, the useful height of a bending resistant cross section is quasi equivalent to the thickness of the wall;

- The required works are expected to be simple to perform, equipment is easy to handle, and does not require skilled labour;

- The invasiveness of the technique is superficial and only affecting joints, similarly to a shallow structural repointing.

- Reinforcement is not visible after repointing;

- The authenticity of historic building is safeguarded;

3.2 Constituents of system

The head of helibars:

Mortar joints of stone masonry walls can be quite narrow. In case of regular carved stone blocks 2 cm spacing is usual. Hence it is important to optimize the shape of the head of the heli-bars, in order to ensure the possibility of insertion and that it would not exceed the plane of the wall surface after application. A cross shape was designed as it can be seen in Figure 20. The shape was optimized to be rounded to provide easier passing, and more space for cables. The rounded edges are also reducing the probability of damage in wires.

Figure 20: Final form of helihead with rounded edges

The helibars:

The helical connector element (see it on Figure 21) can easily penetrate into the mortar due to its special shape. This attribute has been tested on masonry walls in the Laboratory of Structures at University of Minho. Drill holes with a diameter smaller than the connector element were made previously on the wall, Then the helibar's were inserted into the drill hole. The bars could penetrate in a rolling way by simple hammering.

Figure 21: Prototypes of heli-needles: rounded head evolution (a) and original sharp edged head (b). Rectangular cross-section of a ϕ8 helibar (c)

In Chapter 4 - section 4.3 optimization of pre-drilling diameter can be found. Evaluation was based on the comparison of workability and mechanical behaviour of final configurations through experimental pull out tests.

Device for insertion:

For the maximization of simplicity and to avoid damage of the equipment caused by hammering, a new hammer head was proposed. The device consists of a connector part, through which it is applied to the hammer pistol, and a conical head, which is free to rotate with the helibars in the connector part, during the insertion. The special hammer head has the shape and dimensions to allow the helibar to be easily inserted and trapped in it (see representation on Figure 22). The hammer head is also adequate for the full insertion of the helibars, allowing the connectors to be hidden in the joints, as you can see it on Figure 23.

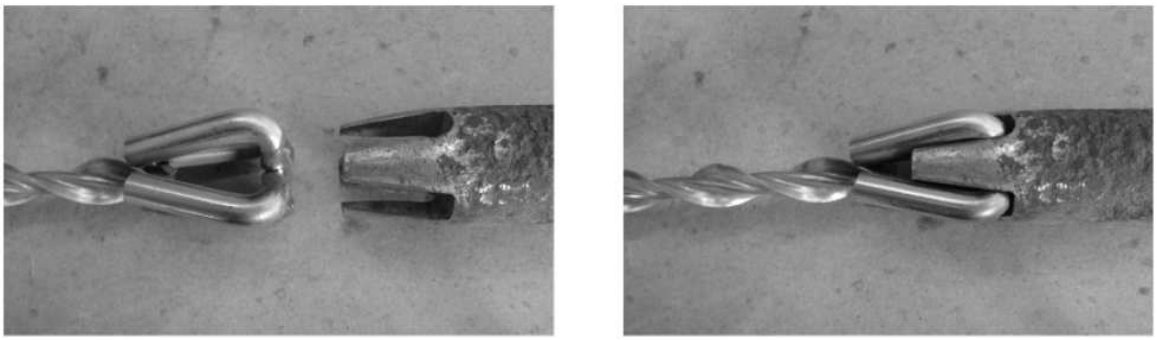

Figure 22: The connection of prototype hammerhead to the anchoring helibars.

Figure 23: Insertion of helibar with the application of drillhead prototype

The structural grid:

Two types of materials were introduced to form the structural grid in the mortar joints. Stainless steel cables and synthetic ropes can be both applicable in terms of workability. As general recommendation, the wires should be straight lined between two connector elements, in order to be immediately activated when out of plane forces are affecting the target wall. To reach this immediate activation, pre-stressing of the ropes might be necessary. Stainless steel wire grid applied to a test specimen can be seen on Figure 24.

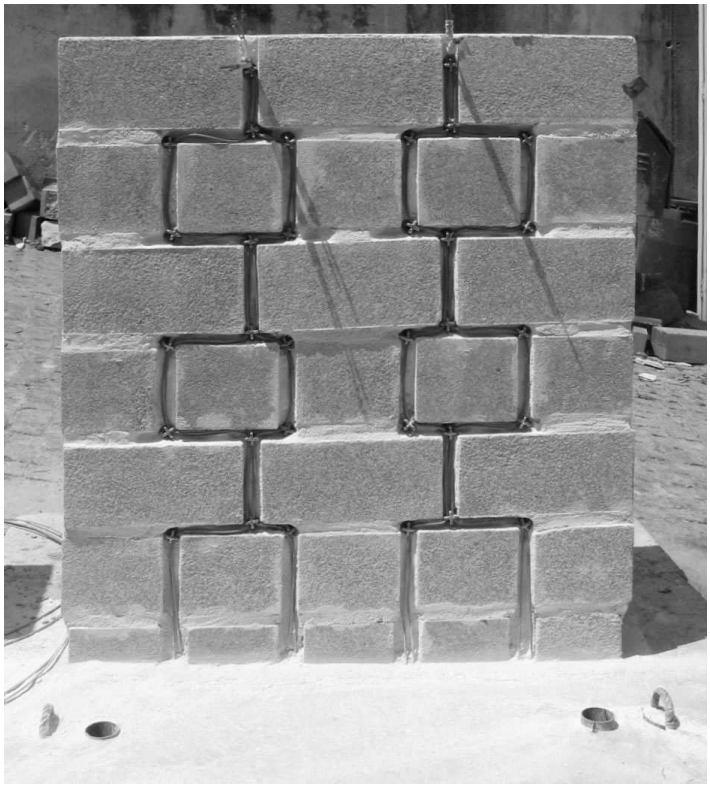

Figure 24: Stainless steel wire grid applied in masonry joints

Starting and finishing connections are playing important role in the efficiency of the method, as forces are expected to be transmitted to the wall there. The bottom connection must be placed lower than the height of the expected plastic hinge. Top connections can be made on both sides of the wall, or – with additional elements for protection on edges – the reinforcement can be passed over the wall and integrate the two sides. The chosen connection types have to be strong enough for load transition. Helibars, injected insertions, or other appropriate connections can satisfy this function.

4

MECHANICAL CHARACTERISATION OF CONSTITUENT ELEMENTS

Introduction:

In the following chapter, experimental investigation on individual constituents can be found. The results were used to conclude on the further development of the proposed strengthening technique, and to make the preliminary calculations for the scaled wall tests. Tensile tests of stainless steel cables; tensile tests of synthetic ropes; pull-out tests of helibars from mortar cylinders;

4.1 Direct tensile test of stainless steel wire ropes

In order to characterize the mechanical properties of wire ropes and to evaluate the efficiency of the hand-made connection types, 13 specimens were subjected to tensile test. The main properties that were to be extracted from the experiments were the tensile strength (f_y ; f_u), corresponding equivalent strains (ε_y ; ε_u) and the elastic modulus (E) of the different cables. During the investigation two series of tests were undertaken related to connection types (single sleeve; doubled sleeves). The results indicated no significant difference between mechanical properties. Therefore the number of aluminium sleeves proved not to influence the strength of any specimen. Figure 25 shows the different connection types, defined by the number of sleeves, and Table 6 lists the specimens for testing.

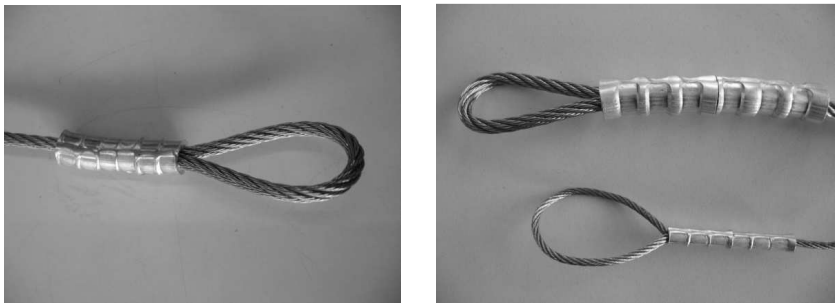

(a) (b)

Figure 25: Single sleeve connection type / CA4 (a); Double sleeve connection type / CA2-CA4 (b)

Table 6: test matrix for cable tests

Name	Diameter [mm]	Number of sleeve	Number of tests	Reference length [cm]
CA2	2	single	3	30,5
CA4	4	single	3	30,5
CA6	6	single	3	37,7-38,3
CA2#2	2	double	2	32-33
CA4#2	4	double	2	34-34,5

Results:

Failure happened in the connections without exception, as it could be expected. The manufacturing of the connection introduces imperfections such as strains and perpendicular confining compression to the fibres, due to deformed sleeves. Such imperfections are creating weak-points determining the localization of failure. However, the breaking forces appeared to be higher than the nominal values for each specimen. As it can be seen in Figure 26 the force-deformation diagrams can be divided into a linear and a non-linear part. The non-linear part allows greater deformations, but is not related

to plastic behaviour. A possible explanation is the sliding of the weave of fibres before failure. See the failed specimens on Figure 27.

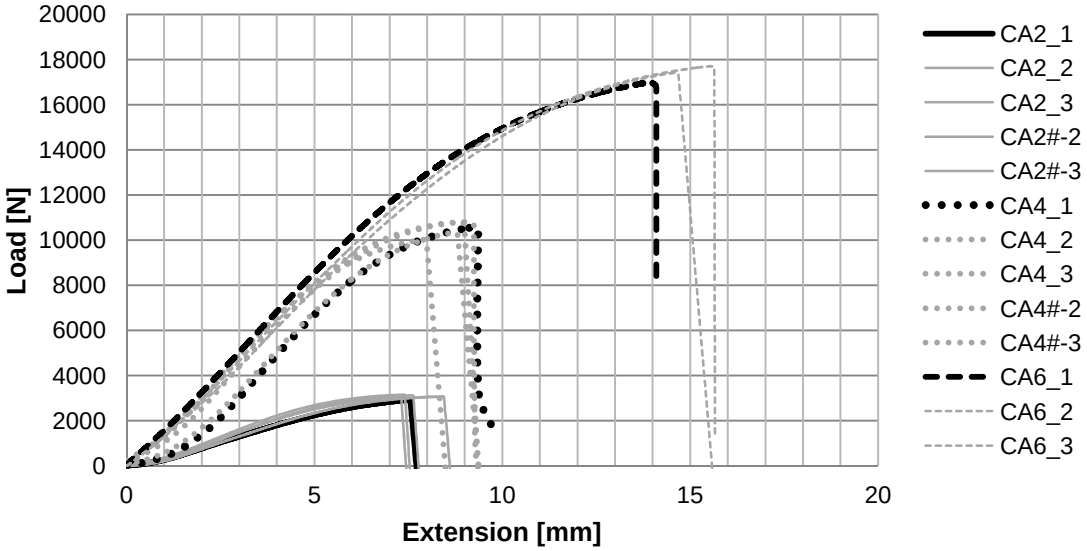

Figure 26: Load-Extension diagram of wire rope tensile tests

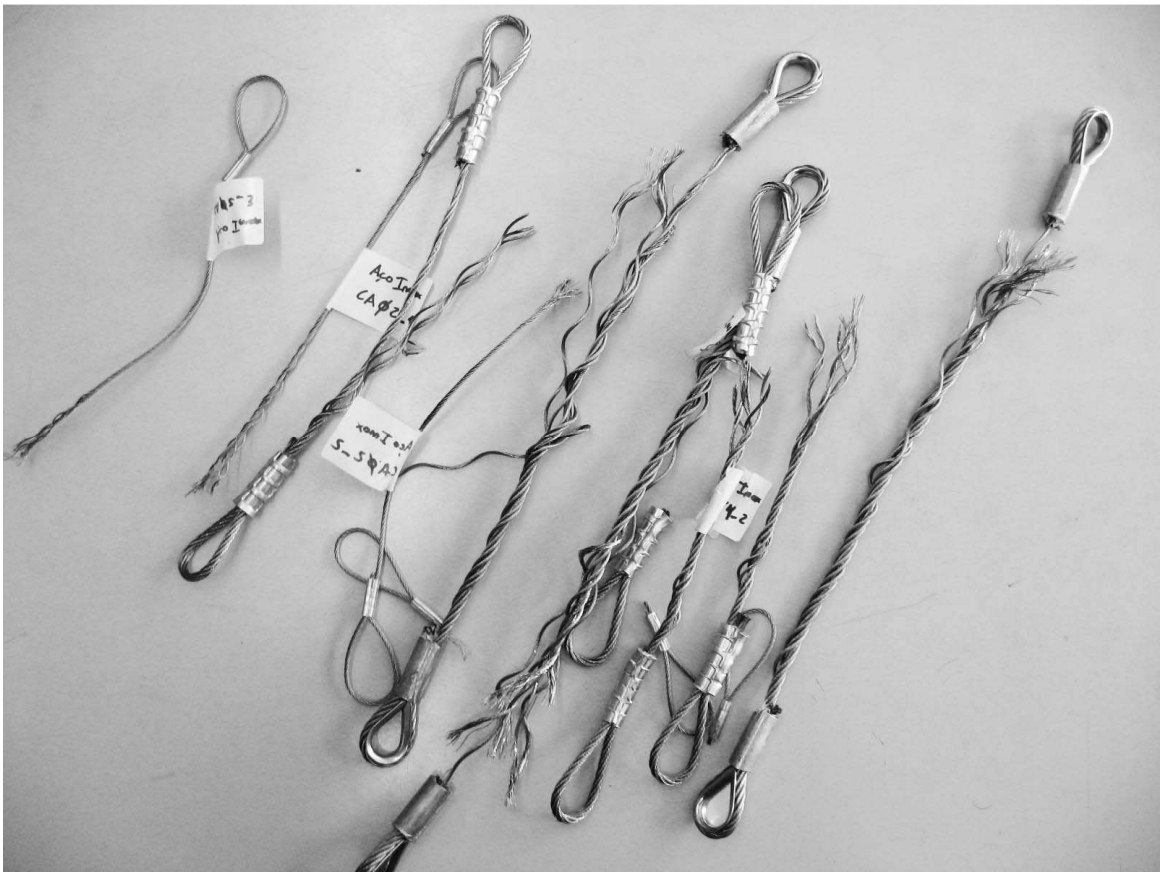

Figure 27: Failed stainless steel wire rope specimens

The mean values of mechanical properties were extracted, and are listed in Table 7. The Young Modulus (E) was taken between the 20% and the 50% of the nominal strength as it is recommended in the ASTM standards for testing wire ropes (A931-96, 2002) . See the corresponding graphs in Figure 28.

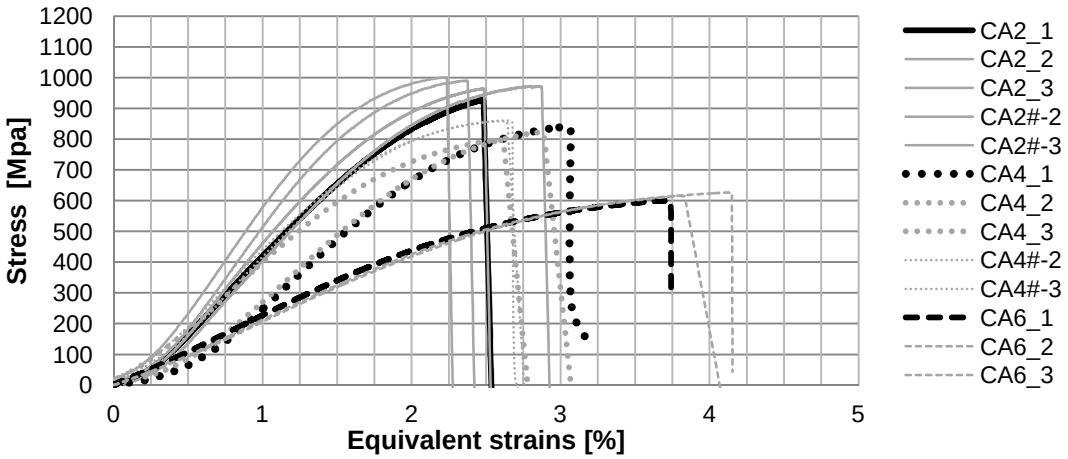

Figure 28: Stress – Strain diagram of wire rope tensile test

Table 7: Mechanical properties of cables

Name of specimen	Elastic limit			Ultimate limit			
	E [N/mm^2]	ε_s [%]	f_y [N/mm^2]	ε_{su} [%]	f_u [N/mm^2]	P_u [kN]	Nominal P_{max} [kN]
CA2-CA2#2	53000	1,350	713	2,55	955	3,00	**2,24**
CA4-CA4#2	44000	1,600	711	3,00	820	10,3	**8,94**
CA6	22300	2,197	490	4,00	614	17,3	**14,0**

Remarks:

The tests can be considered as successful despite the failure in connections, since the results appeared to be better than the nominal values, and the graphs are not showing the signs of early failure.

It was revealed that different cables have significantly different mechanical properties.

The influence of doubled sleeves on the mechanical properties was also investigated and turned out not to affect the results.

Mechanical behaviour of stainless steel cables has non-linearity, but not due to plasticity.

4.2 Direct tensile test of synthetic ropes

Different types of synthetic ropes were subjected to direct tensile test in order to analyze their applicability on masonry walls as alternative reinforcement. Tests were done without the utilization of resins or adhesives, since the application would involve only dry connections (looping and tying).

Synthetic Ropes with Carbon fibre Core (SRCC):

The first series of tests were undertaken with Synthetic Ropes with Carbon fibre Core (herein SRCC-2 and SRCC-4 respecting the diameter) designed by the Department of Civil Engineering at the University of Minho. In case of SRCC-2 the uni-direction inside core is made of 4x1600 tex HTS 5631 carbon fibres protected by 20 yarns of weaved polyester - 10 tex (see Figure 29). SRCC-4 contains 12x1600tex HTS 5631 carbon fibre yarns protected by 20 yarns of weaved polyester - 10 tex.

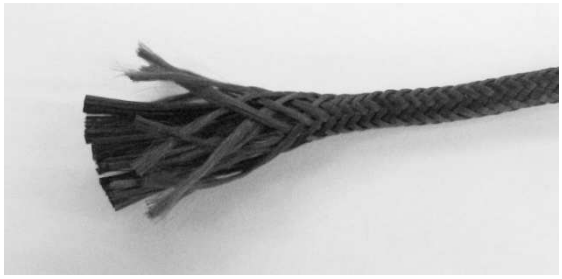

Figure 29: Synthetic rope with carbon fibre core (SRCC-2)

SRCC ropes were designed to be competitive with 4 mm diameter stainless-steel cables in terms of mechanical properties and workability (flexibility and diameter dimension). For experimental investigation SRCC-2 and SRCC-4 specimens were prepared. The reference length of the specimens was set to 100 mm (see physical parameters in Table 8).

Table 8: Physical parameters of SRCC test-specimen types

Name	Equivalent diameter [mm]	Reference length [mm]
SRCC_2	2	100 mm
SRCC_4	4	100 mm

The vulnerability of carbon fibre core against sharp folding, or small diameter curving was expected to be a great disadvantage in terms of workability. For efficient application, special connections might be needed.

Synthetic ropes used in mooring:

A second series of tests were done with high strength synthetic ropes used mainly in mooring (herein MSR). One specimen can be seen in Figure 30. The polymer chords are weaved to form a strand, which has extremely high strength without the usage of inside core (6 mm diameter →19,8 kN). As a consequence, the rope is more resistant to sharp folding and curving, resulting in a more workable product, leaving the chance of creating simple, handmade connections. Physical characteristics are listed in Table 9.

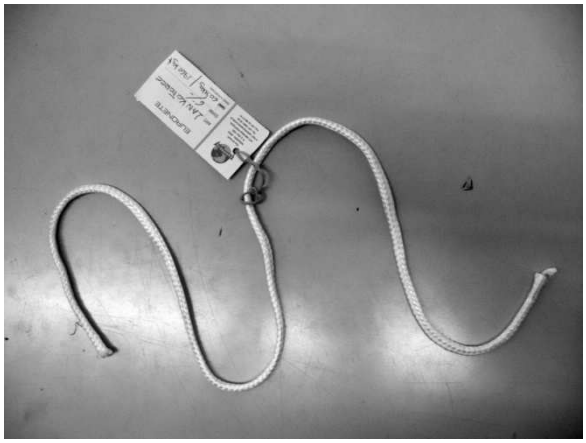

Figure 30: Flexible, high strength mooring synthetic rope

Table 9: Test characteristics for rope test

Name	Equivalent diameter [mm]	Reference length [mm]
MSR1	6	212 mm
MSR2	6	120 mm
MSR3	6	90 mm

A special type of knot was tested in connections with the workable material, as it was able to adapt to folding. The use of knots would increase the workability of the technique, as it is simple to do, very fast, and provides good load transition. See the representation on Figure 31.

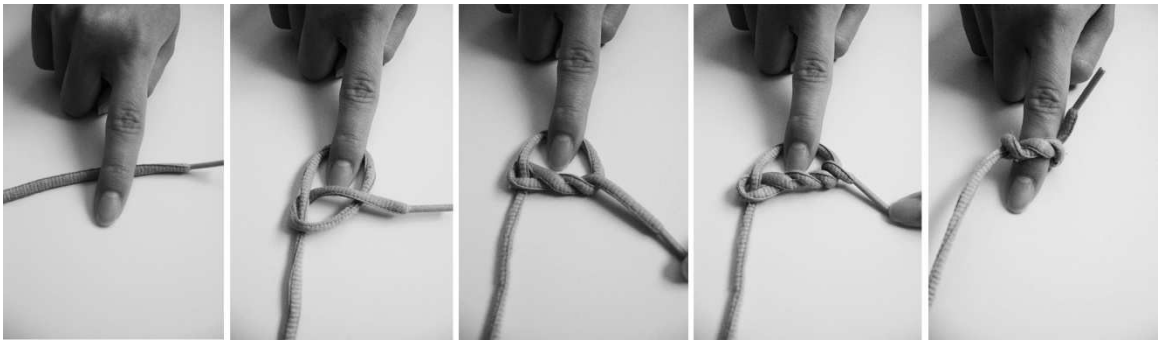

Figure 31: Procedure of knotting the special connection type

Experimental results and evaluation

The resultant graphs of the experiments are given in Figure 32.

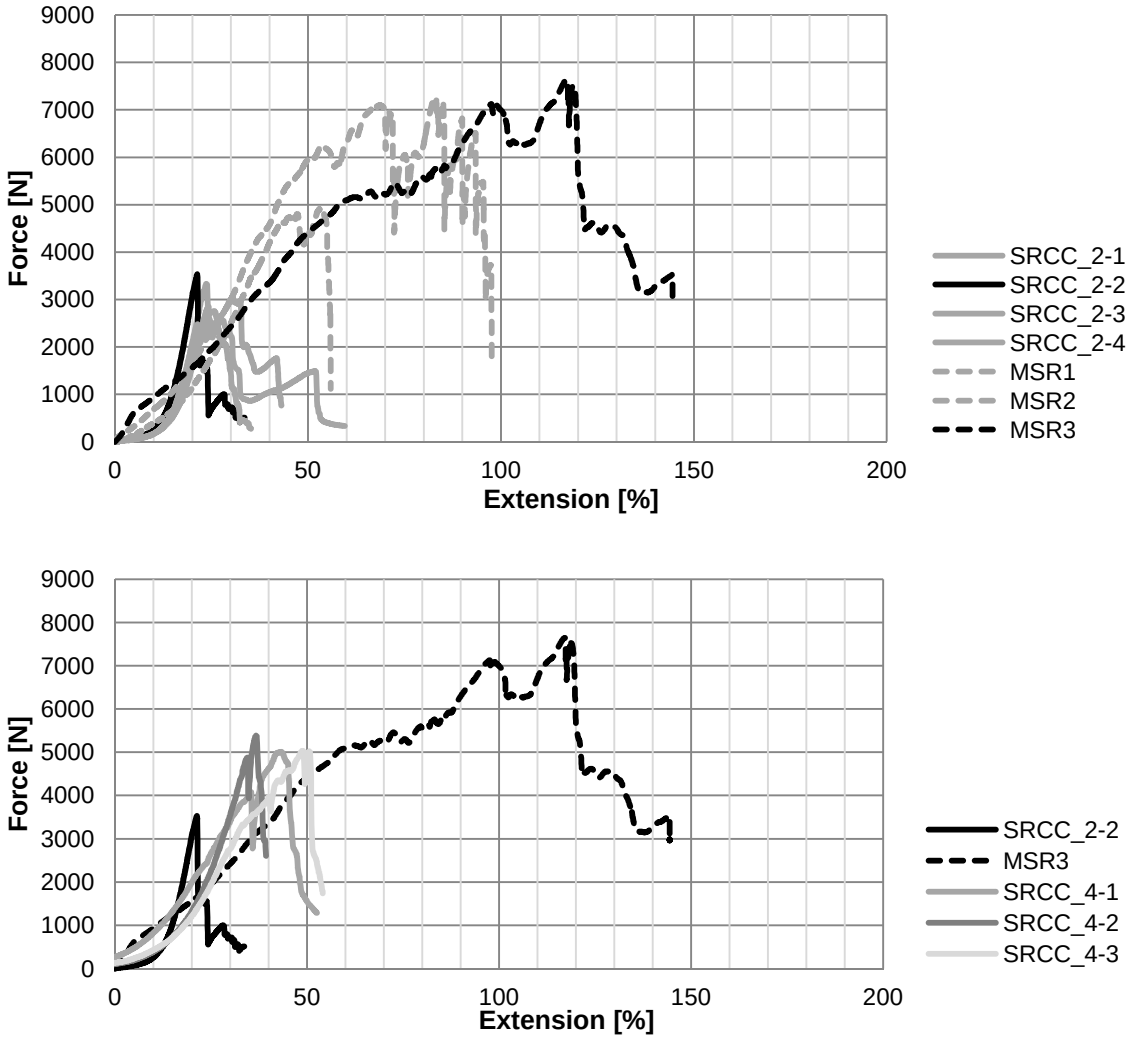

Figure 32: Force-Extension diagrams of synthetic rope tests

The dry connections were vulnerable points in each series of tests. Figure 33 represents the obtained failure loads in percentage, related to the theoretical material and composite ultimate loads. Using dry connections, the results were not closing the real strength of the materials. SRCC-2 reached 20% of the theoretical 15,6 kN; and SRCC-4 provided 11.1% of its theoretical 46.38kN capacity. The MSR reached 32,8 % of its theoretical ultimate load (19.8kN). It is worth noting that dry connections need further development in order to use the capacity of these composites more efficiently.

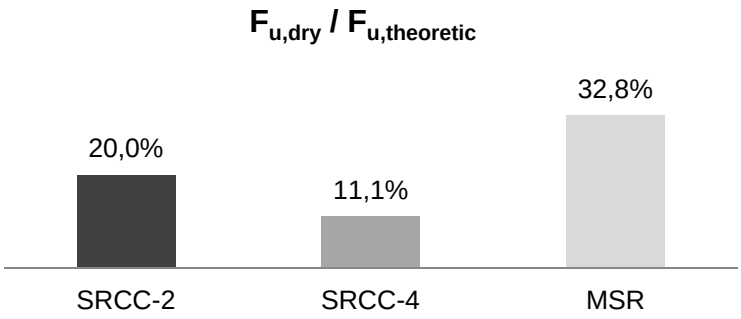

Figure 33: limit of dry connections related to the theoretical capacity

For the proposed application, the SRCC-2 was not proved to be competitive with 4 mm diameter wire ropes, despite its promising theoretical strength (15,6kN). Reaching 3,5 kN as ultimate load, it can be an alternative solution to the usage of 2mm diameter stainless steel cables. The mean stiffness of the composite is 291 N/mm between 30% and 60% of the quasi ultimate load, when the steel cables provide 660 N/mm.

SRCC-4 also provided early failure at 5 kN load during the test compared to its theoretical strength (46.4 kN). The failure was due to the extreme vulnerability of the composite against sharp edges and looping. It can be noted, that increasing the amount of carbon fibre filaments did not provide better results during experimental investigation. The mean value of stiffness was 174,7 N/mm (26,5% of steel cables).

As a conclusion, both SRCC2 and SRCC4 failed to compete with the ϕ4 wire rope in terms of mechanical efficiency. (Note: Stainless steel wire rope is capable of reaching its ultimate capacity (~11 kN) with dry connections).

The use of special knot with MSR caused early failure during the tests. Additional confinement and transversal strains in connection can significantly reduce the strength of the material. The MSR compared to the SRCC provided very low stiffness results. The extracted mean value is 129 N/mm taking into account the initial quasi-linear part of the graphs. The significant difference can be easily represented by comparing the load values at 20% extension. The SRCC almost reaches its peak load (3-3,5kN), while the MSR is only capable of taking 1 kN (as you can see on Figure 32). Due to the low stiffness, and

extremely high deformations, the tested MSR rope cannot be recommended as alternative strengthening for masonry walls.

Pictures representing the test procedures are given in Figure 34; to 38.

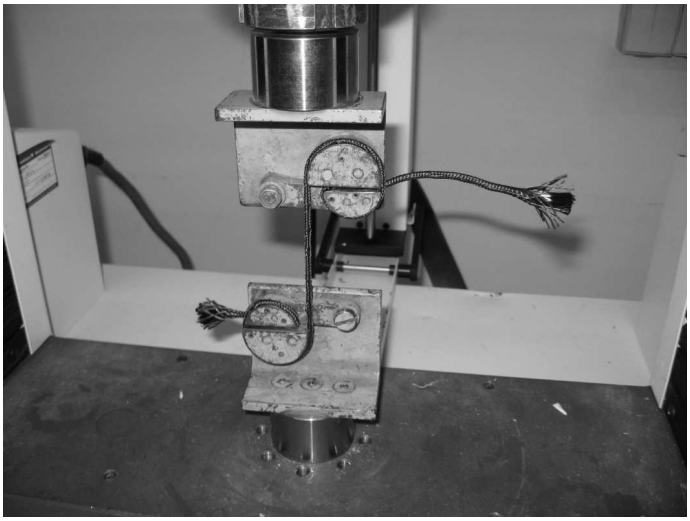

Figure 34: Test apparatus of SRCC experiment

(a) (b)

Figure 35: Failure types of SRCC around the clamps; failure in curving part (a); failure at sharp edge (b)

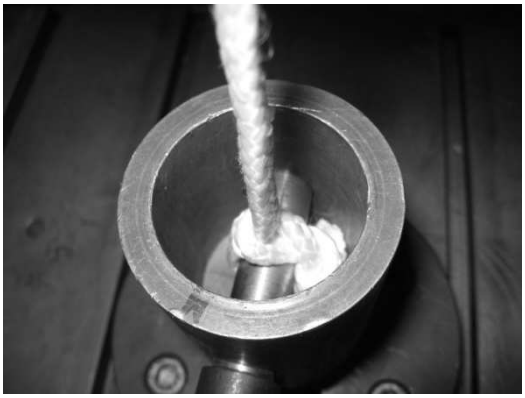

Figure 36: Test set up of MSR

Figure 37: Failed connection

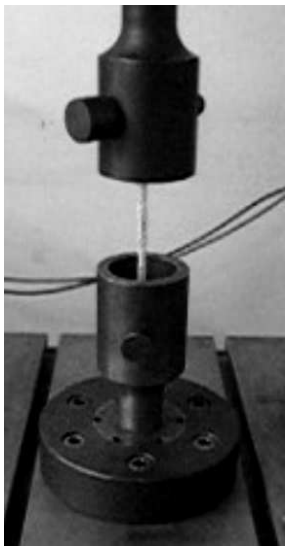

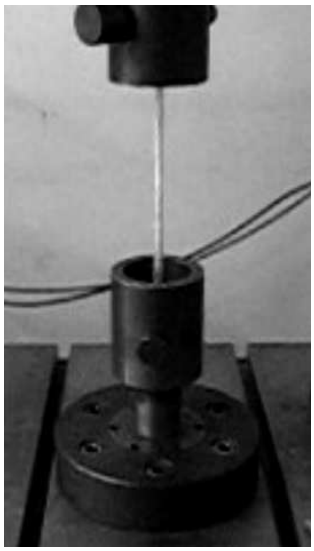

Figure 38: Representation of high deformations of MS / test of specimen n°3

4.3 Pull-out test of helibars

Anchorage force of connector elements was tested by pull-out tests of helibars from cylindrical mortar samples. All together 60 specimens were tested combining different anchorage lengths with helibar diameters and with diameters of pre-drilled holes. The pre-drilled holes were defined by extracting 2 or 4 mm from the diameter of the helibars. Here the "–2 mm" pre-drill is going to appear as weak bond, and the "–4 mm" pre-drill will be referred as strong bond. An overview of combinations is given in Table 10.

Table 10: Overview of specimens for pull-out tests

Mortar cylinder diameter / height [cm/cm]	Anchorage length [relative]	Helibar diameter φ [mm]	Pre-drilled hole diameter [mm]	Number of specimens
5 / 15	8φ	8	6 (weak bond)	5
			4 (strong bond)	5
		10	8 (weak bond)	5
			6 (strong bond)	5
	12φ	8	6 (weak bond)	5
			4 (strong bond)	5
10,5 / 21,5	12φ	10	8 (weak bond)	5
			6 (strong bond)	5
	20φ	8	6 (weak bond)	5
			4 (strong bond)	5
15 / 30	20φ	10	8 (weak bond)	5
			6 (strong bond)	5

Curing time and specimen preparation:

The mortar cylinders were made with Weber Tradition® ready-mixed lime mortar. The amount of water was kept precisely following the instructions in order to limit imperfection factors. Each new mix was marked and documented for later evaluation on the influence of mortar mixture. The cylinders were let to cure exactly 28 days before tests.

Pre-drilled holes with different diameters and length were prepared before the insertion of the corresponding helibars. For the insertion simple hammer was used, and the procedure proved to be workable (as you can see in Figure39). The helibars easily rolled themselves into the mortar cylinders due to their special shape.

Figure39: Preparation of specimens: insertion of helibars by hammering

Before the insertion the helibars were equipped with an aluminium cylinder on the free end to create the appropriate connection to the grips during the procedure. Below the cylinder a cubic element was applied to receive and support the transducers for displacement measure. Resins were used as adhesives to fix these additional elements (see representation on Figure 40).

Figure 40: Representative helibar prepared for pullout test

Test setup:

The tests were undertaken in the Laboratory of Structures, University of Minho. An actuator with 50 kN capacity was attached to reaction frame, and the grips were chosen to fix the helibars. Two Linear Variable Differential Transformers (LVDT) fixed on the helibars; one load-cell and one displacement controller in the actuator were used. See representation of instrumentation on Figure 41 and Figure 42.

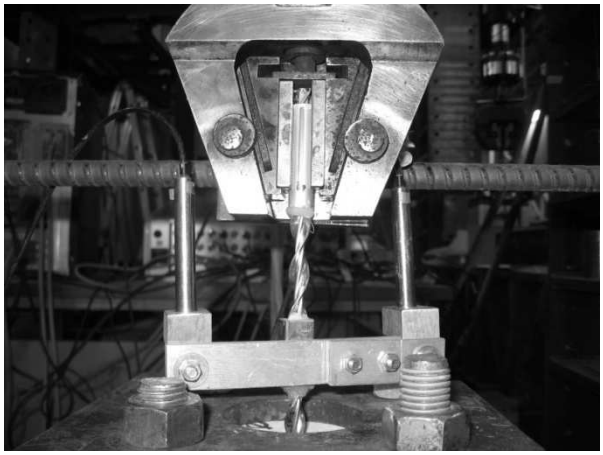

Figure 41: Connection of gripping plates and LVDT-s to the specimen

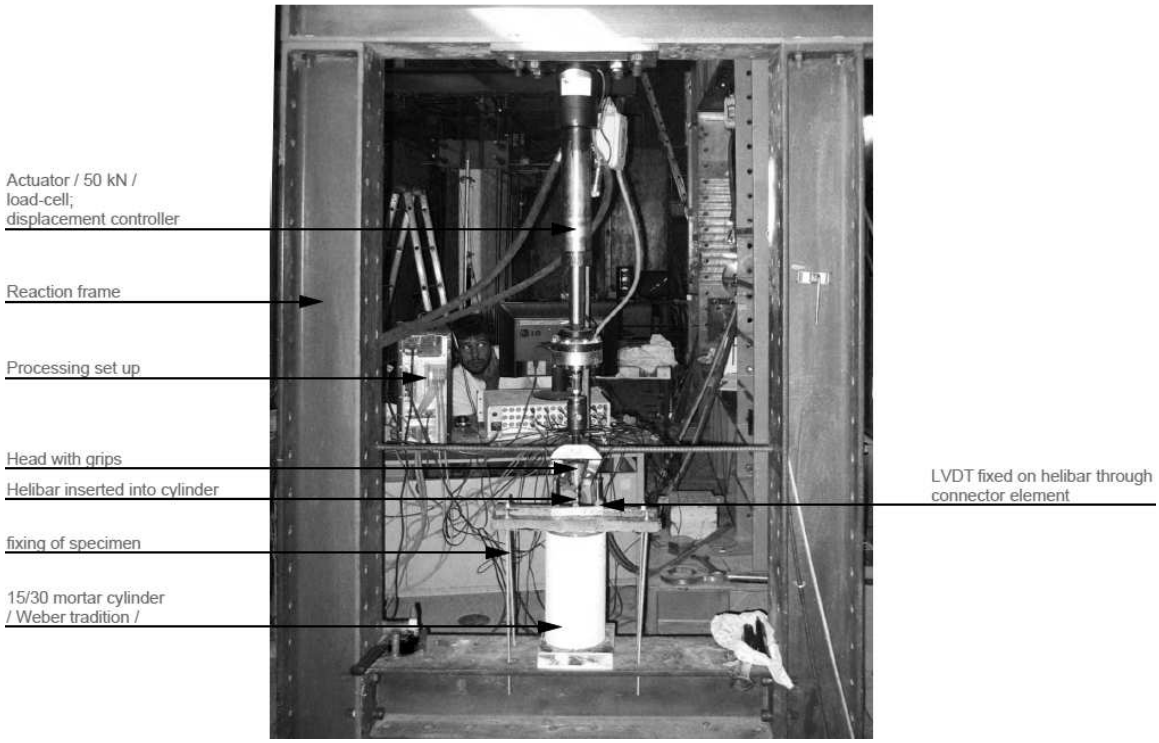

Figure 42: Final test setup with detailing

Procedure:

Displacement control was used during the experiment in order to obtain the full curve of the bond behaviour. The displacement velocities were chosen to obtain maximum force between 1 and 3 minutes as it is recommended in ASTM standard for pull-out tests on concrete cylinders (E488-96, 2003). Final duration of procedure was between 4 and 10 minutes related to different characteristics of test objects.

Results:

Force – Displacement envelopes were obtained by keeping the predrilled-hole diameter as variable. See the corresponding figures from Figure 43 to Figure 48. Comparing the diagrams it can be noted, that the anchorage length and the diameter of the predrilled hole influenced the results. The greater diameter of the helibar did not contribute significantly to develop higher bonding strength. However, greater deformability of ϕ8 helibars showed during the tests with higher anchorage lengths (20ϕ8; strong bond). These procedures were stopped due to the significant, rotational lengthening of the anchor (plastic deformation). Same rotational lengthening was observed in 12ϕ8 and 20ϕ10; strong bond tests, but the deformation remained elastic. Significant deformations of ϕ10 mm helibar showed exceptionally during the first test of 20ϕ10; strong bond. On Figure 48 the jumping in the graph shows the point of the LVDT removal, due to dangerous torsion movement.

It is worth noting that the envelopes corresponding to different pre-drills are well separated in the diagrams, except the case of 20ϕ10 (Figure 48), where the envelopes are showing overlapping. It means that the higher anchorage length reduces the effect of pre-drilled hole dimension. In the same diagram, great widths of envelopes are likely due to imperfections caused by the pre-drilling procedure. The significant free length of the driller was accompanied with instable out-of-axis movement. This imperfection caused small incontrollable increase in the diameter of the drill-holes.

For comparison, see the mean values of maximum pullout forces and stiffness's in Table 11.

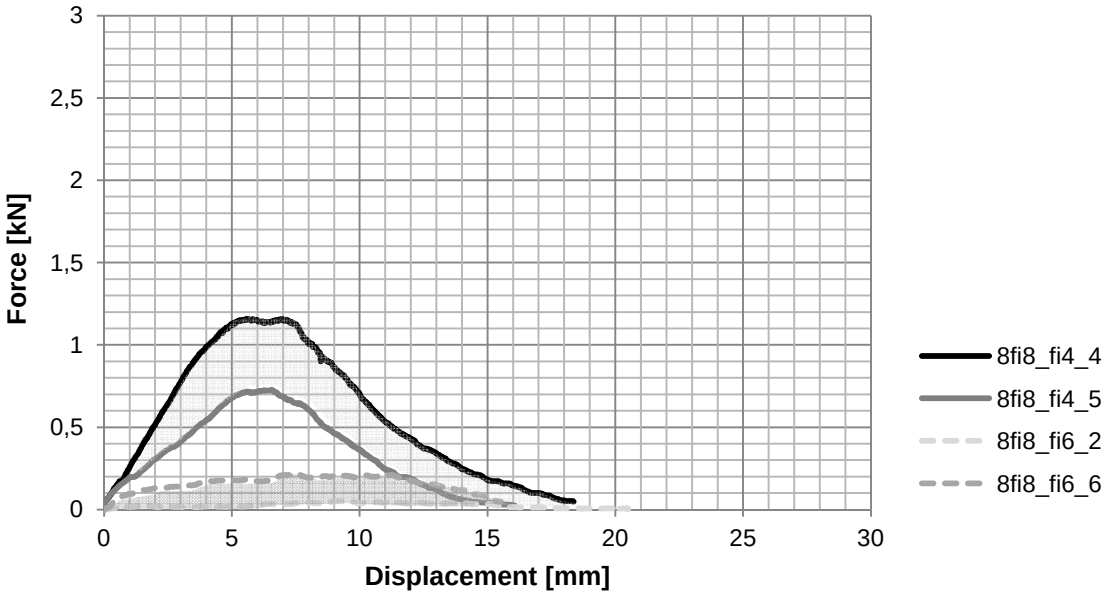

Figure 43: Comparison of Force-Displacement envelopes for 8ϕ8 anchors with two different predrilled holes

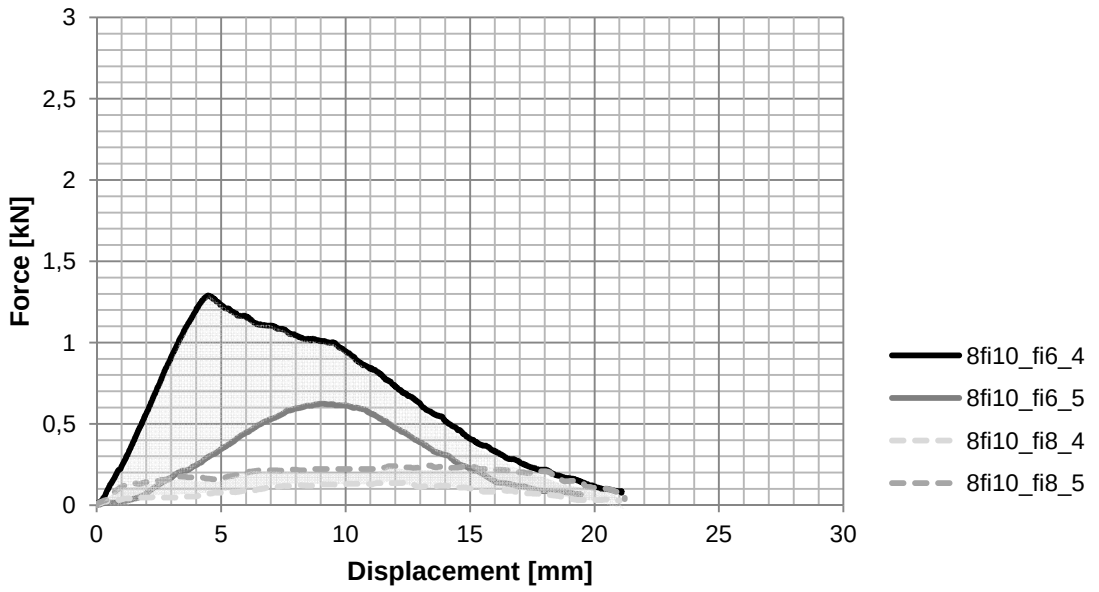

Figure 44: Comparison of Force-Displacement envelopes for 8ϕ10 anchors with two different predrilled holes

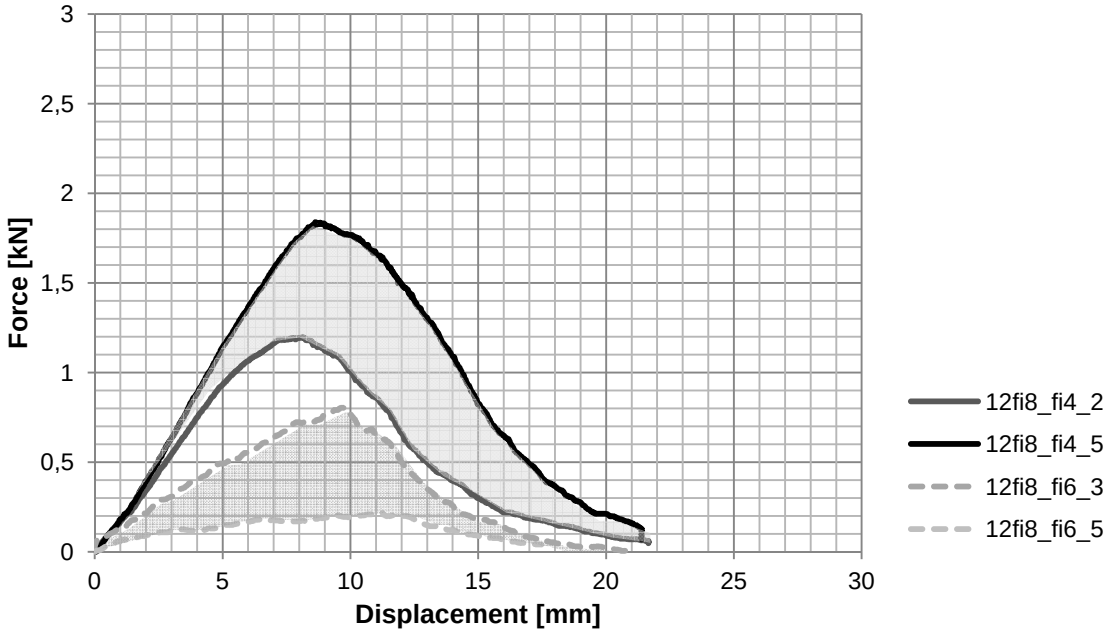

Figure 45: Comparison of Force-Displacement envelopes for 12ϕ8 anchors with two different predrilled holes

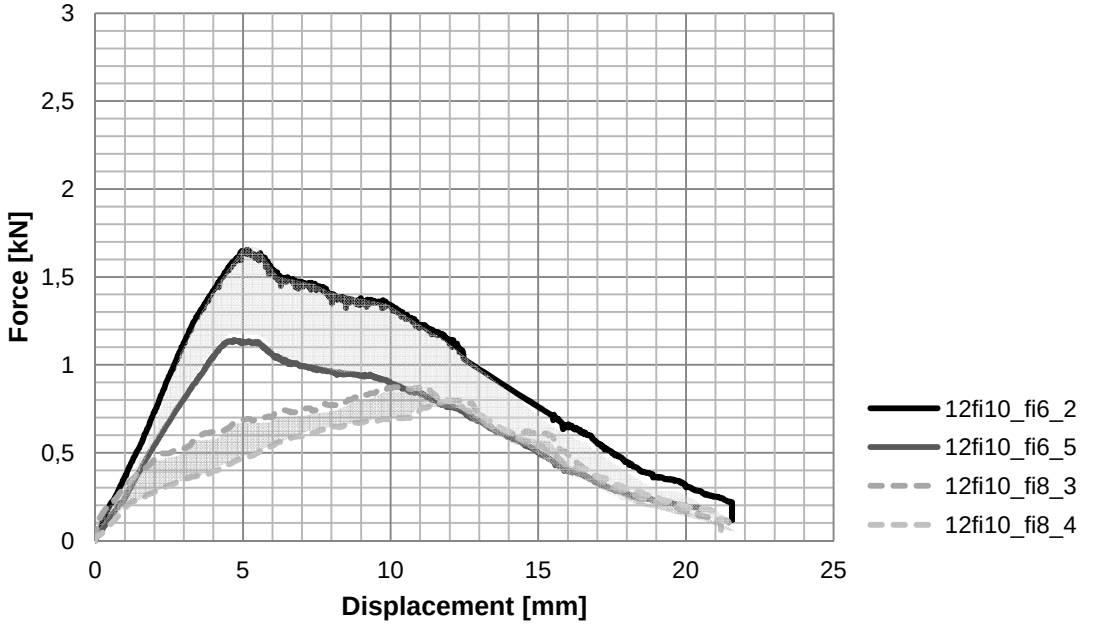

Figure 46: Comparison of Force-Displacement envelopes for 12ϕ10 anchors with two different predrilled holes

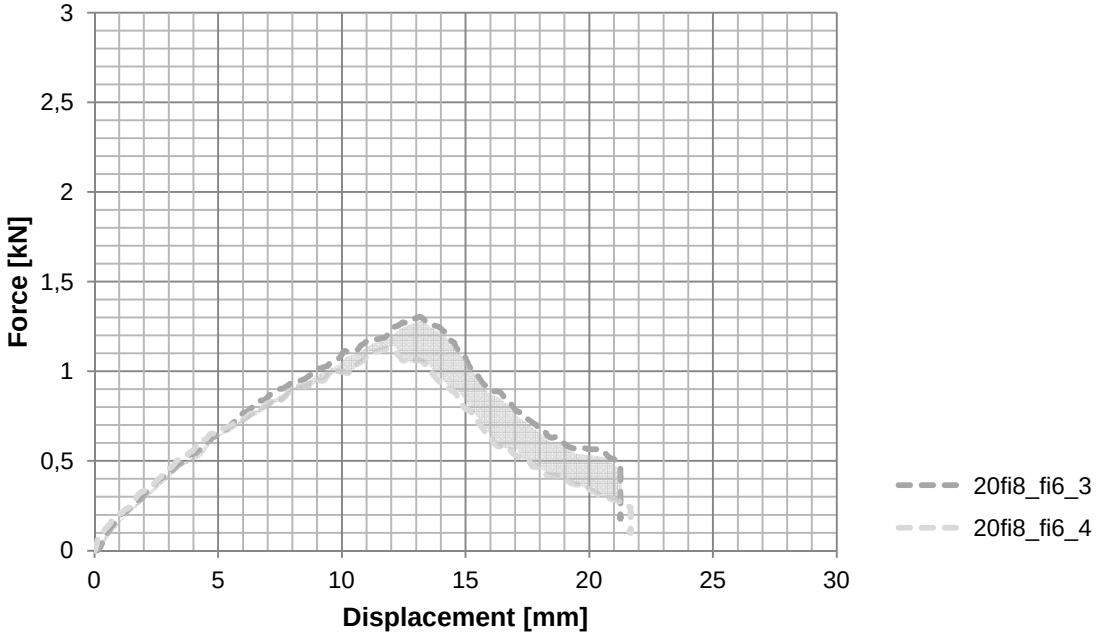

Figure 47: Comparison of Force-Displacement envelopes for 20ϕ8 anchors with two different predrilled holes

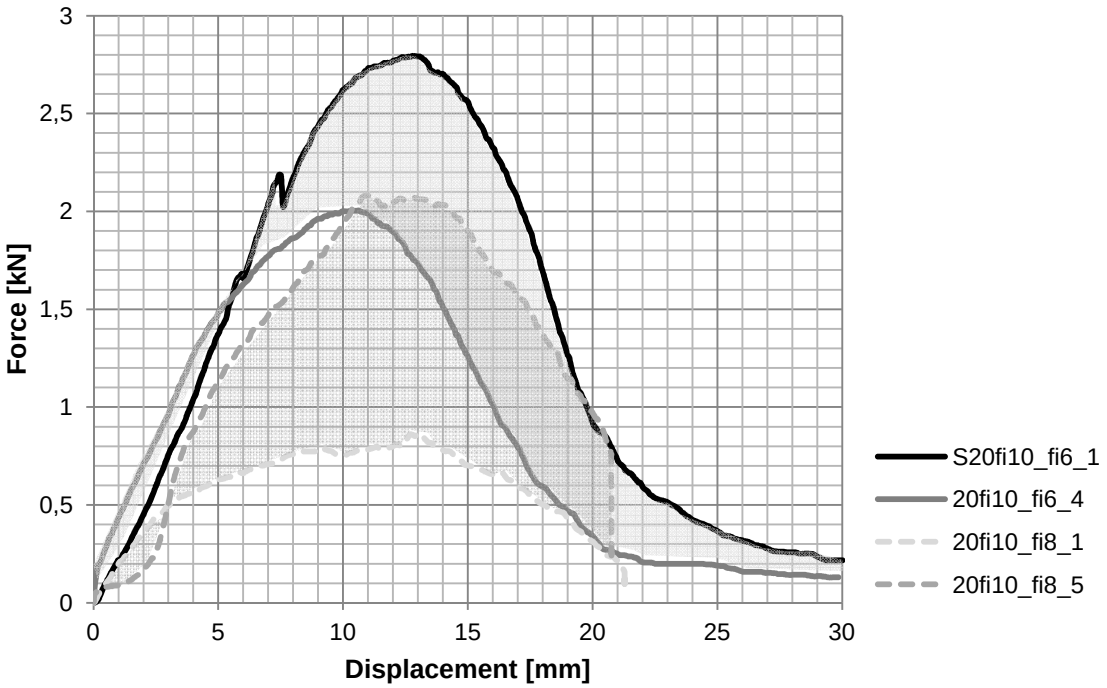

Figure 48: Comparison of Force-Displacement envelopes for 20ϕ10 anchors with two different predrilled holes

Table 11: Corresponding bond forces of anchors

Anchorage length	Strong bond (pre-drill: –4)		Weak bond (pre-drill: –2)	
	Ultimate Force [kN]	Stiffness [N/mm]	Ultimate Force [kN]	Stiffness [N/mm]
8ϕ8	0,935	176,7	0,143	-
8ϕ10	0,903	181,9	0,211	-
12ϕ8	1,364	193,8	0,323	55,79
12ϕ10	1,482	294,6	0,602	-
20ϕ8	1,955 (note: plastic def.)	-	1,065	97,42
20ϕ10	2,480	293,9	1,583	176,6

On Figure 49 linear interrelation between force and anchorage length is represented. The wider pre-drill does not affect the level of increase (0,013 for strong bond and 0,012 for weak bond in case of ϕ10 mm helibars); but causing a descending of the linear graph. In case of helibars with 8 mm diameter the level of increase seems to match. However, the failure of tests with 20ϕ8 specimens did not allow the evaluation of the level of increase.

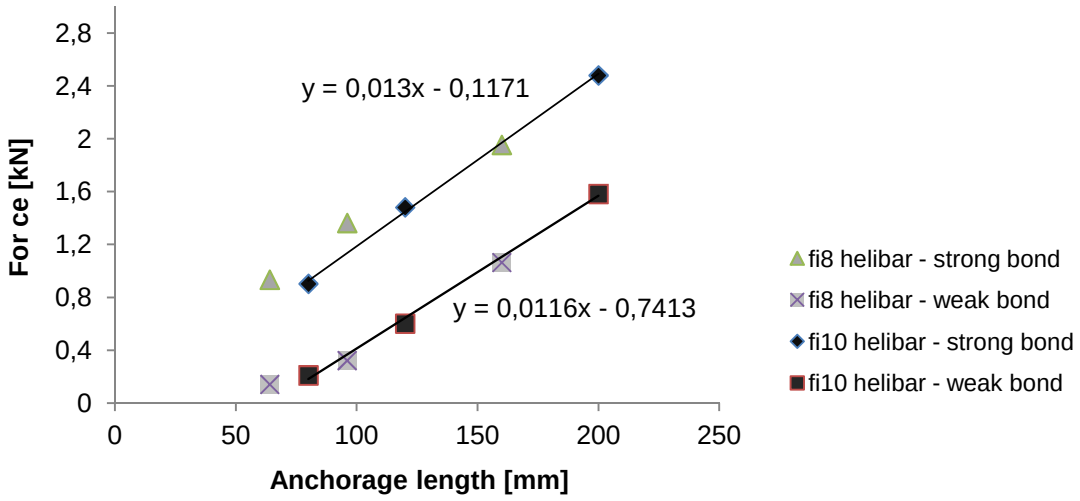

Figure 49: Interrelation between mean anchorage forces and anchorage length

Remarks:

The helical shape of the special bar allows a rotational movement not only during insertion, but also during the pull-out actions. In the experimental investigation these rotations were stopped with the grips, but in reality this effect can reduce the observed pullout strength. Rotational lengthening happened and caused plastic deformation in case of ϕ8 mm helibars, when high de-bonding forces were possible to be applied (20ϕ8, strong bond).

The anchorage length and the diameter of the predrilled hole influenced the results. The greater diameter of the helibar did not contribute significantly to develop higher bonding strength.

The diameter of the prior drill hole did not influence the difficulty in the insertion of the helibars. Since the results are significantly higher with strong bond type it is not advisable to use bigger drill holes.

$$d_{\text{pre-drill}} < \phi_{\text{helibar}} - 4 \text{ mm}$$

Further investigation on the pullout performance without pre-drilling is recommended, since the adaption of hammering machine allows easy insertion. This workability issue was discovered after the pullout tests.

The results are acceptable for the proposed strengthening technique, allowing evaluation of the strength of the anchor in axial direction. However, the participating anchors will be subjected to greater out-of-axis actions. In order to evaluate the complex behaviour further investigation is needed on out-of-axis performance.

5

ANALYTICAL INVESTIGATION

Introduction

In the present chapter an analytical study was prepared to investigate cost efficiency issues, and to define the amount of reinforcement to be applied on wall specimens for bending tests. It also aims to provide an analytical guide for designing the proposed technique for future practice.

5.1 Cost efficiency estimation

A preliminary study was prepared to compare the mechanical performance and cost efficiency of different strengthening materials that are used for external strengthening in practice. In Table 12, a list of reinforcing materials can be seen with physical and mechanical parameters. The "applicable strength / weight ratio" of these materials was introduced and used for further comparison (see Figure 50).

Table 12: Comparison of reinforcing materials; Introduction of applicable strength/weight ratio

Strengthening material	**"Net" size [mm × mm]**	**weight of grid [g/m^2]**	**tensile strength [kN/m]**	**Applicable strength/weight ratio [kN/kg]**	**Ultimate strain [%]**
Carbon fibre (CFRP)	20 × 20	80	35,2	**440**	1,75
Alkali resistant fibreglass (GFRP)	25 × 25	225	45,0	**200**	< 3
Reinforcing steel net φ6/200 (A500-ϕ6)	200	1074	61,0	**57**	~10
Stainless steel cables 4 φ4 (cable-ϕ4)	-	392	40,0	**102**	4-5

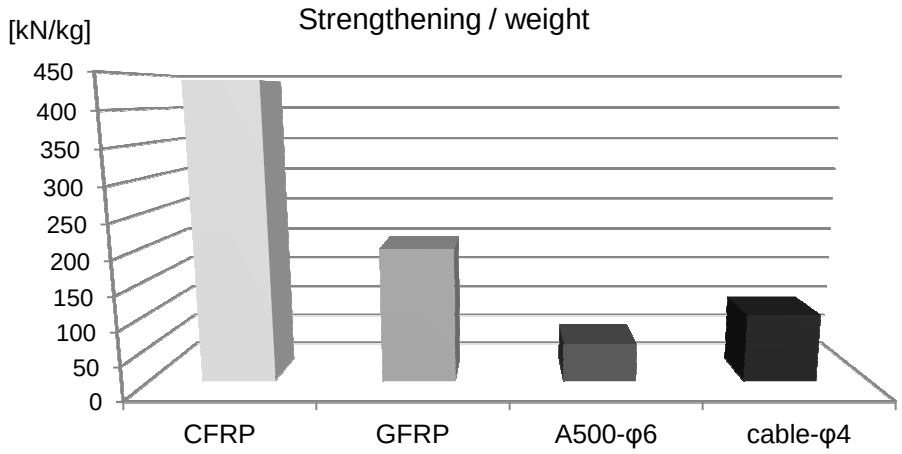

Figure 50: Diagram of the amount of strengthening force that can be utilized from one kilogram of the compared reinforcing materials [kN/kg]

Following this path, it is possible to compute the amount of material that is necessary for a specific level of strengthening. The amount of strengthening was chosen to be 100 kN, and a cost estimation was plotted in Figure 51 with the prices obtained from the European market.

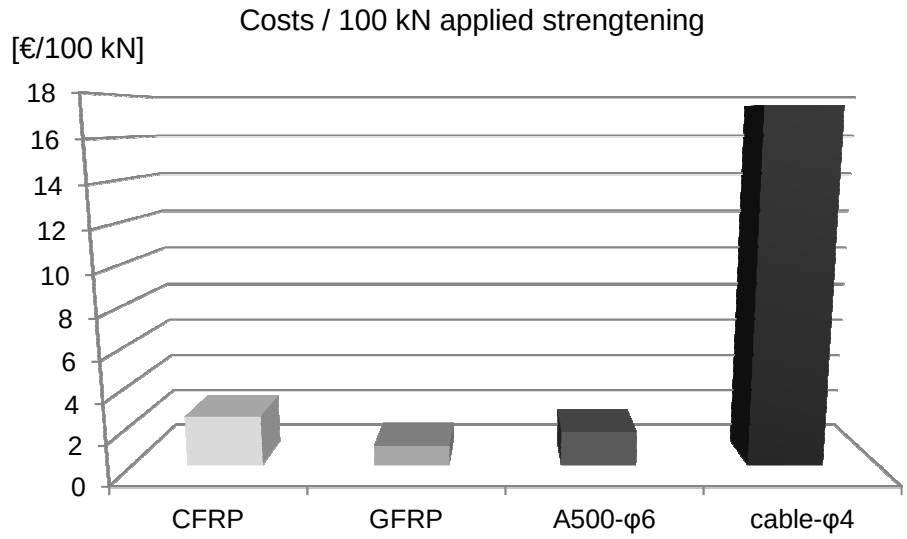

Figure 51: Costs of materials related to 100 kN of strengthening

It is known that the price of fibre reinforced polymers is very high. However, according to the cost efficiency estimation, a higher level of mechanical improvement can be reached by using these materials. It is important to note, that only theoretical values of mechanical performances were used, and that in reality these theoretical values are hard to be reached due to the vulnerability, and bonding nature of these special composites.

The aim of present cost efficiency study was to understand this issue, since the market prices of different materials are often hard to compare because of the different reference values (Note: reference values were varying between price/mass; price/length; price/area).

5.2 Practical range of strengthening

As both mechanical and practical issues are constraining the applicability and efficiency of the technique, simple calculations were done to define the range of applicability.

The calculations were based on the Eurocode 6 recommendations for externally reinforced masonry. (EC6-6.6.2) (See also in 2.3.4). The mechanical constraint represents the preferred failure mode, according to which the amount of strengthening should be chosen in a way that failure would happen in the compressed zone (recommendation of research group). The minimum compressed area providing this type of failure was calculated from the geometry of walls with different thicknesses.

The practical constraint comes from a physical point of view. Stone masonry walls are built with reasonable block sizes. For maximum strengthening two 6mm diameter wire ropes were chosen to fit each joint, and the presence of 5 joints / meter were assumed (20 cm long blocks). This assumption is the lower bound of the usual block sizes. The practicable forces were calculated in the cases of walls with different thicknesses.

Different failure modes are going to be referred as: mode_1 – failure on the compressed edge; and mode_2 – rupture of the reinforcement on the tensioned side.

On Figure 52, utilized strengthening forces are plotted against the scale of thicknesses of a defined masonry wall type. To give an explanation, in case of a 40 cm thick wall the sum of strengthening forces that can be utilized with the practical maximum amount of wire ropes is around 117 kN. In this case the preferred failure mode is satisfied, as the value lies in the upper region of the diagram, above the limit line. However, as can be seen, the wire ropes are not closing their capacity (180kN), reaching only 65%. Therefore it can be stated that reinforcing a 40 cm thick wall of the masonry type with practical maximum amount of wire ropes would not be cost efficient.

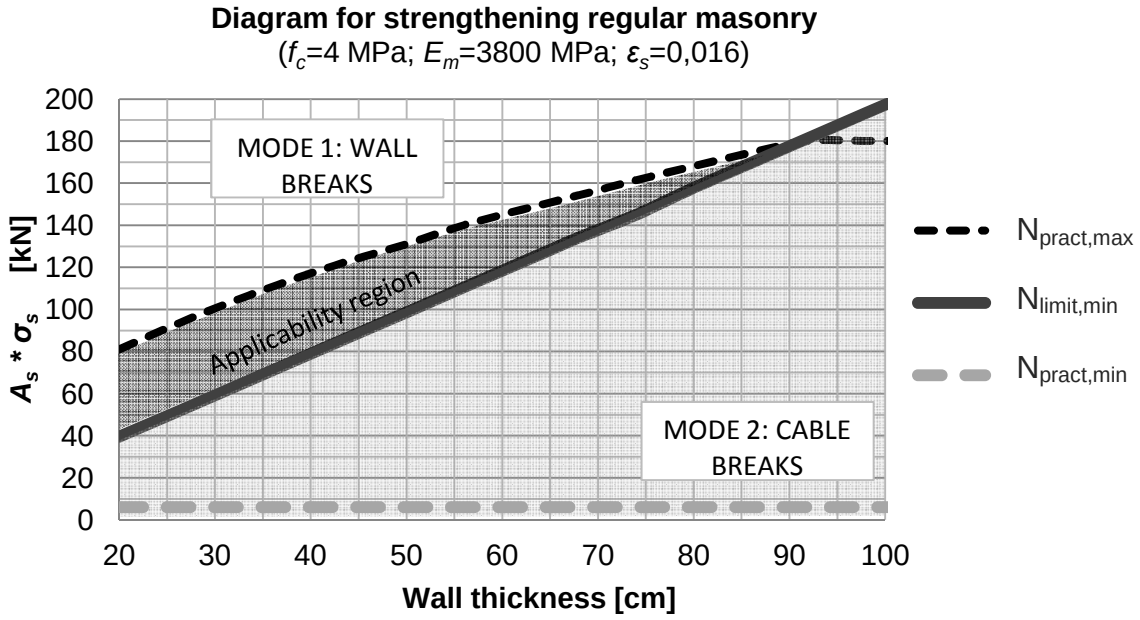

Figure 52: Range of applicability

The practical range of strengthening graph is important to give an idea about the efficiency of the chosen reinforcement amount. However, it is crucial to have a design abacus to see the resistant curve of the structures to be strengthened concerning the axial forces and bending moments, as well as the different failure modes.

5.3 Design abacus

The analytical study also involved the proposal for a design abacus, namely the reduced axial force (n) – reduced bending moment (m) interaction curve for masonry walls strengthened with the proposed technique. The geometrical features and the chosen material laws are represented in Figure 53.

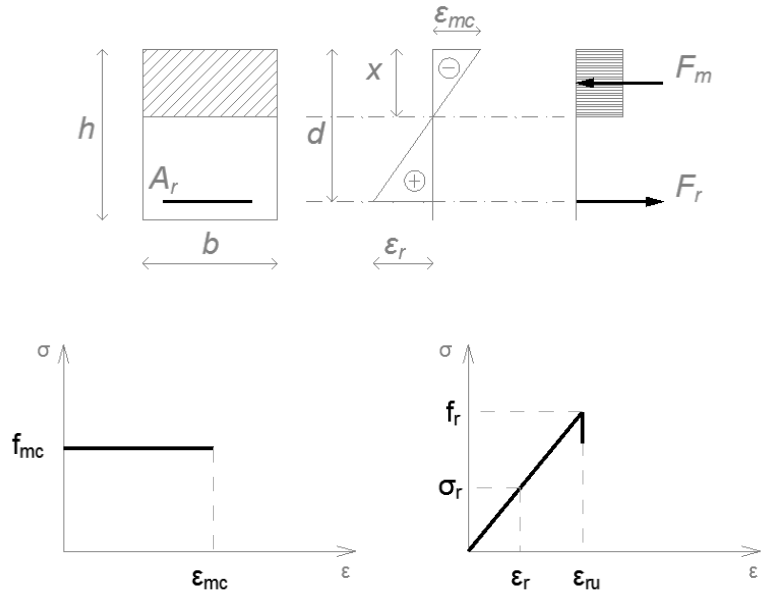

(a) (b)

Figure 53: Geometrical features; and material laws: for masonry (a), and for wire ropes /synthetic ropes (b)

where:

h=	height of cross-section
b=	width of cross section
d=	effective height of reinforced cross-section
x=	height of compressed area
ε_{mc}=	ultimate strain of masonry
ε_r=	strain of reinforcement
ε_{ru}=	ultimate strain of reinforcement
A_r=	area of reinforcement
F_m=	compression force on cross-section
F_r=	tensile force on cross-section
fmc=	masonry strength
σ_r=	stress state of reinforcement
f_r=	strength of reinforcement

The equilibrium equations were calibrated respecting the previous two different failure types, and the interaction of the resultant curves was studied.

Failure mode 1 – the wall fails ($\varepsilon_{mc} = \varepsilon_{mu}$)

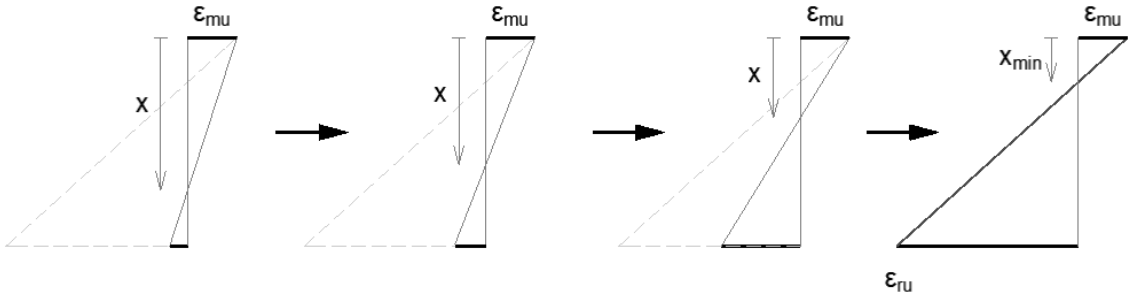

The corresponding equilibrium equations are:

$$F_m + F_r = N_{Ed} \tag{12}$$

$$F_r\left(d - \frac{h}{2}\right) + F_m\left(\frac{h}{2} - \frac{x}{2}\right) = M_{Ed} \tag{13}$$

Failure mode 2 – reinforcement fails ($\varepsilon_r = \varepsilon_{ru}$)

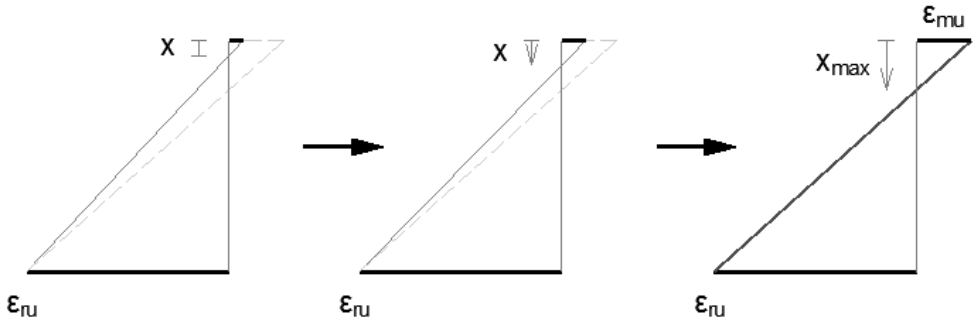

The corresponding equilibrium equations are:

$$F_m + F_{ru} = N_{Ed} \tag{14}$$

$$F_{ru}\left(d - \frac{h}{2}\right) + F_m\left(\frac{h}{2} - \frac{x}{2}\right) = M_{Ed} \tag{15}$$

In order to non-dimensionalize the equations the following formulas were adapted

$$\zeta = \frac{x}{h} \tag{16}$$

$$m = \frac{M_{Ed}}{h^2 f_{mc} * 1000} \tag{17}$$

$$n = \frac{N_{Ed}}{h\, f_{mc} * 1000} \tag{18}$$

$$\mu = \frac{A_r E_r \varepsilon_{mu}}{h f_{mc}} \tag{19}$$

$$\mu^* = \frac{A_r F_r}{h f_{mc}} \tag{20}$$

$$\nu = \frac{d}{h} \tag{21}$$

and the following equations were extracted from geometrical rules

$$\sigma_r = E_r \varepsilon_m \left(\frac{d}{x} - 1\right) \tag{22}$$

$$\zeta\_\min = \frac{x_{min}}{h} = \frac{\varepsilon_{mu} d}{h(\varepsilon_{ru} + \varepsilon_{mu})} \tag{23}$$

Using Equations (16) to (23), the equilibrium Equations (12); (13) are rewritten as

$$n = \zeta - \mu \left(\frac{\nu}{\zeta} - 1\right) \tag{24}$$

$$m = \mu \left(\frac{\nu^2}{\zeta} - \nu - \frac{\nu}{2\zeta} + \frac{1}{2}\right) + \frac{\zeta}{2} - \frac{\zeta^2}{2} \tag{25}$$

…and the equilibrium Equations (14); (15) are taking the form of

$$n = \zeta - \mu^* \tag{26}$$

$$m = \mu^* \left(\nu - \frac{1}{2}\right) + \frac{\zeta}{2} - \frac{\zeta^2}{2} \tag{27}$$

Two different graphs of the corresponding failure modes are represented in Figure 54 and Figure 55.

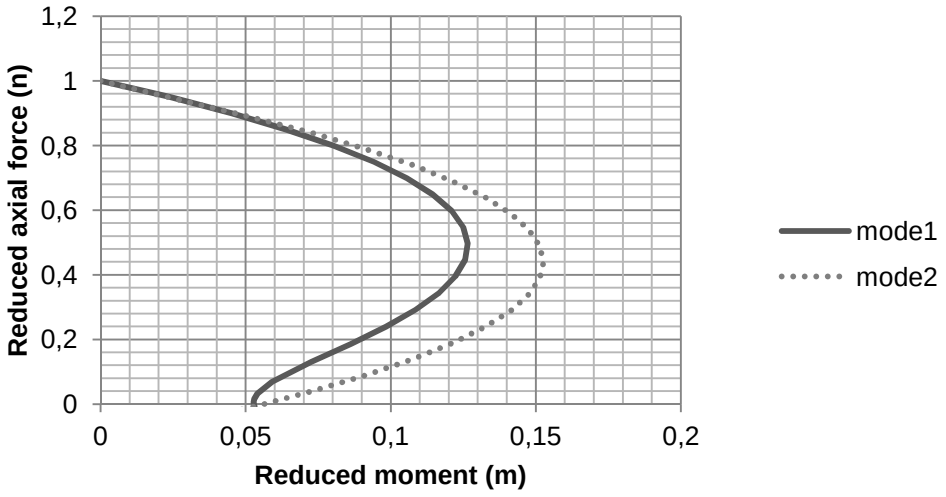

Figure 54: n-m interaction curve of different failure modes; Corresponding thickness of wall is small (h=32 cm)

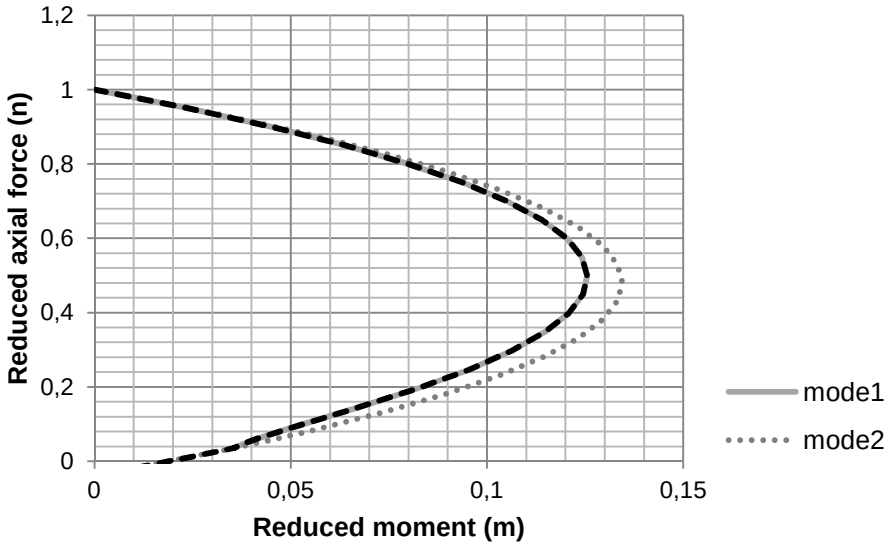

Figure 55: n-m interaction curve of different failure modes; Corresponding thickness of wall is significant (h=100 cm)

As the diagrams reflect it, the intersection of the graphs can change from the involvement of both failure modes (Figure 55) to the involvement of only one of the two modes (Figure 54). Figure 55 clearly shows that increasing the axial load can change the governing failure type. Without axial force the governing failure type would be the rupture of the reinforcing cables (mode_2), but increasing it the failure type changes to mode_1, which is the crushing in the compression side.

Figure 56 presents the influence of the amount of strengthening. As the reinforcing wires can only work in tension, they are not contributing to the compression capacity of the strengthened wall. Hence, there is no significant difference between the graphs when $n >$ ~0,5. It is also worth noting that the diagrams are changing the combination of failure modes due to the changing amount of reinforcement. Given a high amount of reinforcement (here 15ϕ4 mm), the structure is showing mode_1 failure (failure on compressed edge). If the amount of reinforcement is kept low (2ϕ4 mm), the wall fails according to mode_2 (immediate rupture of reinforcement).

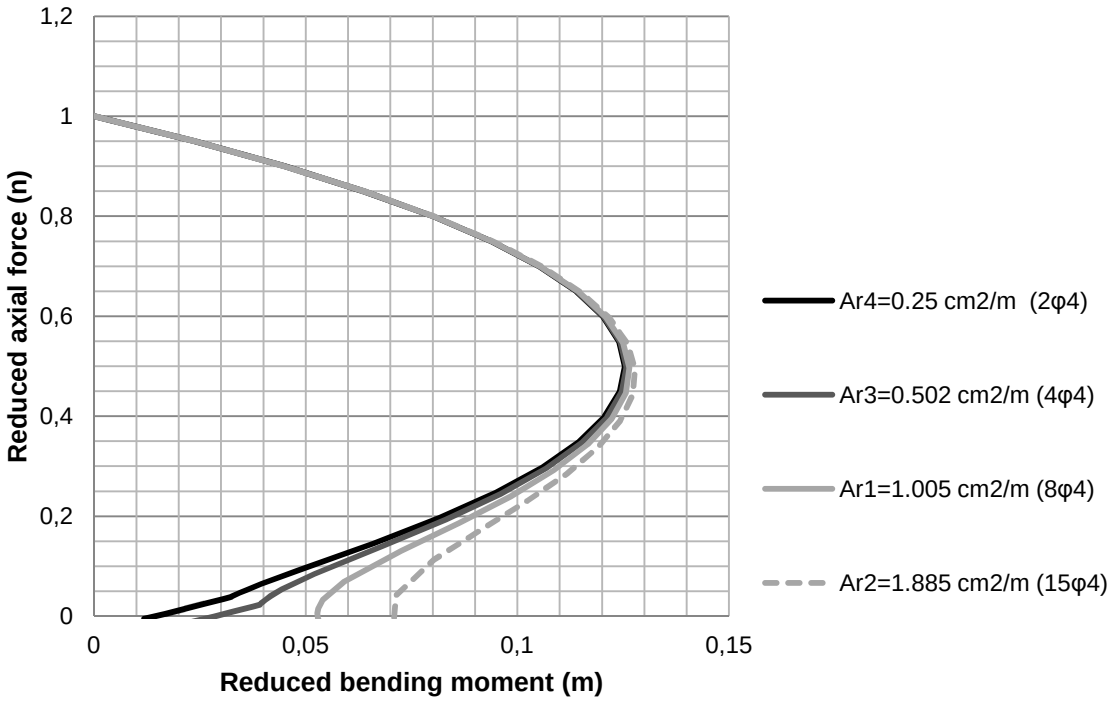

Figure 56: n-m interaction curve for different amount of strengthening (h=32 cm)

The design abacus is an effective tool for the determination of resistance of walls reinforced with the proposed technique. Its applicability will also be presented through a case study and in the evaluation of the wall bending tests.

6

SCALED MASONRY WALL TESTS

Introduction

In this chapter scaled stone masonry walls were tested with and without the application of the proposed strengthening technique. The tests were undertaken after a reduced curing time of 21 days, and conclusions were based on the relation between mechanical performance, applicability and workability issues. Description of the specimens, instruments, test procedure and discussion of results are next in the following sections.

6.1 Specimens and test procedure

Six scaled masonry walls were tested under monotonic out-of-plane loads. Each specimen was made as double leaf, regular stone wall, 1,1 m high and 0,95 m long with a thickness of 32,5 cm, cantilevering from a reinforced concrete slab, with the dimensions of 140 / 118 / 25 (see representation on Figure 57). Granite stones were used as units, and Weber Tradition® lime mortar was used as binder, which provided 4 MPa strength during preliminary compression tests after 28 days of curing. Cantilevering specimens were to reproduce the worst conditions occurring in the case of out-of-plane actions. In order to eliminate inherent problems of bed-joints between slabs and walls, granite stones were placed on the top of the slabs during the casting, sinking with the 2/3 of their volume. The walls were subsequently constructed on the top of the bare stone support.

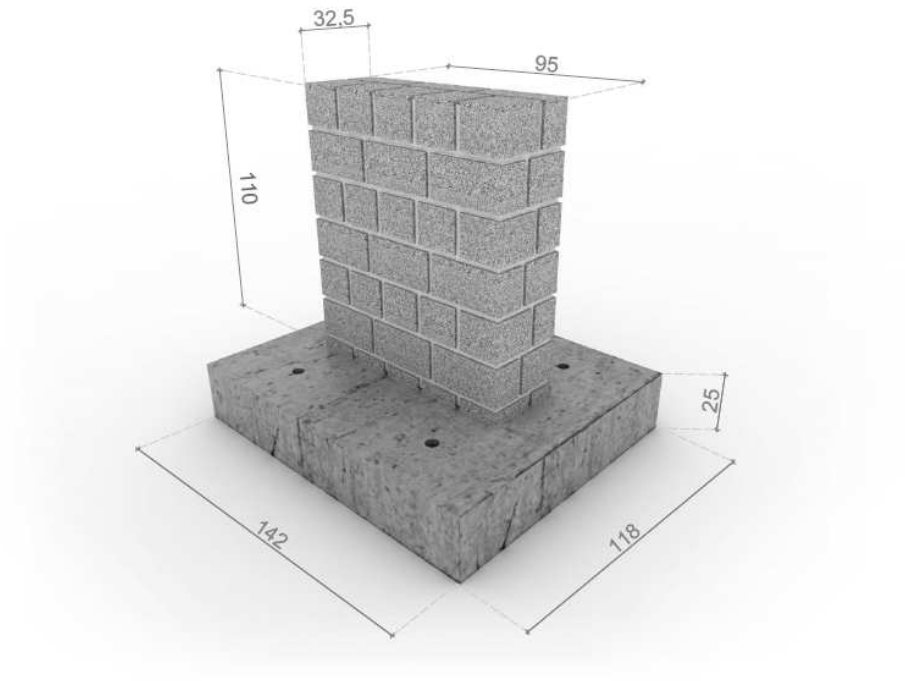

Figure 57: Dimensions of specimens

Two un-strengthened specimens (URW) were tested together with 4 strengthened walls, out of which one was strengthened with ϕ4 mm stainless steel cables (StRW.1). After evaluating the performance of StRW.1 it was decided to prepare the next wall with ϕ2 mm cables to increase the performance (StRW.2). Subsequently another wall was prepared with the ϕ2 mm wire ropes, as the results were promising (StRW.3). The 6th specimen was prepared with SRCC-ϕ4 synthetic ropes (SYRW) to see its workability and applicability related to the technique.

Lateral out-of-plane monotonic displacement with periodically increased velocity was applied along the top joint of the walls: First period was defined to capture the elastic range of the behaviour (top displacement: d_1=0-2mm; v_1= 0,005 mm/sec); increased velocities were used for the record of non-linearity (d_2=2-6mm; v_2= 0,010 mm/sec; d_3=6-10mm; v_3= 0,020 mm/sec; d_4=10-50mm; v_4= 0,030 mm/sec).

6.2 Workability issues of strengthening technique:

During the first tests of application different obstacles had to be passed, and decisions had to be made on the rest of the procedures. The design of the reinforcement was based on theoretical calculations of a system, which is under development. Consequently, workability issues highly affected the mechanical performance of the chosen reinforcement type leading to changes on the next test objects.

The most important workability issues affecting mechanical performance were:

- the behaviour of helibar prototypes as constituent of the reinforcement;
- the behaviour of ropes (wire or synthetic);
- the importance of pre-stressing,
- the type of bottom and top connections of reinforcement (load transition points)

Behaviour of helibars:

As it was discussed previously, the helibar connector elements have a complex design with the main aim of protecting the wire ropes from passing sharp edges. The helihead has a clever shape in order to fulfil this function. Problems occurred however, in the welded connection between the head and the bar, as its low rigidity allowed easy deformations Due to this disadvantage the wire ropes touched the sharp edges of stones, and suffered early failure (see it on Figure 58). Another issue was the rigidity of the helibar itself, but the major problems were found in the welding. The way of development lies in the strengthening of the connections between the helihead and the bar, and choosing higher diameter helical bars (ϕ12 mm is recommended).

(a) **(b)**

Figure 58: Connector element deformed due to transversal loading (a); wire rope failure due to attachment to sharp edged stone (b)

Behaviour of ropes:

One wall was tested with synthetic ropes used as reinforcement. The composite was not proved to be workable in the system, as the vulnerability of carbon fibre core needed special attention. Therefore the application became time consuming and stressful with uncertainties in keeping the soundness of the composite (as you can see it on Figure 59).

Figure 59: Imperfections in SRCC synthetic ropes

The observed imperfections however did not influence the test performance, as the ropes showed exceptionally high elongation, due to which the reinforcement was not activated during the test. For this reason the test results of SyRW won't be discussed furthermore.

Development is possible by changing the type of synthetic rope. However, it is worth noting that finding the most adequate type in terms of workability and mechanical performance needs persistent investigation.

Importance of pre-stressing:

Theoretically the ropes are immediately activated when the load is applied. In reality the curvature of the inserted grid allows adjustment and small movements of reinforcement in the joints, hence the activation of the system is not immediate. This problem was partly solved by assuring a pre-stress on the ϕ2 mm cables. The application was rather hard, as it had to be repeated several times, due to the adjusting deformations of heliheads. Pre-stressing was applied in every second vertical joint, and on the top of the

specimen. See the device for pre-stressing on Figure 60. Significant increase in mechanical performance was observed. The results are discussed in section 4.2.4.

Figure 60: Pre-stressing of cables

Bottom and top connections of reinforcement (load transition points):

Bottom and top connections had to be secured carefully, as they functioned as load transition points. Bottom connection was created by fixing the ropes to the deep reinforcement of the concrete slabs. Connection types are shown on Figure 61 for cables and synthetic ropes respectively.

Figure 61: Bottom connections of cables and ropes to reinforced concrete slab

Top connections were created respecting the existence of pre-stressing. If pre-stressing was applied, steel reaction plates were used on top of the cleaned joints for load transition

(see it on Figure 62). If not, the reinforcement was fixed to the last row of helibars with aluminium sleeves for cables, and with knots in case of synthetic ropes.

Figure 62: Prestressed top connection with load distributing steel plate

6.3 Test setup:

The test setup is represented on Figure 63. Each specimen was instrumented with 7 sensors: 2 x 2 transducers along target lines corresponding to the position of cracking and crushing around the base; 2 transducers were placed below the load application to measure out of plane displacement, and to catch signs of torsion. One LVDT was applied on the actuator.

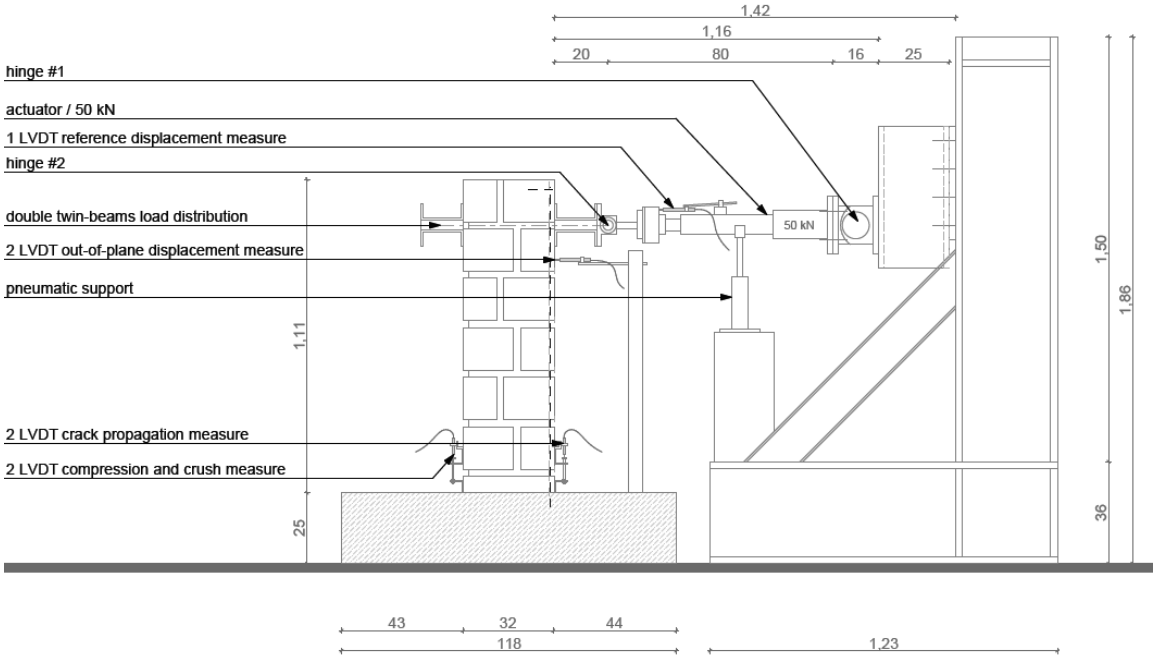

Figure 63: Final set up for masonry wall tests

The actuator was connected to the reaction frame with a hinge, and was supported by pneumatics in its mid-span. The loading plate was connected to the actuator by a second hinge, allowing the system to adjust vertical displacements. For the load distribution, a pair of twin beams was fixed on the wall, tied and stressed at the cantilevering ends.

6.4 Results:

During flexural tests, the masonry walls attained two main limit states:

1) The cracking limit state occurred when applied load F_{cr} (and corresponding top deflection d_{cr}) induced cracking of the section.

2) Subsequently, maximum resistance was attained (F_{max}, d_{Fmax}).

For safety reasons the ultimate limit state was not closed during the experiments. The tests were stopped in different stages after reaching the maximum resistance.
An overview of results is given in Table 13, and the behavioural curve is given in Figure 64.

Table 13: Bending test results

Name of specimen	F_{cr} [kN]	d_{cr} [mm]	F_{max} [kN]	d_{Fmax} [mm]	Stiffness_section 1 K_{s1} [kN/mm]	Stiffness_section 2 K_{s2} [kN/mm]
URW.1	0,4	0,6	1,7	6,8	0,67	0,31
URW.2	0,4	0,5	2,0	8,4	0,80	0,90
StRW.1_ϕ4	1,4	0,9	2,3	4,0	1,55	0,41
StRW.2_ϕ2	1,8	0,4	3,3	8,6	4,50	1,44
StRW.3_ϕ2	1,3	1,5	2,4	6,2	1,62	0,26

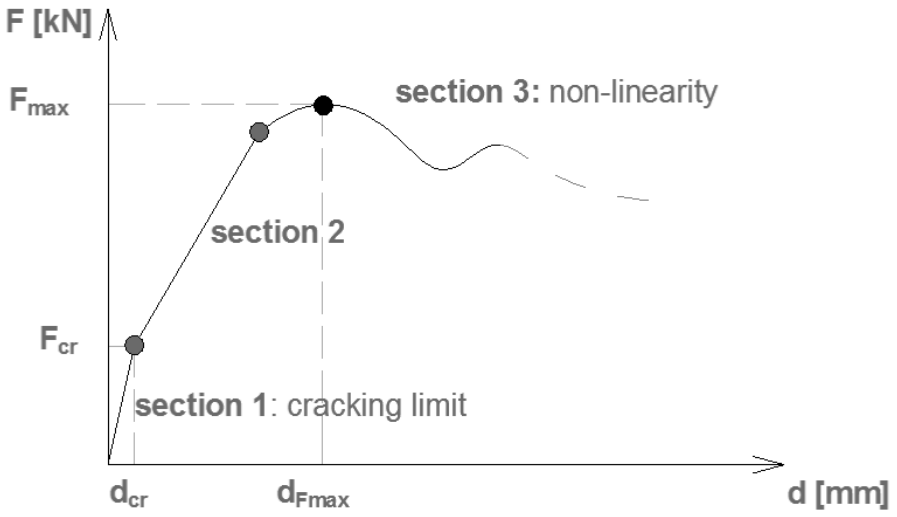

Figure 64: force-deflection curve of bending tests

Unreinforced walls:

Failure mode of each specimen was collected. The unreinforced walls failed with one-one major crack propagation as it is represented on Figure 65, Figure 66 and Figure 67.

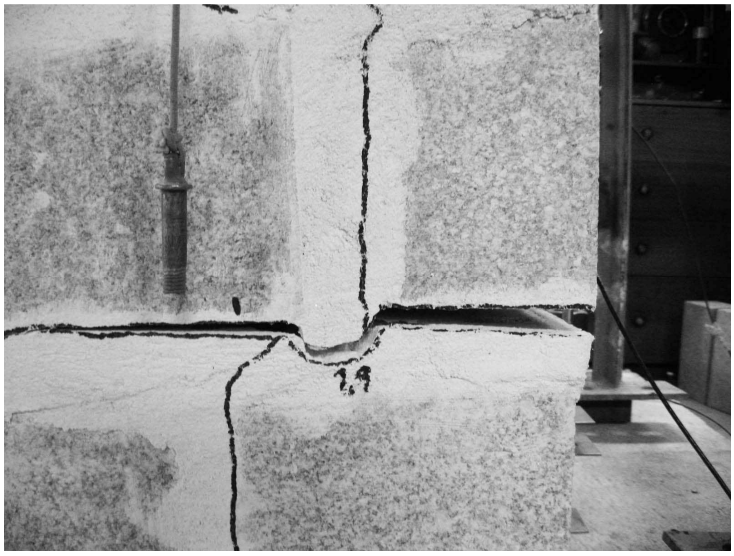

Figure 65: Cracked state of URW.2

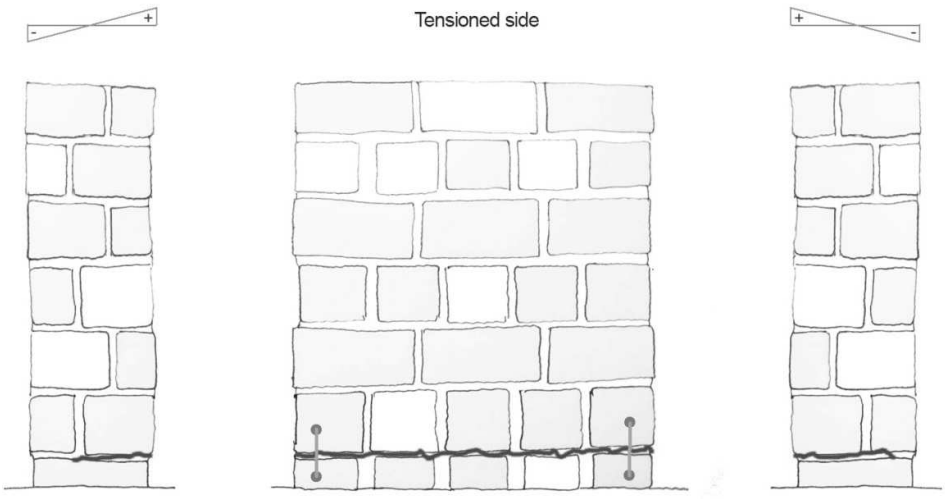

Figure 66: Rocking failure mode of URW1

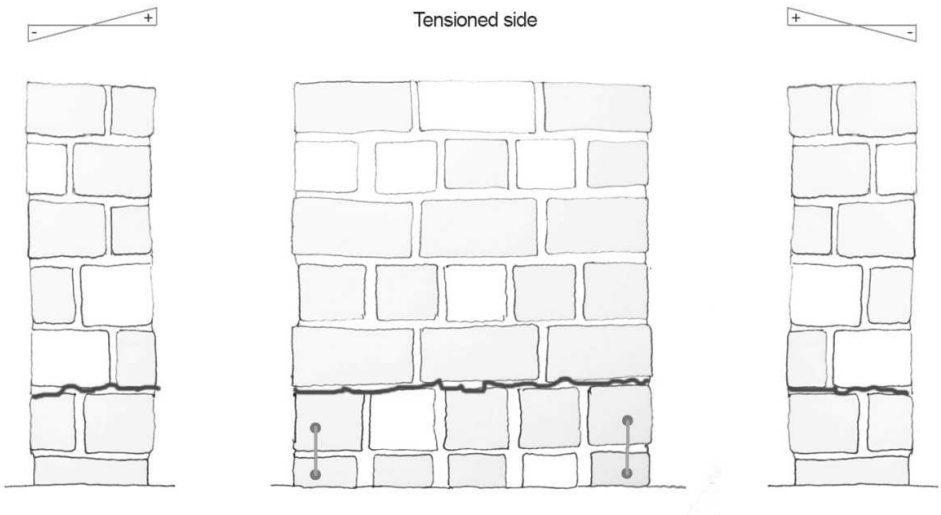

Figure 67: Rocking failure mode of URW2

For preliminary calculations 0,1 MPa was used as tensile strength, and the horizontal load to reach the cracking limit was estimated as 2,24 kN. Both of the unreinforced walls provided unexpectedly low values ($F_{cr,URW.1}$=0,4 kN; $F_{cr,URW.2}$=0,4 kN). According to these values the tensile strength was calculated again with elastic theorem and gave a near zero value (0,0033 MPa). This could be due to the low curing time of lime mortar and due to the appearance of non-visible damages during transportation. The existence of these damages makes elastic estimation of tensile strength questionable.

Cracking was expected in the first joint over the base. Despite the expectations URW.2 provided crack propagation in the second joint, but with the same force of cracking limit state (see also the applied force-curvature graph on Figure 68 for the good definition of cracking). Hand calculations using kinematic approach verified that the same amount of force can cause cracking in different levels. Physical differences must have influenced the localization of the first crack. Indeed, URW.2 suffered cracking during transportation (see on Figure 69), which was not observed in case of URW.1. This imperfection is likely to cause a jump in the localization of the bending crack, since the prior cracks appeared also in the discussed second joint. Other physical differences are likely to show in the obtained maximum forces of resistances ($F_{max,URW1}$= 1,7 kN; $F_{max,URW2}$= 2 kN), and in the stiffness's of the walls ($K_{URW1,s1}$=0,67 kN/mm; $K_{URW2,s1}$=0,8 kN/mm), but these differences can be simply referred as variation of test results. Deeper understanding of these results is not possible because of the low number of test specimens. The resultant Force-deflection diagrams are visible on Figure 70.

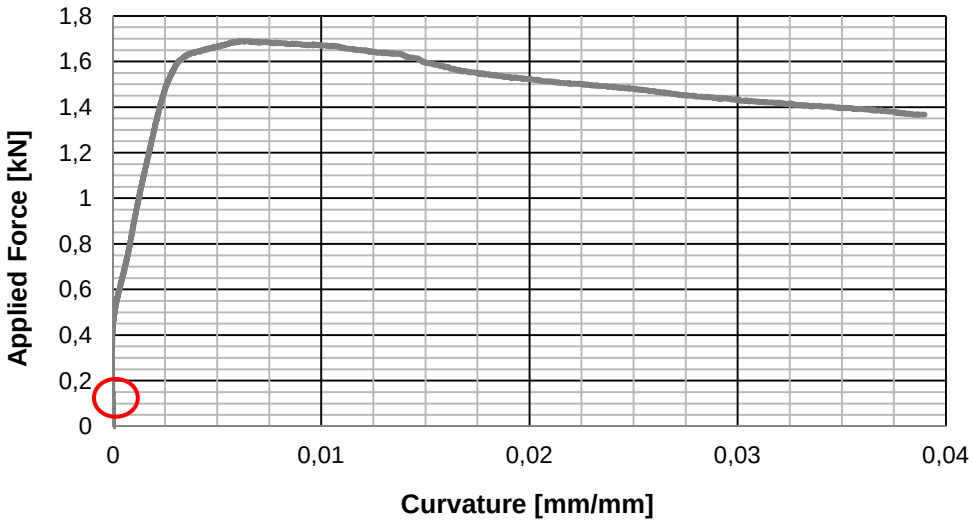

Figure 68: Applied force-curvature diagram of URW.1 for the definition of cracking

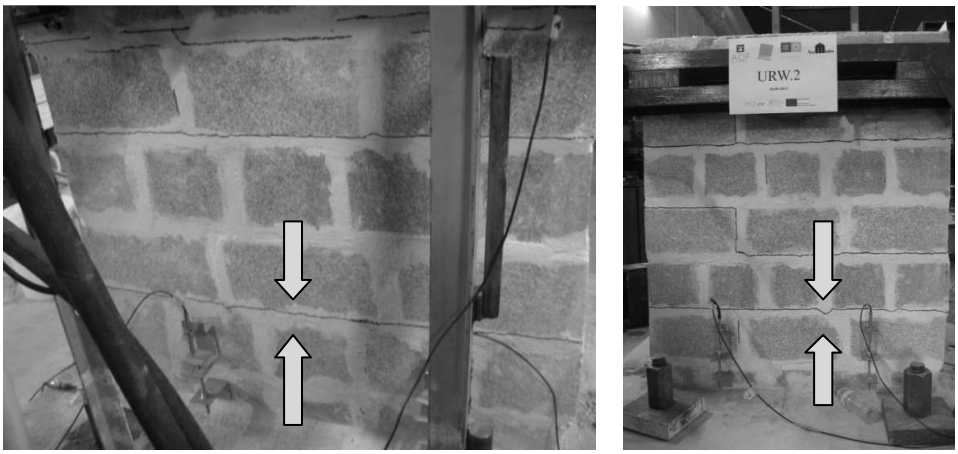

Figure 69: Prior cracks on URW2

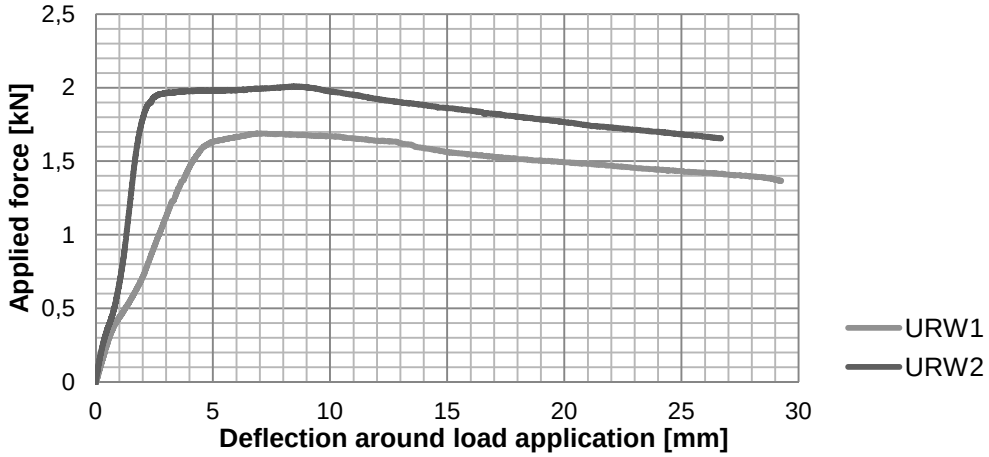

Figure 70: Force-deflection diagram of unreinforced walls

Strengthened walls:

Figure 71 to 76, are showing the failure maps of strengthened walls. Clear advantage of the applied technique appears immediately in the distributed crack patterns (higher energy dissipation capacity). Pre-tensioning was applied on StRW.2-3 but the way of application was not efficient on StrW.3, most likely because of the human factor and difficulties. The increased performance due to efficient pre-stressing (StRW.2) can be followed on Figure 73, Figure 74 as well as on Figure 77.

Figure 71: Cracked state of StRW.1

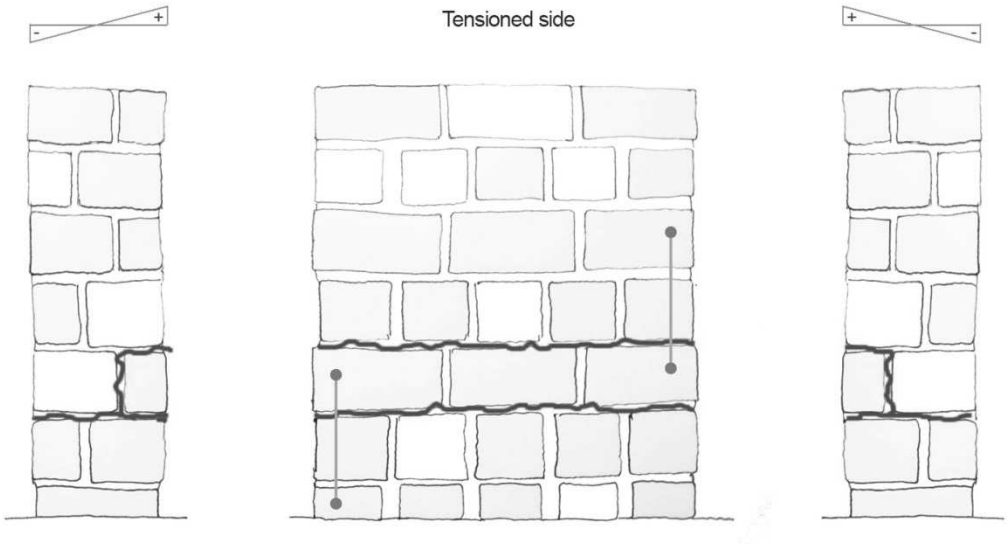

Figure 72: Rocking failure mode of StRW.1 with ϕ4 wire ropes

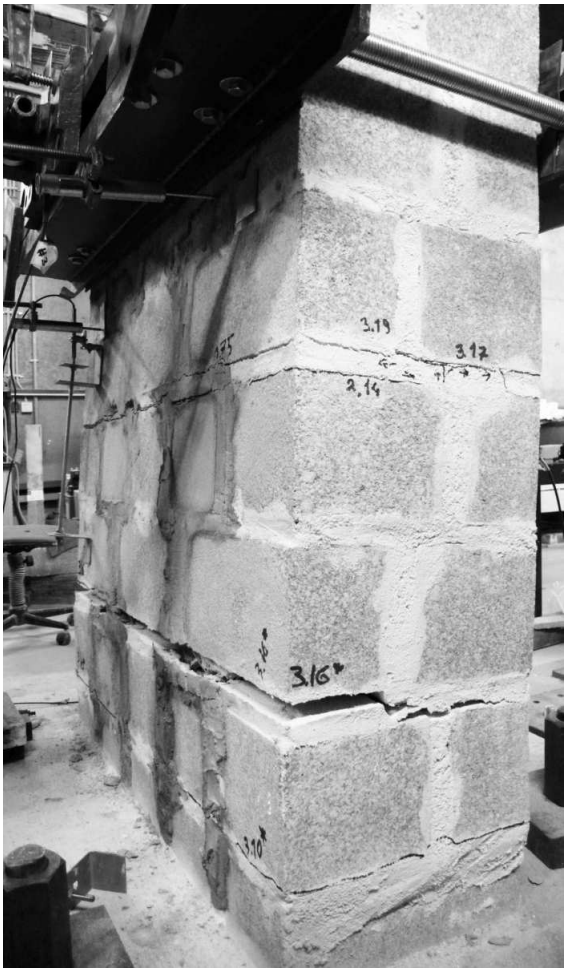

Figure 73: Cracked state of StRW.2

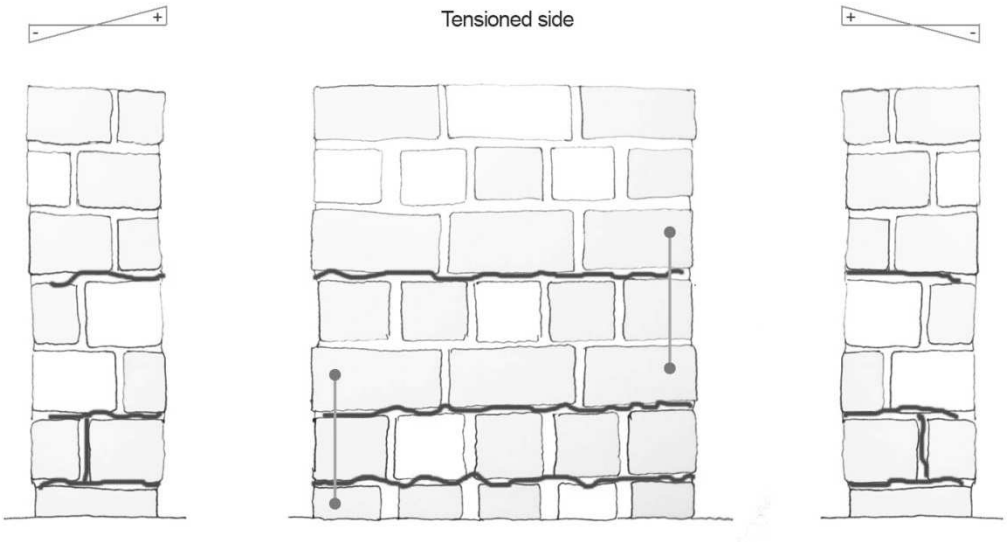

Figure 74: Rocking failure mode of StRW.2 with ϕ2 wire ropes

Figure 75: Cracked state of StRW.3

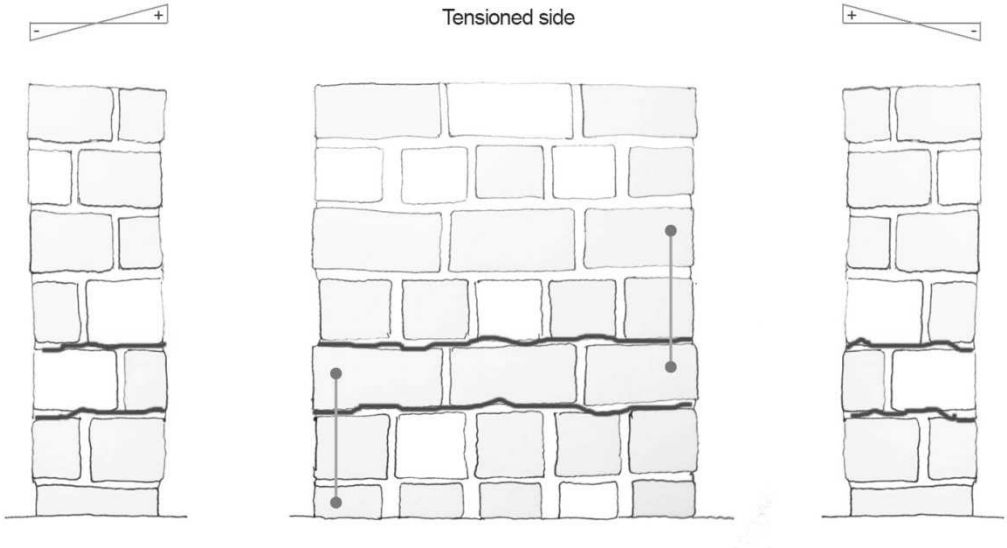

Figure 76: Rocking failure mode of StRW.3 with ϕ2 wire ropes

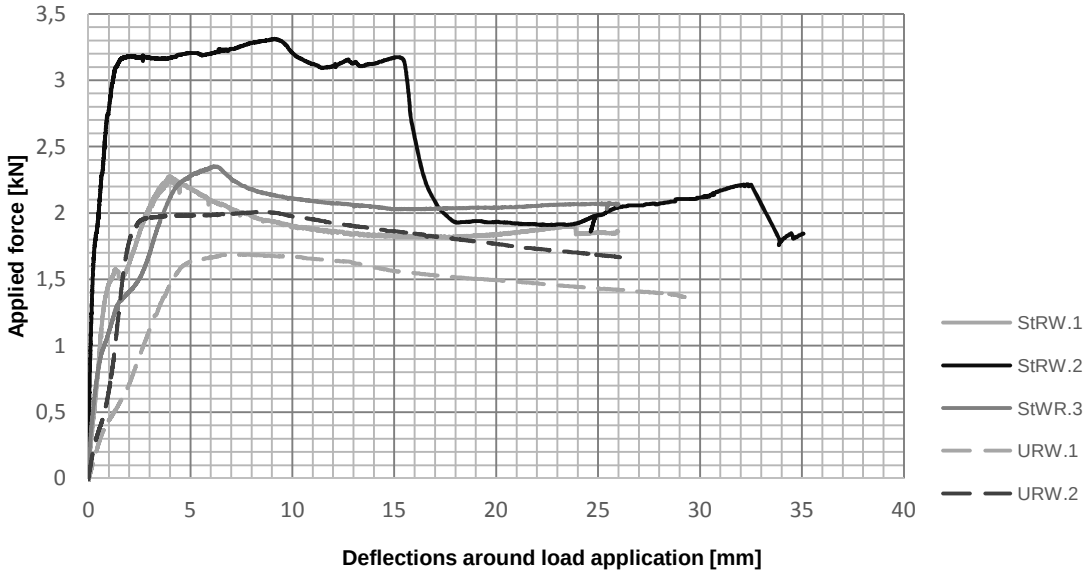

Figure 77: Force-deflection diagrams of reinforced walls

Preliminary calculations were done to estimate the bending resistance of the strengthened walls, however only STRW.2 provided close values, due to the more efficient pre-stressing. The maximum horizontal load on top corresponding to maximum resistance was estimated as 4,92 kN, and STRW.2 provided 3,3 kN. The difference could be caused by different factors, such as the real efficiency of the pre-stressing and the adequacy of estimated masonry properties.

Without efficient pre-stressing the maximum resistance of the walls did not increase significantly ($F_{max,StRW.1}$= 2,3 kN; $F_{max,StRW.3}$= 2,4 kN compared to $F_{max,URW.1}$= 1,7 kN; $F_{max,URW.2}$= 2,0 kN). Remarkable increase was only observed, when reasonable pre-stress was applied in case of StRW.2 ($F_{max,StRW.2}$= 3,3 kN). However, the stiffness, and the force of cracking limit state increased in each case of reinforced walls ($F_{cr,StRW.1}$= 1,4 kN; $F_{cr,StRW.2}$= 1,8 kN; $F_{cr,StRW.3}$= 1,3 kN compared to $F_{cr,URW.1}$= 0,4 kN; $F_{cr,URW.2}$= 0,4 kN. And the stiffness' of STRW.2 in different sections: $K_{StRW.2\_s1}$= 4,5 kN/mm; $K_{StRW.2\_s2}$= 1,44 kN/mm compared to $K_{URW1\text{-}2\_s1\text{-}2}$ < 1 kN/mm). Overall it can be stated that the technique is capable of

- increasing the stiffness and plastic behaviour of walls against out of plane actions,
- raising the limit state of cracking (F_{cr}), and
- increasing the maximum resistance if adequate pre-stressing is applied.

It was worth comparing the effects on StRW.2 with the theoretical resistance. The design abacus was prepared for the test object by choosing 4ϕ2 mm wire ropes as reinforcement and setting the mechanical and geometrical properties of the wall to be adequate. To estimate the Young Modulus, dynamic identification was used (E=3500 MPa). The

compression strength of the wall was chosen to be 4 MPa. As it was predicted, Figure 78 verifies that wire ropes would fail first under the test conditions (a cable broke during the test of StRW.2). The mode_1 curve represents failure on the compressed edge, and mode_2 curve represents failure due to rupture in reinforcement. The axial force-bending effects are represented with a point in the left side of the resistance curve. “n” was calculated from the self-weight and the additional weights of the wall using equation 18 (n=0,017), and “m” was calculated from the applied moment on the 1st joint cross-section (m=0,063) using equation 17.

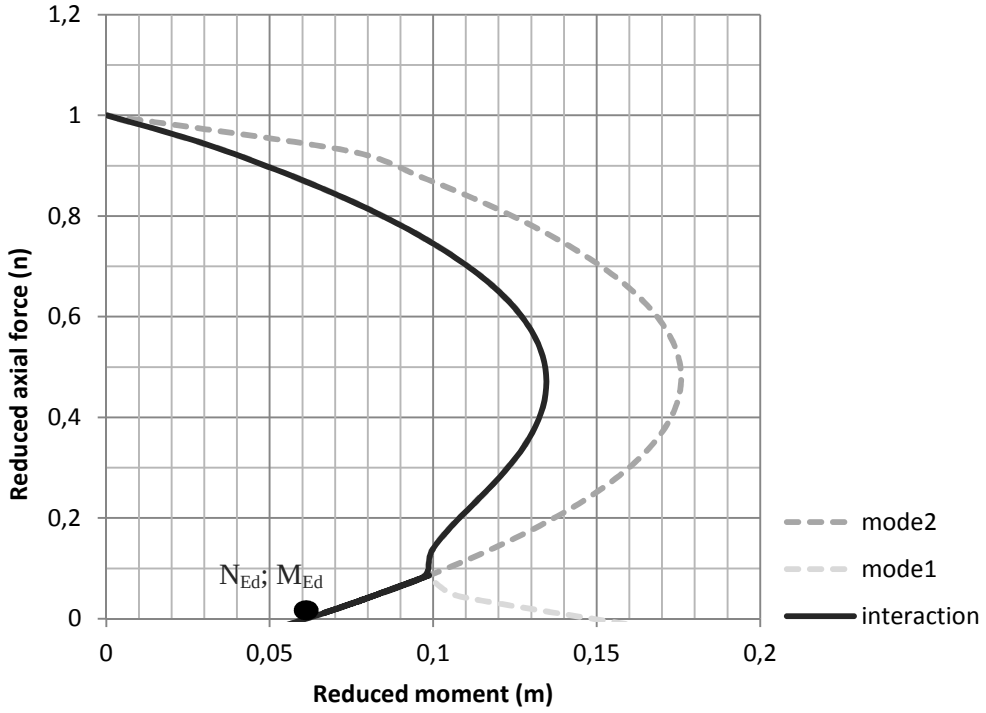

Figure 78: comparison of effects presented by experiments with the theoretical resistance in design abacus

6.5 Remarks:

Workability and applicability of the proposed technique was studied together with the mechanical performance of the reinforced specimens during the experiments. The special connector elements proposed in current research proved the necessity of further improvement in their stiffness. The importance of pre-stressing was clearly supported by the experimental results, as the maximum resistance of the StRW.2 wall increased with 78%. As a practical issue, the application of this pre-tensioning needs further development to improve its workability.

Despite the obstacles and problems in the first applications of the proposed technique during the experimental investigation, it is really promising, and worth improving.

Fields of future improvement:

- stiffness of helibars
- protection of wire ropes
- device for pre-tensioning
- alternative synthetic rope type

7

CASE STUDY: GUIMARÃES CASTLE

Introduction:

In the following chapter a case study of the Alcáçova wall is presented (Guimarães Castle; Portugal). Practical and analytical investigation on the theoretical application of the new technique is next, together with a literature review about the historical structure.

7.1 Brief history of Guimarães Castle

In the 10th century, Countess Mumadona Dias ordered the construction of the castle on the top of the hill named Monte Latito, in order to protect the neighbouring new monastery and growing village from the Muslims invasions. The recognition of the Portuguese nation is attached to the activities of the countess which gives a special importance to the defensive building.

The castle was remodelled and expanded in the 11th century, when Count D. Henrique and his wife D. Teresa settled in Guimarães. D. Afonso Henriques was born here, who after fighting for independence became the first king of Portugal. Trough the 12th century till the 16th the castle was continuously improved, when it lost its defensive importance and became the city jail. In the following century it mostly functioned as a royal barn, when in 1653 the castle was announced to be a ruin. In 1836 its demolition was publicly debated.

The situation was reversed in the 19th century. The castle was classified as "first class historical monument" and some properties around the monument were expropriated in order to enhance its image (DGEMN, 1937; Fernandes, 2011).

7.2 The Alcáçova wall

The Castle of Guimarães has a pentagon shaped plan with 8 towers as it can be seen on Figure 79.

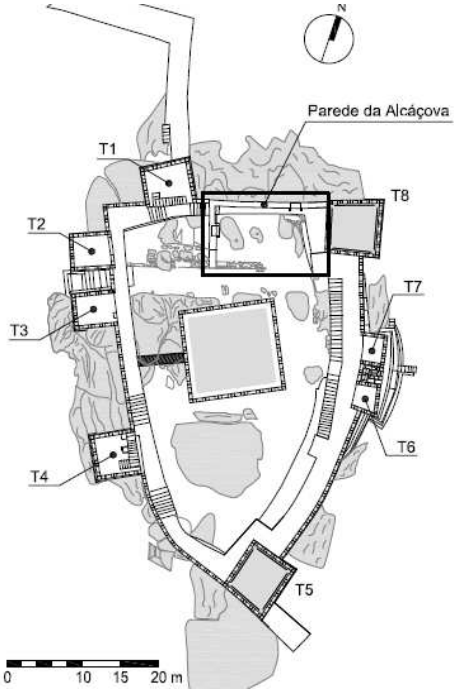

Figure 79: site plan of Guimarães Castle; localization of Alcáçova wall

In the present situation a wide part of the northern wall (the Alcáçova wall) is standing without any transversal bracings. It is known that the wall was the northern facade of a building, and played its role in supporting the buildings floors, but now it lacks these transversal structures.

A recent investigation was carried out at the University of Minho, and pointed out the wall's extreme vulnerability in transversal direction. The situation was studied with on-site non-destructive tests (Moreira, 2010), as well as with the help of numerical models (Fernández, 2012). The numerical investigation in Yhosimi W. E. Fernández's work pointed out, and evaluated the vulnerability, giving comparable results for two different types of numerical models. (micro-models and macro-models with homogenization). See the structural safety in Table 14.

Table 14: Capacity results of numerical study (Fernández, 2012)

Joints	Heterogeneous model (% of self-weight)	Homogeneous model (% of self-weight)	Accuracy of homogeneous model
Weak mortar	8,9	6,9	80%
Strong mortar	34,4	31,6	90%

Fernández could well estimate the global overturning mechanism of the wall through numerical modelling, as it is represented in Figure 80.

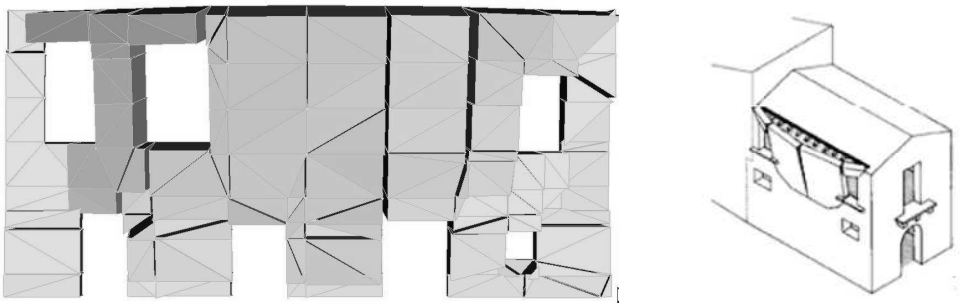

Figure 80: Global mechanism of Alcáçova wall (Fernández, 2012)

Structural intervention was planned based on the gathered information. Internal anchoring system was designed to increase the structural safety of the target wall (see the plans on Figure 81 and Figure 82).

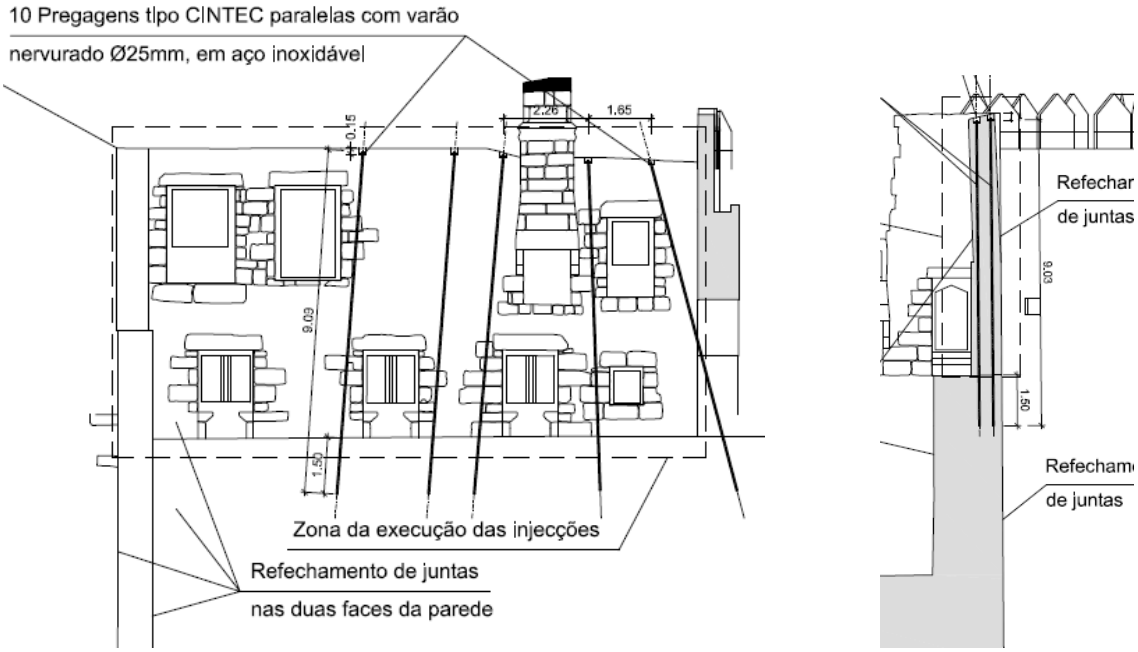

Figure 81: Front view and cross-section of strengthening Alcáçova wall

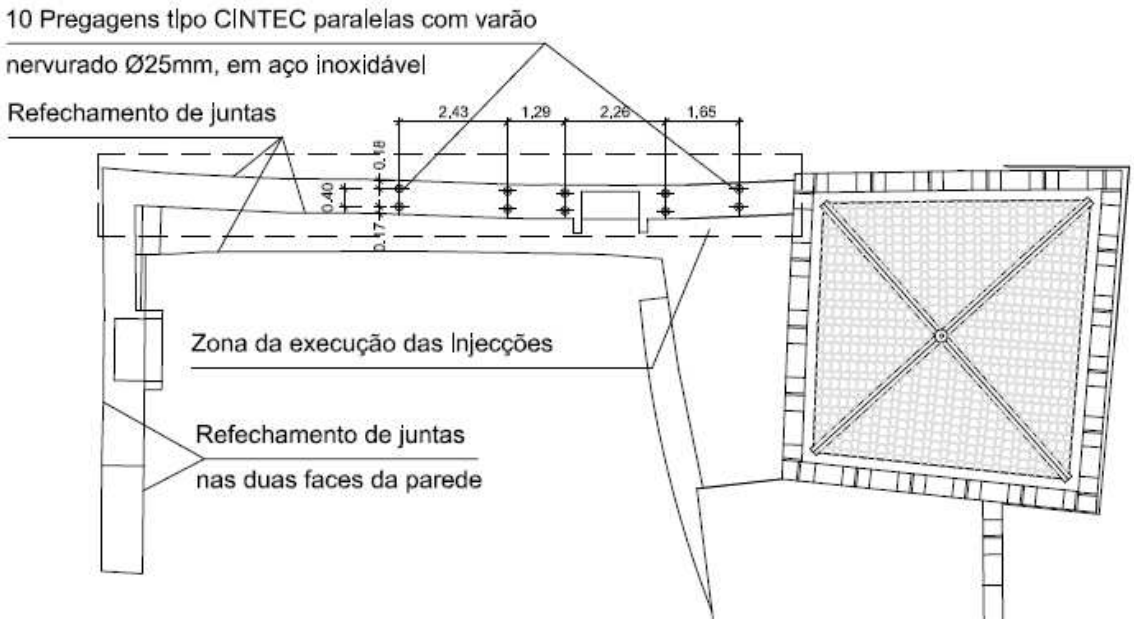

Figure 82: Plan of strengthening Alcáçova wall

7.3 Proposal for alternative strengthening

In the following section, the applicability of the proposed technique is being discussed as an alternative to the designed strengthening system for improving the safety level of the Alcáçova wall.

Geometrical study of the wall was done by Fernández previously. The joint texture of the wall is represented in Figure 83. Mean values were extracted from his statistical study of block dimensions, and are given here: 59,81 cm length / 33,55 cm height. The wall has a three leaf configuration with two external leaves made of granite with an average thickness of 35-40 cm of each leaf. The middle is poor quality rubble masonry, with gaps as it was reported after the non destructive investigation (see on Figure 84).

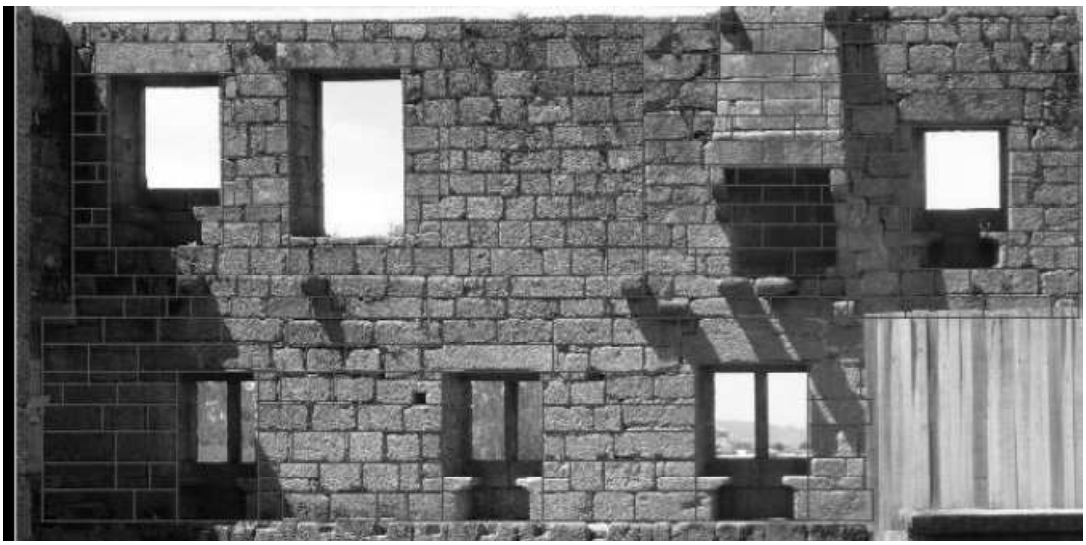

Figure 83: Joint texture of Alcáçova wall (Fernández, 2012)

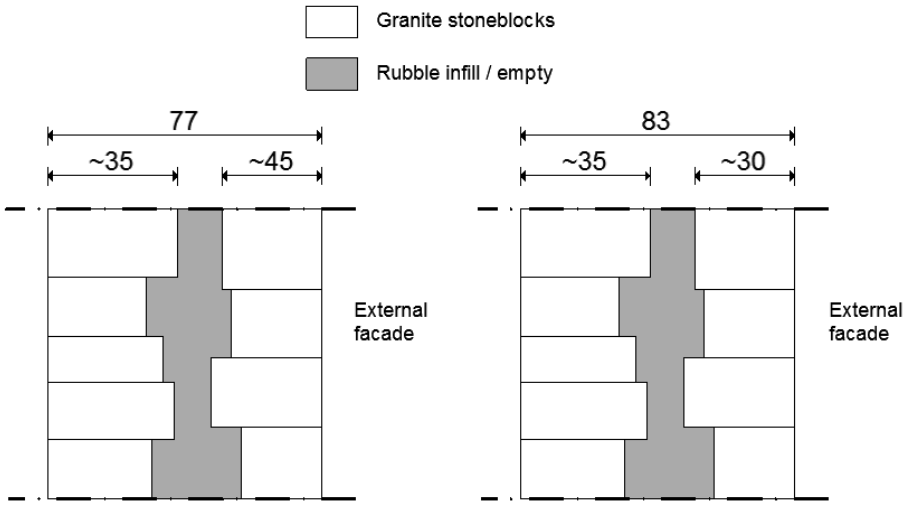

Figure 84: Leaf configuration of Alcáçova wall (Moreira, 2010)

The gathered information was eligible to estimate a practical maximum of the amount of strengthening for the proposed technique. The number of joints per meter is 1,672. Taking into account 2×ϕ4 mm stainless steel wire ropes in each vertical joint, the practical maximum would be 3,34 wire rope per meter.

Calculations to estimate the practical maximum amount of strengthening were done by considering 2; 4 and 8 MPa as compressive strength and 3800 MPa as elastic-modulus for the masonry. The mechanical properties of wire ropes were taken from experimental results presented in the thesis work (values are listed in Table 15). In case of the 77 cm thick wall the amount of forces that are possible to be utilized in reinforcement ("*f*") respecting the compressive strength of masonry ("σ_{mc}") are listed in Table 16.

Table 15: Mechanical properties of constituents

Material	Maximum strength	Young Modulus	Maximum strain
granite masonry	2; 4; 8 MPa	3800 MPa	0,5 ‰
steel wire ropes	711 MPa	44000 MPa	16 ‰

Table 16: Efficiency of practical maximum reinforcement

Masonry compressive strength σ_{mc} [MPa]	Force in wires *f* [kN/m]	Failure type and efficiency of wires
2	8,09	mode_1; 27%
4	29,84	mode_2; 100%
8	29,84	mode_2; 100%

7.4 Strengthening with stainless steel wire ropes

Calculations for the improvement of Alcáçova wall were done by using kinematic approach. The geometrics of the overturning mechanism can be seen on Figure 85.

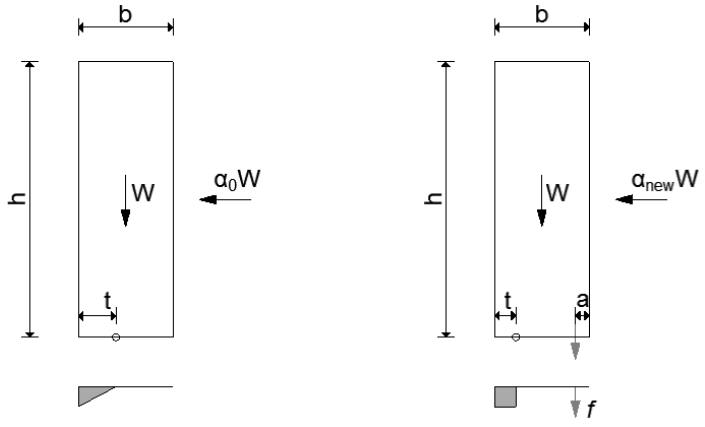

(a) (b)

Figure 85: Geometrics of overturning mechanisms: un-strengthened (a) and strengthened wall (b)

Where

h = height of the wall
b = Thickness of the wall
t = width of compressed edge; position of plastic hinge
a = distance of reinforcement from external surface
W = self-weight of wall
α_0 = seismic multiplier
f = Force applied with reinforcement (kN/m)

Safety evaluation:

From the moment equilibrium equation of the un-strengthened wall, α_0 multiplier can be calculated. The position of the rotational hinge was taken as

$$t = \frac{2N}{\sigma_{cmax}} \tag{28}$$

Elastic behaviour of the masonry was supposed. Using the equations from section 2.4.2 the safety level of the wall was estimated (see Table 17). The Damage Limit State assures that the wall would remain in the elastic range in case of minor excitations. The Ultimate Limit State assures that the wall would only suffer repairable damages in case of a defined major earthquake. (For further information see Eurocode 8, 2004).

Table 17: Safety evaluation of un-strengthened wall part

Masonry compressive strength σ_{mc} [MPa]	α_0	**DLS** = 0,084	**ULS** = 0,106
2	0,058	K.O.	K.O.
4	0,079	K.O.	K.O.
8	0,089	O.K.	K.O.

Calculation of strengthening:

For the calculation of the amount of force needed for the external flexural strengthening of the wall, model "b" was adapted from Figure 85. The position of the rotational hinge was taken as

$$t = \frac{N}{\sigma_{cmax}} \tag{29}$$

And the amount of force ("*f*") was calculated from the equation of moment equilibrium, considering α_{ULS} *as 0,106*, and α_{DLS} *as 0,084.*The corresponding strengthening necessities in case of σ_{mc}=2 MPa are the following.

$$f_{ULS}=24,7\ kN/m$$

$$f_{DLS}=4,89\ kN/m$$

In this case the wire ropes are able to provide *8,09 kN/m* for strengthening, which is enough to satisfy the damage limit state, but not the ultimate limit state.

It is important to use the design abacus, proposed in present thesis work (section 5.3) to see the complete resistance curve of Alcáçova wall, and to verify the failure modes and results by positioning the different limit states on the diagram. The bottom cross-section has an axial load composed by the self weight of the wall ($N_{Ed}=154\ kN$) and a bending effect coming from the applied seismic forces acting on the mass centre of the wall ($M_{Ed,ULS}=62,46\ kNm$; $M_{Ed,DLS}=49,6\ kNm$). The design abacus was prepared for Alcáçova wall with the proposed strengthening and the effects are represented together with the graph (see it on Figure 86). Using equation 17 and 18; $n=0,101$; $m_{ULS}=0,054$ *and* $m_{DLS}=0,043$.

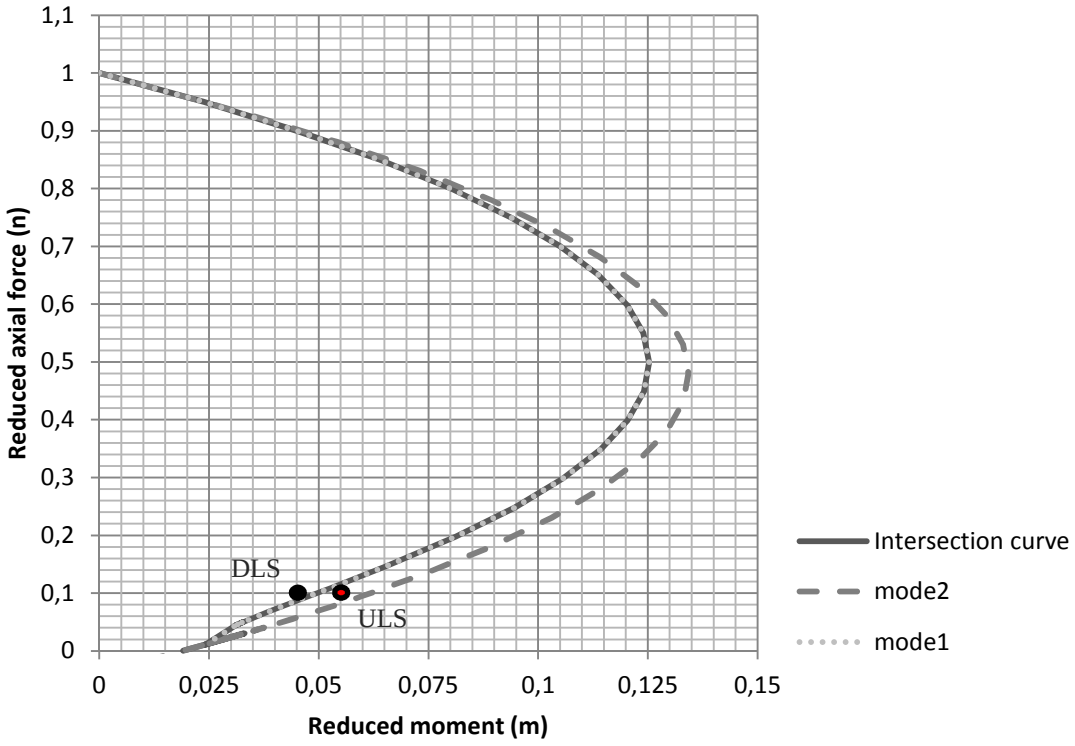

Figure 86: Reduced moment,-axial force interaction curve for Alcáçova wall (σ_{mc}=2 MPa)

The calculations were repeated with the assumption of a higher compressive strength of Alcáçova wall. The results of the calculations are listed in Table 18. As we can see, assuming different mechanical characteristics for the masonry highly influences the results, as assuming 4 or 8 Mpa for the masonry compressive strength satisfied the ultimate limit. It is also worth noting that the increase in the compression strength

contributed to the change of the failure type, and the full utilization of the reinforcement's capacity.

Table 18: Results of the analysis for strengthening Alcáçova wall

masonry compression strength	α_0	α_{new}	**improvement**	**DLS =0,084**	**ULS =0,106**
σ_{mc}=2 MPa	0,058	0,087	150,7%	OK	K.O.
σ_{mc}=4 MPa	0,079	0,124	158,1%	OK	OK
σ_{mc}=8 MPa	0,089	0,131	146,7%	OK	OK

7.5 Remarks

The investigation was done to see the applicability of the technique on an existing historical construction. It has been shown that geometrical issues are giving constraints to the applicable amount of reinforcement in the joints, and that the awareness of the real mechanical characteristics of the masonry is crucial, as these properties highly influence the results. Efficiency can be improved also by choosing a different type of reinforcement. Present research involved 3 specific types of stainless steel cables, but other products can have better performance. Synthetic ropes are also promising materials as reinforcement, and worth investigating, as it was discussed in previous chapters.

8

CONCLUSIONS

8.1 Final evaluation of research

The research was successful in investigating the applicability and workability of the new technique and to make the first steps in the definition of the mechanical performance, by applying and testing it on real structures. The key issues to be concentrated on are the pre-stressing of the reinforcing grid, the improvement of proposed anchor elements, and the extended research to find or develop the appropriate synthetic rope type, that can be used as alternative strengthening.

The design abacus – presented in the analytical study – was used as a powerful tool to define the interaction of failure modes and the resistance of a strengthened wall through the experimental research and also in the case study of Alcáçova wall.

Numerical modelling is recommended in the future. For this purpose, extended experimental results are necessary about the bond behaviour of the improved anchor elements. In order to define theoretical curves, it is important to plan further pull-out test in axial direction and also new tests in transversal direction, since both phenomena is involved in the function of the element. Pre-stressing can solve the problem of initial adjustment of the reinforcing grid, forcing the wire ropes to be straight lined between anchors. It is possible to eliminate most of these uncontrollable imperfections that would make the numerical modelling difficult.

8.2 Ideas for further development

Pre-tensioning:

Pre-stressing was applied successfully on one of the test specimens. The utilization of these forces was rather difficult in the geometrical conditions (workability issues). Other problems were the uncertainties in the amount and distribution of the applied forces (mechanical issues). Due to the deformability of the tested anchor elements, the cables had to be stressed in - at least - each horizontal joint. Improving the anchors might solve this problem and the procedure won’t need several repeat during the application.

It is possible to adapt an altered tool for pre-tensioning, which would be able to adjust to the special geometrical constraints (Figure 87). However, the implementation needs further research and a designed guideline for appropriate pre-tensioning.

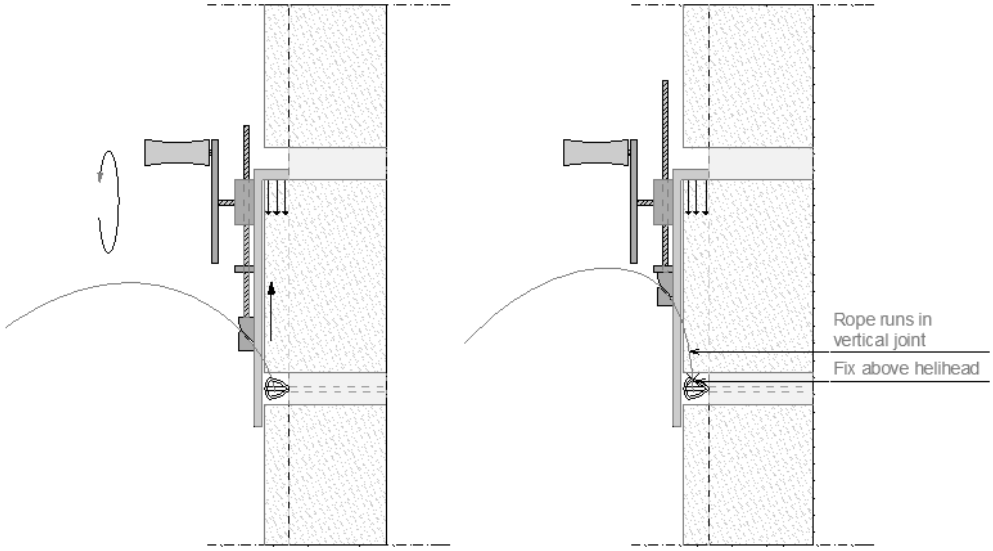

Figure 87: Sketch of adapted pre-tensioning tool

Protection of cables:

The most important function of the helihead is the protection of the wire ropes by preventing the passage around sharp edges. However, this function was lost during the experiments due to the significant deformations in the welded connection between the bar and the head. This connection has to be strengthened and the transversal performance of the helibar inserted into mortar joint needs to be tested to see the adequacy of the system. For better performance, higher values in diameter of helibar also should be used (ϕ12). Further investigation is necessary.

Alternative materials for grid:

Different synthetic ropes were tested as alternative materials to form the reinforcing grid. These attempts failed due to the high deformations and to the vulnerability of the ropes, extremely decreasing efficiency. Further research is needed in the developing field of these composites and materials to find the best solution, which is able to adapt 90° folding and the use of dry connections. One promising material is the Kevlar rope, which is extremely workable, and not vulnerable to transversal effects. Despite the promising physical and mechanical characteristics (3ϕ2 mm strand suffered slipping at ~40 kN when it was tested with resins in anchor at the Laboratories of Textile Materials in University of Minho), it suffered early failure during tests of simple tied connections. However, it is still an open question if the material would be able to close its high capacity with sleeves used in connection, or with other types of dry connections. Other issue is the question of compatibility between the material and connector sleeve element that needs further investigation. If adequate performance could be reached this way, Kevlar ropes could compete with the stainless steel wire ropes with their absolute non-corrosiveness, greater flexibility and remarkable mechanical properties.

9

REFERENCES

A931-96, 2002. Standard Test Method for Tension Testing of Wire Ropes and Strand. *ASTM*.

Barros, Varma, Sena-Cruz & Azevedo, 2008. Near surface mounted CFRP strips for the flexural strengthening of RC columns: Experimental and numerical research. *Engineering Structures,* Volume 30, pp. 3413-3425.

Bernat, Gil, Roca & Escrig, 2013. Experimental and analytical study of TRM strengthened brickwork walls under eccentric compressive loading. *Construction and Building Materials,* Volume 44, pp. 35-47.

Binda, Modena & Baronio, 1993. Strengthening of masonries by injection technique. *Proc. of 6° NAMC,* Volume Vol. I, pp. 1-14.

Binda, Modena, Baronio & Abaneo, 1997. Repair and investigation techniques for stone masonry walls. *Construction and Building Materials,* pp. 133-142.

Borri, Castori, Corradi & Speranzini, 2011. Shear behavior of unreinforced and reinforced masonry panels subjected to in situ diagonal compression tests. *Construction and Building Materials,* Volume 25, pp. 4403-4414.

Churilov & Dumova-Jovanoska, 2013. In-plane shear behaviour of unreinforced and jacketed brick masonry walls. *Soil Dynamics and Earthquake Engineering,* Volume 50, pp. 85-105.

Circolare-C8A, n.d. Appendice al cap. C8.

CNR-DT, 200/2004. Guide for the Design and Construction of Externally Bonded FRP Systems for Strengthening Existing Structures.

DGEMN, 1937. *O Casleto de Guimaraes.* Porto: s.n.

E488-96, 2003. Standard Test Methods for Strength of Anchors in Concrete and Masonry Elements. *ASTM*.

EN-1052-2:1999, n.d. Methods of test for masonry - Part2: Determination of flexural strength.

EN-1052-2, 1999. Methods of test for masonry - Part2: Determination of flexural strength.

Esmaeeli, Manning & Barros, 2013. Strain hardening fibre reinforced cement composites for the flexural strengthening of masonry elements of ancient structures. *Construction and Building Materials,* pp. 1010-1021.

Eurocode-6, 2005. EN 1996-1-1: Design of masonry structures - Part 1-1: General rules for reinforced and unreinforced masonry structures.

Eurocode-8, 2004. EN 1998-1: Design of structures for earthquake resistance - Part 1: General rules, seismic actions and rules for buildings.

Fernandes, E., 2011. *Guia de Arquitectura de Guimaraes.* s.l.:Argumentum.

Fernández, Y. W. E., 2012. *Characterization of the response of quasi periodic masonry: Geometrical investigation, homogenization and structural application,* Guimaraes: s.n.

Gelmi, Modena & Zaninetti, R. a., 1993. Mechanical characterization of stone masonry structures n old urban nuclei. *Proc. of 6" NAMC,* Volume I, pp. 505-5 16.

Griffith, Kashyap & Ali, M., 2012. Flexural displacement response of NSM FRP retrofited masonry walls. *Construction and Building Materials, http://dx.doi.org/10.1016/j.conbuildmat.2012.06.065,* Volume http://dx.doi.org/10.1016/j.conbuildmat.2012.06.065.

Ismail & Ingham, 2012. In-situ and laboratory based out-of-plane testing of unreinforced clay brick masonry walls strengthened using near surface mounted twisted steel bars. *Construction and Building Materials,* Volume 36, pp. 119-128.

Ismail, Laursen, Jason & Ingham, 2009. Out-of-plane testing of siemically retrofitted URM walls using posttensioning.

Lazzarini, Laursen & McDaniel, n.d. Out-of-plane seismic performance of unreinforced masonry walls retrofitted with unbonded post-tensioning tendons.

Magenes, Modena, Porto & Morandi, 2009. Seismic Behaviour and Design of New Masonry Buildings:Recent developments and Consequent Effects on Design Codes. *Eurocode 8 Perspectives from the Italian Standpoint Workshop,* pp. 199-212.

Magenes & Penna, 2009. *Existing Masonry Buildings: General Code Issues and Methods of Analysis and Assessment; Eurocode 8 Perspectives from the Italian Standpoint Workshop,* pp. 185-198.

Milani, 2013. Lesson learned after the Emilia-Romagna, Italy, 20–29 May 2012 earthquakes: A limit analysis insight on three masonry churches. *Eng Fail Anal, http://dx.doi.org/10.1016/j.engfailanal.2013.01.001*.

Moreira, S., 2010. *Relatório ensaios não-destrutivos no Castelo de Guimarães,* Guimarães: s.n.

Papanicolaou, Triantafillou & Lekka, 2011. Externally bonded grids as strengthening and seismic retrofitting materials of masonry panels. *Construction and Building Materials,* Volume 25, pp. 504-514.

ANNEX I. – Resultant graphs of pullout test

8φ8 _φ4 /strong bond/

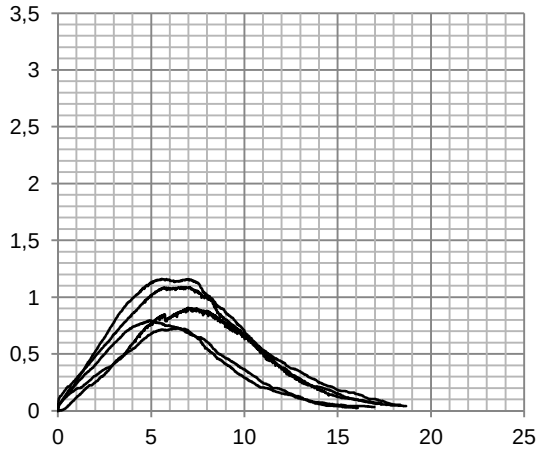

8φ8 _φ6 /weak bond/

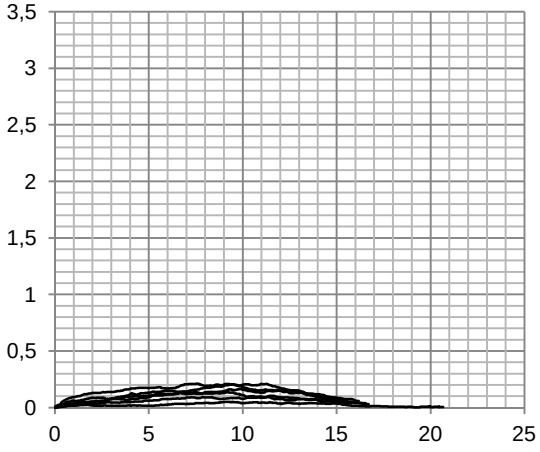

8φ10 _φ6 /strong bond/

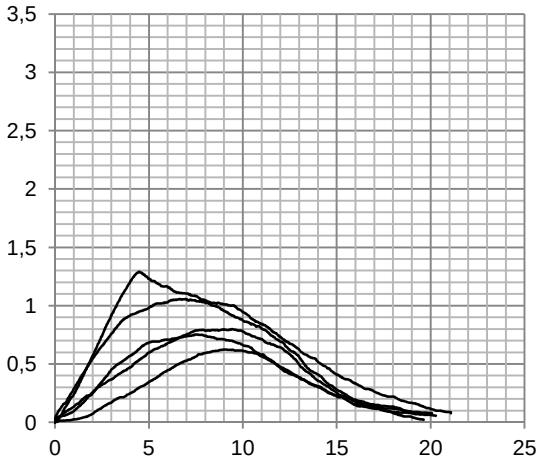

8φ10_φ8 /weak bond/

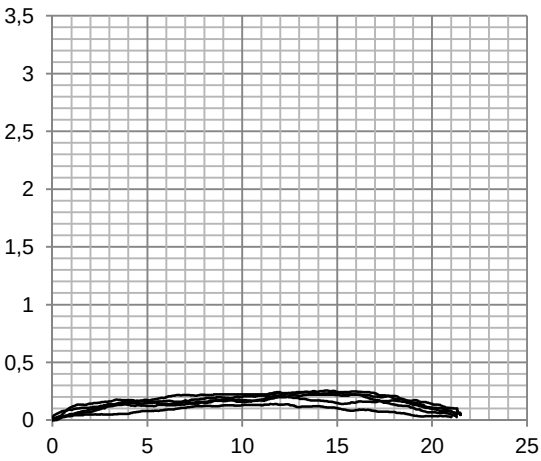

12φ8 _φ4 /strong bond/

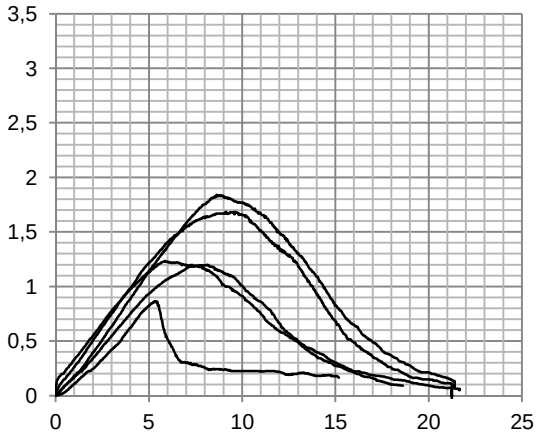

12φ8 _φ6 /weak bond/

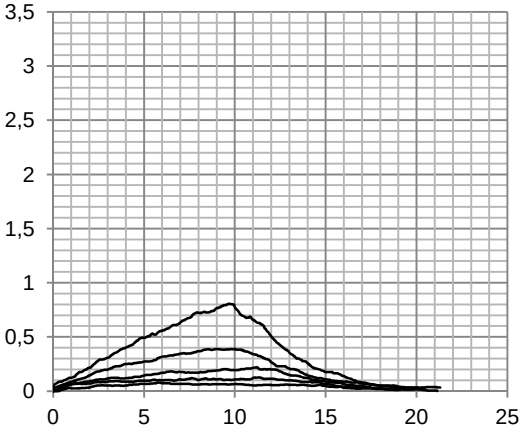

12φ10_φ6 /strong bond/

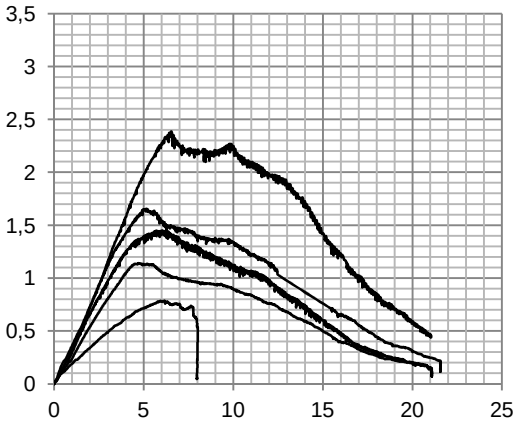

12φ10_φ8 /weak bond/

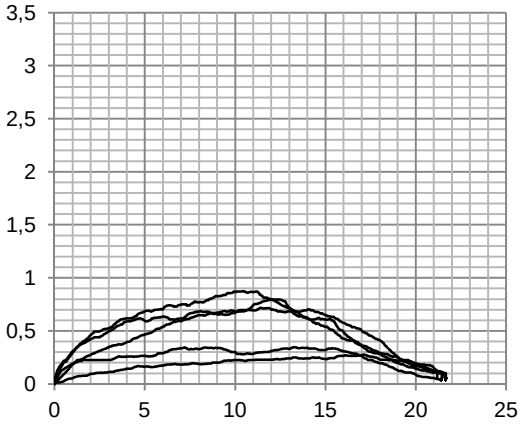

20φ8 _φ6 /weak bond/

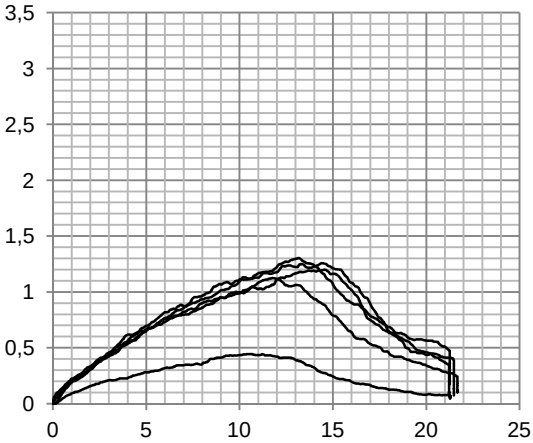

20φ10_φ6 /strong bond/

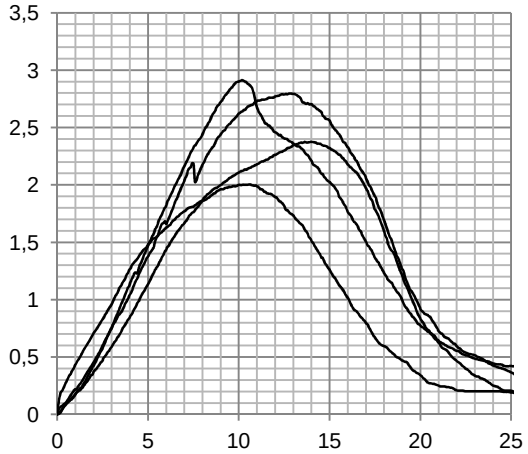

20φ10_φ8 /weak bond/